



**TRIBHUVAN UNIVERSITY
INSTITUTE OF ENGINEERING
PULCHOWK CAMPUS**

THESIS NO.: M-381-MSREE-2021-2023

**Machine Learning Approach for Fault Detection and Diagnosis of PV
Modules**

by

Kabina Maharjan

A THESIS

**SUBMITTED TO THE DEPARTMENT OF MECHANICAL AND
AEROSPACE ENGINEERING IN PARTIAL FULFILLMENT OF THE
REQUIREMENTS FOR THE DEGREE OF MASTER OF SCIENCE IN
RENEWABLE ENERGY ENGINEERING**

**DEPARTMENT OF MECHANICAL AND AEROSPACE ENGINEERING
LALITPUR, NEPAL**

NOVEMBER, 2023

COPYRIGHT

The author has agreed that the library, Department of Mechanical and Aerospace Engineering, Pulchowk Campus, Institute of Engineering may make this thesis freely available for inspection. Moreover, the author has agreed that permission for extensive copying of this thesis for scholarly purposes may be by the professor(s) who supervised the work recorded herein or, in their absence, by the Head of the Department wherein the thesis was done. It is understood that recognition will be given to the author of this thesis and the Department of Mechanical and Aerospace Engineering, Pulchowk Campus, Institute of Engineering for any use of the material of this thesis. Copying or publication or the other use of this thesis for financial gain without the approval of the Department of Mechanical and Aerospace Engineering, Pulchowk Campus, Institute of Engineering, and the author's written permission is prohibited. Request for permission to copy or to make any other use of the material in this thesis in whole or in part should be addressed to:

Head

Department of Mechanical and Aerospace Engineering

Pulchowk Campus, Institute of Engineering

Lalitpur, Nepal

**TRIBHUVAN UNIVERSITY
INSTITUTE OF ENGINEERING
PULCHOWK CAMPUS**

DEPARTMENT OF MECHANICAL AND AEROSPACE ENGINEERING

The undersigned certify that they have read, and recommended to the Institute of Engineering for acceptance, a thesis entitled “Machine Learning Approach for Fault Detection and Diagnosis of PV Modules” by Kabina Maharjan in partial fulfilment of the requirements for the degree of Master of Science in Renewable Energy Engineering.

Supervisor, Assist. Prof. Arbin Maharjan
Department of Electrical Engineering
Pulchowk Campus

Supervisor, Assist. Prof. Laxman Motra
Deputy Head
Department of Mechanical and Aerospace Engineering
Pulchowk Campus

External Examiner, Dr. Laxman Pd. Ghimire
Assistant Director
Alternative Energy Promotion Centre

Committee Chairperson, Dr. Sudip Bhattra
Head
Department of Mechanical and Aerospace Engineering

November 28, 2023

ABSTRACT

Fault analysis in solar Photovoltaic (PV) arrays is a crucial aspect that helps to increase the PV system's efficiency, safety, and reliability. Faults and defects, if not detected, not only compromise the system's generation but also accelerate system aging and jeopardize the functionality of the overall system. Currently, the solution involves manual monitoring by system operators, but this approach is time-consuming, prone to inaccuracies, and poses safety risks. Therefore, it is imperative to implement automatic detection and diagnosis methods to detect faults to ensure the PV systems' safety and reliability. Existing techniques either lack the precision to provide detailed fault information or are overly complex. This research introduces a fault detection and diagnosis method in solar PV systems using a machine learning approach. The research extends to defining normal conditions and four distinct fault categories for the proposed fault detection and classification algorithm. A predictive model is prepared using a machine learning approach to forecast the DC output power. The trained Multilayer Neural Network (MNN) model is found to have the Root Mean Square Error (RMSE) of 6.74 and 6.11 for the training and validation sets. By analyzing the difference between the power predicted by the MNN model and the actual PV system power, the predefined fault types in the PV modules are detected. The proposed approach offers rapid detection and high accuracy. Simulation results demonstrate the effectiveness of this method in identifying and diagnosing Maximum Power Point Tracking (MPPT), open-circuit string, module, and partial shading faults in PV systems.

ACKNOWLEDGEMENT

I express my sincere gratitude to my project supervisors, **Assist. Prof. Arbin Maharjan** and **Assist. Prof. Laxman Motra (DHOD)**, as well as program coordinator **Assoc. Prof. Dr. Hari Bahadur Darlami of Master of Science in Renewable Energy Engineering**, for their invaluable guidance, insightful lessons, and inspiration throughout this research.

My heartfelt thanks go to the **Department of Mechanical and Aerospace Engineering** for providing a crucial platform for applying the engineering knowledge acquired during my Master's program.

I extend my appreciation to **Narayan Dhakal, Factory Operation Director at Time Pharmaceutical Factory**, for generously providing data and resources essential for the success of this research.

I am indebted to my family and colleagues for their unwavering support and encouragement during the entire duration of the study.

Furthermore, I wish to express my gratitude to the authors and publishers of the various sources that have played a pivotal role at every stage of this research.

TABLE OF CONTENTS

COPYRIGHT	2
ABSTRACT	4
ACKNOWLEDGEMENT	5
TABLE OF CONTENTS	6
LIST OF FIGURES	8
LIST OF TABLES	10
LIST OF ABBREVIATIONS	11
CHAPTER ONE: INTRODUCTION	13
1.1 Background	13
1.2 Problem Statement	15
1.3 Objective	17
1.3.1 Main Objective.....	17
1.3.2 Specific Objectives	17
1.4 Assumptions and Limitations	17
1.4.1 Assumptions.....	17
1.4.2 Limitations	18
CHAPTER TWO: LITERATURE REVIEW	19
2.1 World Scenario of Renewable Energy	19
2.2 Faults in PV System.....	20
2.3 Advanced Fault Identification Methods.....	25
2.4 Machine Learning Approach Based Fault Diagnosis	27
2.4.1 Multi-Layer Neural Network (MNN)	28
2.4.2 Radial Basis Function (RBF) Neural Network	28
2.4.3 Probabilistic Neural Network (PNN).....	29
2.4.4 Deep Neural Networks (DNN)	29

2.4.5 Other Neural Networks	29
CHAPTER THREE: METHODOLOGY	30
3.1 System Description	31
3.2 Data Collection	32
3.3 Data Preprocessing.....	33
3.3.1 Data cleaning	34
3.3.2 Normalization	34
3.4 Multilayer Neural Network Model	34
3.5 Optimization	37
3.6 Multilayer Neural Network Training	37
3.7 Fault Detection and Diagnosis	38
CHAPTER FOUR: RESULTS AND DISCUSSION	41
4.1 Data Preprocessing.....	41
4.2 Multilayer Neural Network-Based Solar PV System Modelling.....	43
4.3 Fault Detection and Diagnosis	50
CHAPTER FIVE: CONCLUSION AND RECOMMENDATION	56
5.1 Conclusion	56
5.2. Recommendation	56
REFERENCES.....	57
Appendix A: Correlation Between Irradiance and Temperature Before and After Normalization	62
Appendix B: Error Comparison Power Data Sheet	63
Appendix C: Time Pharmaceutical Factory, Nawalpur, Nepal, Hourly Meteorological Data Report Logsheet	77
Appendix D: System Parameters During Open-Circuit String Fault and Module Fault	91

LIST OF FIGURES

Figure 2.1: Location and structure-based DC side fault classification of PV system..	24
Figure 3.1: Research flowchart	31
Figure 3.2: Google Earth map of solar PV plant installed in Time pharmaceutical factory	32
Figure 3.3: Architecture of MNN [39].....	36
Figure 3.4: Fault detection and diagnosis model flowchart.....	40
Figure 4.1: Solar irradiance normalization process (input data): (a) before normalization; (b) after normalization	41
Figure 4.2: Ambient temperature normalization process (input data): (a) before normalization; (b) after normalization	41
Figure 4.3: Solar PV output power normalization process (input data): (a) before normalization; (b) after normalization	42
Figure 4.4: Correlation between inputs and output (a) before normalization; (b) after normalization	42
Figure 4.5: RMSE of training and validation sets for different no. of neurons	44
Figure 4.6: Final ANN architecture	45
Figure 4.7: Best Performance of ANN	45
Figure 4.8: Neural network training error histogram.....	46
Figure 4.9: The gradient value, the Mu value, and the validation check value of the trained ANN model.....	46
Figure 4.10: Neural network training regression	47
Figure 4.11: Full-month comparison between PV output forecasting using the MNN Model and measured PV output (May, 2023).....	48
Figure 4.12: Correlation between forecasted and measured value for both training and validation sets.....	48
Figure 4.13: Full-month comparison between PV output forecasting using the MNN Model and measured PV output (June, 2023).....	49
Figure 4.14: Zoom out of comparison between MNN model forecast and measured value over June 21,2023	50

Figure 4.15: Fault detection and diagnosis model	52
Figure 4.16: Fault indicator for normal condition and MPPT failure.....	53
Figure 4.17: Fault indicators for open-circuited string and module fault	54
Figure 4.18: Fault indicator for MPPT fault	55

LIST OF TABLES

Table 1.1: Production capacities per energy source of Nepal [4]	14
Table 2.1: Solar PV system fault classification [25].....	23
Table 3.1: Technical specifications of solar modules installed at site	33
Table 4.1: MNN model result	44
Table 4.2: RMSE and accuracy of forecasted power.....	50
Table 4.3: Tested fault cases	51

LIST OF ABBREVIATIONS

AC	:	Alternating Current
AEPC	:	Alternative Energy Promotion Centre
ANN	:	Artificial Neural Network
BP-PSO	:	Back Propagation-Particle Swarm Optimization
DANN	:	Detection Artificial Neural Network
DC	:	Direct Current
DNN	:	Deep Neural Network
DoED	:	Department of Electricity Development
FF-ANN	:	Feed-Forward Artificial Neural Networks
FPGA	:	Field Programmable Gate Array
FC	:	Honey-Comb
ISE	:	Integrated Software Environment
GW	:	Giga Watt
KELM	:	Kernel-Based Extreme Learning Machine
MNN	:	Multilayer Neural Network
MPP	:	Maximum Power Point
MPPT	:	Maximum Power Point Tracking
MS	:	Monitoring System
MW	:	Megawatt
NARX	:	Nonlinear Autoregressive Network
NASA	:	National Aeronautics and Space Administration
NEA	:	Nepal Electricity Authority

NN	:	Neural Network
NOCT	:	Nominal Operating Cell Temperature
PNN	:	Probabilistic Neural Network
RBF	:	Radial Basis Function
RES	:	Renewable Energy Systems
ReLU	:	Rectified Linear Unit
RMSE	:	Root Mean Square Error
RPV	:	Residential Photovoltaic
SP	:	Series-Parallel
STC	:	Standard Testing Condition
TCT	:	Total-cross-Tied
XSG	:	Xilinx System Generator

CHAPTER ONE: INTRODUCTION

1.1 Background

Fossil fuels have numerous harmful environmental effects, including climate change, greenhouse gas emissions, global warming, and air and water pollution. Experts forecast that fossil fuel reserves will be depleted by 2030. To promote sustainability, researchers are exploring eco-friendly, cost-effective, and practical energy production methods. Renewable energy, particularly solar photovoltaic (PV) systems, is emerging as a crucial solution for addressing climate change and achieving sustainable development. PV systems are popular due to their environmental benefits and the ability to harness clean, endless solar energy. Many countries are adopting strategic energy plans to facilitate the installation of large-scale PV systems, aiming to reduce reliance on traditional fossil fuels, lower electricity costs, and leverage the unique advantages of PV systems [1].

As the global shift towards renewable energy gains momentum, grid-connected solar PV systems are gaining prominence as a major contributor to large-scale electricity production. Nepal possesses substantial potential for implementing a solar energy infrastructure. The country receives an average of 3.6 to 6.2 kWh of solar radiation per square meter per day, with approximately 300 sunny days annually, rendering it an ideal location for solar power generation. The potential theoretical annual output of Residential Photovoltaics (RPV) varied from 637 GWh in Kathmandu to 50 GWh in Butwal. Furthermore, the cumulative RPV potential from urban households in Nepal was approximated to be around 6.5 TWh per year [2]. The Government of Nepal's 2018 white paper outlines a vision for renewable energy integration in the national energy matrix to ensure energy security, targeting 5-10% contribution from renewable sources in the power generation mix [3]. The promotion of renewable energy in Nepal has played a pivotal role in extending clean energy access to its populace. As of now, approximately 55 MW of electricity has been generated from mini/micro-hydro and solar energy, facilitated by the Alternative Energy Promotion Center (AEPCC), providing clean electricity solutions to 3.6 million households. This achievement has reached 18% of the total population and has fostered the creation of 30,000 jobs within this sector [3]. According to the Department of Electricity Development (DoED), till June 2023 many licenses had been issued for solar projects, where for construction 21

projects had a total capacity of 133.56 MW, and for survey 44 projects had a total capacity of 747.6 MW.

Table 1.1: Production capacities per energy source of Nepal [4]

Energy source	Total in Nepal	Percentage in Nepal	Percentage USA	Per capita in Nepal	Per capita USA
Fossil fuels	0.00 kWh	0,0 %	59,9 %	0.00 kWh	2.05 kWh
Nuclear power	0.00 kWh	0,0 %	19,5 %	0.00 kWh	0.67 kWh
Solar energy	317.04 m kWh	2,6 %	3,2 %	10.38 kWh	0.11 kWh
Wind power	24.39 m kWh	0,2 %	8,3 %	0.80 kWh	0.28 kWh
Water power	11.85 bn kWh	97,2 %	7,0 %	388.00 kWh	0.24 kWh
Tidal power plants	0.00 kWh	0,0 %	0,0 %	0.00 kWh	0.00 kWh
Geothermic	0.00 kWh	0,0 %	0,4 %	0.00 kWh	0.01 kWh
Biomass	0.00 kWh	0,0 %	1,7 %	0.00 kWh	0.06 kWh

However, boosting the performance of solar PV systems requires addressing various One of the factors affecting the PV module's performance is the accumulation of dust, with temperature, relative humidity, and cloud cover having subsequent impacts. Exposing the module for 23 days can result in a 15.29% reduction in energy output. The power output and conversion efficiency can experience decrease of 2.6% and 0.49%, respectively. Additionally, relative humidity is found to contribute to a reduction in energy output by 4.3 Wh/m²/day [5]. Furthermore, throughout the PV plant's lifetime, several faults on the DC side or AC side of the system can occur causing reduction in the output power of the system [6]. The effectiveness of PV systems can be compromised by exposure to diverse weather conditions, including

soiling and temperature fluctuations, leading to electrical and mechanical problems like cracked cells and short circuits [7]. With such exposure, there is a growing need for methods to maintain performance, minimize revenue losses and downtime, and swiftly detect, classify, locate, and mitigate faults in PV systems. One approach to achieve this is by implementing a Monitoring System (MS) within the PV plant. This system monitors electrical and meteorological variables, manages plant operations (e.g., remote access), identifies malfunctions and errors, and reports performance and benchmarking data, either locally or remotely, to the grid operator through a communication system. A fault detection algorithm designed for PV systems serves the purpose of accurately estimating electricity generation during regular operation and identifying any faults within the PV system. This capability empowers operators to promptly implement corrective measures, preventing prolonged periods of under-performance. By minimizing power losses caused by faults, the implementation of such algorithms contributes to enhancing the overall performance of PV systems [8]. However, relying solely on the analytical based MS face limitations in the reliability of their application in these systems due to the absence of on-site measurements and comprehensive specifications for PV systems [9].

Typically, techniques for detecting and classifying PV faults focus primarily on the most common types, such as open-circuit, short-circuit, and module mismatch. Various approaches have been used in fault classification, including visual methods [10], thermographic image analysis [11], and mathematical methods [12] that employ theoretical and simulated models of PV plants. More recently, machine learning-based techniques have been proposed, which have shown improved classification performance in different scenarios, particularly in dealing with shadowing and PV module degradation. Nevertheless, it's important to note that many of these methods are based on simulated data, and the authors often do not provide a comprehensive analysis of techniques for online fault classification.

1.2 Problem Statement

Solar photovoltaic (PV) power emerges as a significant and versatile renewable energy source, finding applications ranging from utility-scale installations to residential rooftops, and it has a widespread global presence. Projections suggest that by 2050, it is expected to contribute approximately 11% to the world's total electricity generation [13]. This is primarily due to its reliability, sustainability, and the fact that it does not

deplete over time, making it an environmentally friendly choice. The increasing adoption of solar energy is influenced by factors such as concerns about climate change, declining costs of PV technology, and government policies promoting the use of renewable energy. As a result, solar energy has become a substantial contributor to the global electricity supply. Consequently, the installation of these systems is on the rise. Recognizing the significant potential of small rooftop PV systems, there is a growing emphasis on research to enhance their quality and performance.

The performance of solar PV systems can be impacted by various issues, including degradation, partial shading, and open or short circuits. A recent study revealed that five-minute average climatic and performance data indicated up to 18.9% power loss due to system faults, encompassing component failure, inverter shutdown, shading, inverter MPPT failure, and other issues [14]. Research has shown that safety concerns or power drops can mask the true lifespan of PV modules, with common failures like laminate discoloration, cell part isolation, and delamination causing an average power loss of around 10% [15]. Moreover, the occurrence of faults such as open-circuit string faults, Maximum Power Point Tracking (MPPT) faults, and shading faults in solar photovoltaic (PV) systems poses significant challenges and demands attention due to their adverse impact on system performance, reliability, and overall energy output. These faults can lead to substantial power losses, reduced energy harvest, and even complete system failures if not promptly detected and addressed.

The impact of these faults extends beyond mere energy losses, as they can compromise the long-term reliability and lifespan of the PV system. Furthermore, in the context of the global shift towards renewable energy sources, the economic implications of inefficient solar power generation underscore the importance of addressing these specific faults. Addressing challenges associated with PV modules and their operation is crucial not only for maximizing the energy yield and economic viability of solar PV systems but also for promoting the widespread adoption of solar energy as a sustainable and reliable power source. Developing effective fault detection and mitigation strategies for these issues is essential to ensure the optimal functioning and longevity of solar PV installations, contributing to the overall success of renewable energy initiatives. Despite the implementation of conventional protective devices within a photovoltaic (PV) system, faults within a PV array might go unnoticed [16].

Achieving this objective involves implementing strategies such as monitoring and fault detection. However, the complexity of these fault scenarios requires advanced techniques for accurate and timely detection. The intricate fault patterns associated with solar modules, characterized by nonlinear relationships and dynamic environmental influences, demand an adaptable and efficient approach. Moreover, diagnosing issues with photovoltaic modules is challenging due to their similar appearance despite varying qualities. Defects and faults, often invisible or missed, require specialized methods for identification. Machine learning techniques excel in capturing and learning from the multifaceted nature of the data. Their ability to autonomously discern complex patterns, adapt to evolving conditions, and generalize well to diverse fault scenarios makes them indispensable for accurate and comprehensive fault detection.

1.3 Objective

1.3.1 Main Objective

The main objective of this study is to detect and diagnose faults of the solar modules by using machine learning approach.

1.3.2 Specific Objectives

The specific objectives of the project are:

- To develop a real-time solar PV power forecasting model and evaluate its performance
- To develop a fault detection method for the solar modules of the solar PV plant.
- To test the proposed fault detection method under different faulty conditions.

1.4 Assumptions and Limitations

1.4.1 Assumptions

- The collected real-time dataset is representative of various real-world conditions in the PV system.
- The meteorological data and historical records of the PV system are accurate and complete.
- The configuration and components of the PV system remain consistent throughout the study period.

1.4.2 Limitations

- This study is designed to detect and diagnose only four specific types of faults in PV modules.
- The precise location of the faults within the PV arrays isn't identified in this study.
- The effectiveness of the proposed method has not been experimentally validated in real-world PV installations.

CHAPTER TWO: LITERATURE REVIEW

2.1 World Scenario of Renewable Energy

There is a noticeable acceleration in the global energy transition, marked by various indicators that anticipate significant changes in both energy supply and demand in the upcoming decades. The analysis underscores the role of rapid innovation, particularly in the decreasing costs of renewable technologies and supportive technologies like batteries, which are facilitating this ongoing transition. According to the International Energy Agency (IEA), renewable energy capacity witnessed substantial growth, with renewable electricity capacity increasing by 45% between 2015 and 2020. Solar and wind power have been particularly prominent in this expansion, with decreasing costs contributing to their widespread adoption. Additionally, various countries have set ambitious renewable energy targets to further accelerate the transition. For example, by 2050, the European Union aims that out of the final energy consumption, 32% would be produced through renewable energy. Research forecasts that by 2050, renewable power will constitute 58% of total renewables deployment, with variable renewable power contributing to 60% of overall energy generation, a substantial increase from the current 10% [17]. Attaining significant proportions of variable renewable energy requires a substantial transformation in the energy industry, as demonstrated by successful approaches in top-performing nations. Successful operation of these systems requires a systemic approach that integrates various innovations. It is crucial that advancements in technology must be accompanied by the creation of innovative market structures and business strategies that are in harmony with the features of emerging technologies.

In the context of energy consumption, Nepal consumed 7741 Gigawatt-hour (GWh) of electricity in 2020, mainly derived from hydropower sources [18]. Despite possessing a theoretical hydropower potential of 83,000 Megawatt (MW), with about 40,000 MW considered economically viable, Nepal faces challenges due to its relatively small geographic size of 147,516 km² [19]. The significant interest and investment in hydropower must be carefully considered, taking into account the premium on land in Nepal. Any shift in land-use, particularly towards large-scale hydro dams, could result in substantial and lasting environmental and social impacts, including flooding and resettlements.

Nepal's solar potential is immense, estimated at 50,000 terawatt-hours per year—7,000 times greater than its current electricity consumption and 100 times greater than the water resource [20]. However, harnessing this solar power growth necessitates balancing and storage services, similar to those provided by pumped storage hydropower. The Global Pumped Hydro Atlas identifies 2,800 suitable storage sites in Nepal, exceeding the requirement even when the country catches up with developed nations. Crucially, none of these sites requires damming rivers, thereby eliminating potential high environmental and social costs. Looking ahead, Nepal aims to install 200 watts of solar panels per person annually over the next 50 years, mirroring the deployment rate seen in Australia, where solar and wind systems are effectively reducing electricity costs. To meet energy consumption levels per capita seen in developed countries without relying on fossil fuels (by electrifying nearly all energy services), approximately 40 square meters of solar panels per person, with a nominal power capacity of around 10 kilowatts, will be needed. Some of this solar panel area can be integrated into rooftops, with the majority co-located with agricultural spaces. Notably, leveraging the cost-effectiveness of solar energy allows developing countries like Nepal to skip the fossil fuel era and directly transition to zero emissions—a critical move to limit global warming to 1.5 degrees Celsius, as emphasized by the Intergovernmental Panel on Climate Change [21].

2.2 Faults in PV System

In [22], the factors contributing to the degradation and failure of PV technology has been explored. The study highlighted the significant impact of climatic conditions, such as solar irradiance, high temperatures, and relative humidity, which can reduce the efficiency of solar cells by over 70%. These conditions lead to a substantial decrease in the overall efficiency of solar cells. Additionally, the study identified that soft shading can affect the current of PV modules without altering the voltage. In contrast, hard shadowing's impact on the performance of photovoltaic modules depends on whether cells in the module are partially or completely shaded. The research emphasized the importance of considering different parameters when assessing the functioning of the solar PV modules.

The solar energy has garnered considerable attention for electricity generation, with the widespread adoption of photovoltaic (PV) systems globally due to technological advancements in the field. However, to ensure optimal performance, these PV systems

require accurate continuous assessments and monitoring. Different nature of faults, ranging from permanent to temporary defects or failures, can affect solar PV systems, presenting a issue in identifying and locating system faults accurately, cost-efficiently and promptly. An effective fault detection system is essential to minimize damage caused by faulty PV modules and safeguard the system against potential losses. In [23] different classifications of PV faults and fault detection techniques has been explored. Special emphasis is given to thermography technique due to its benefits in identifying, diagnosing and location various fault types. The study provides a comprehensive overview of diagnosis of the PV system defects including detection, classification and locating, drawing insights from contemporary literature. The integration of thermal imaging is highlighted as a non-destructive and efficient method for effectively discovering and locating failures. The investigation also delves into several computational approaches employed in analysing the failures in the solar PV system, which includes statistical approaches and machine learning techniques.

The faults pose a significant risk of power losses in residential solar PV systems. Different natures of fault are used in [14] and a unique techniques of fault analysis is used to determine the power losses that occur when the different types of the faults are introduced in the system. The nature of faults is shading-free non-zero efficiency fault, faults with zero system efficiency, zero efficiency for short time period and shading fault. The research highlighted that brief faults have the capability to cause substantial system losses, with one monitored system experiencing an annual power loss of 23%. The causes of the system faults can vary, and the solutions may differ accordingly. Despite the diverse reasons, the study stressed the importance of detecting and quantifying the impacts of these brief faults to ensure effective mitigation strategies.

The identification and analysis of faults in photovoltaic (PV) systems play a pivotal role in making sure that the system is safe and power output of PV arrays is optimized. These faults not only diminish the efficiency and power output of the system but also shorten its operational lifespan. Among the commonly encountered PV faults are shading faults, single or double line-to-line, single or double line-to-ground, and arc faults, while less common but more severe faults include system degradation, hotspots, connection faults and faults in the bypass diode of the solar modules.

Existing fault identification methods, as delineated in this study, exhibit several limitations that may lead to the misidentification of faults. The mathematical formulation of different faults in the solar PV system, is followed by a critical analysis of their efficiency, precision, complexity, and consistency [24]. The findings presented in this work contribute to a comprehensive understanding of the nature and causes of PV faults. Importantly, this research serves as a valuable reference and provides suggestions for both studies and the PV manufacturing engineering to enhance fault identification capabilities in solar systems.

Table 2.1: Solar PV system fault classification [25]

Fault Location	Fault	Cause	Impact	Detection Technique
PV Panel Fault	Delamination	Overexposed to direct sunlight	<ul style="list-style-type: none"> All the faults in the panel will result in the reduction of solar panel output and increase the burden on the DC-DC converter 	<ul style="list-style-type: none"> Visual inspection Thermography based detection Image processing-based fault identification Signal processing-based detection
	Cell crack	Physical damage		
	Diode shorting	Overexposed to direct sunlight		
	Snail trail	Moisture in atmosphere		
	Glass crack	Physical damage		
Combination box fault	Oxidation	Environmental impact	<ul style="list-style-type: none"> Power flow reduction 	<ul style="list-style-type: none"> Visual inspection and signal-based monitoring
	Corrosion	Environmental impact		
Power converter fault	Bond wire melting	Thermal joints overheating	<ul style="list-style-type: none"> Cause stress on the inverter operation, wear out in the inverter components, and reduces the inverter's operating lifetime 	<ul style="list-style-type: none"> Temperature-sensitive electrical parameters operating characteristics-based monitoring, using signal, and learning approaches Thermal model, and physics-based modeling approaches
	Bond wire lift-off	Overheating		
	Bond wire cracking	Bond wire stress		
	Aluminum corrosion	Environmental impact		
	Substrate crack	Thermal stress on substrate		
	Die delamination	Power electronic switch overheating		
Filter fault	Thermal overstress	Overheating	<ul style="list-style-type: none"> Increase in the harmonics at the inverter (AC side) Poor power quality False trip signal 	<ul style="list-style-type: none"> Monitor output signals and use learning-based approaches Thermal image-based learning approaches
	Crack in dielectric	Sudden temperature change		
	Electrolyte leakage	Expose to thermal stress during storage		
	Electrolyte evaporation	Expose to thermal stress during storage		
Battery fault	Ageing	Stress factors	<ul style="list-style-type: none"> Active cathode/anode material loss Capacity fade Thermal run-away Power fade Longer charging time 	<ul style="list-style-type: none"> Thermal inspection Data-driven models for state of health estimation Remaining useful life prediction measures characteristics and capacity estimation Incremental capacity analysis
	Cooling loss	Lithium plating/dendrite formulation		
	Cell failure	Electrolyte decomposition		
	Battery management system failure	Converter control circuit failure		

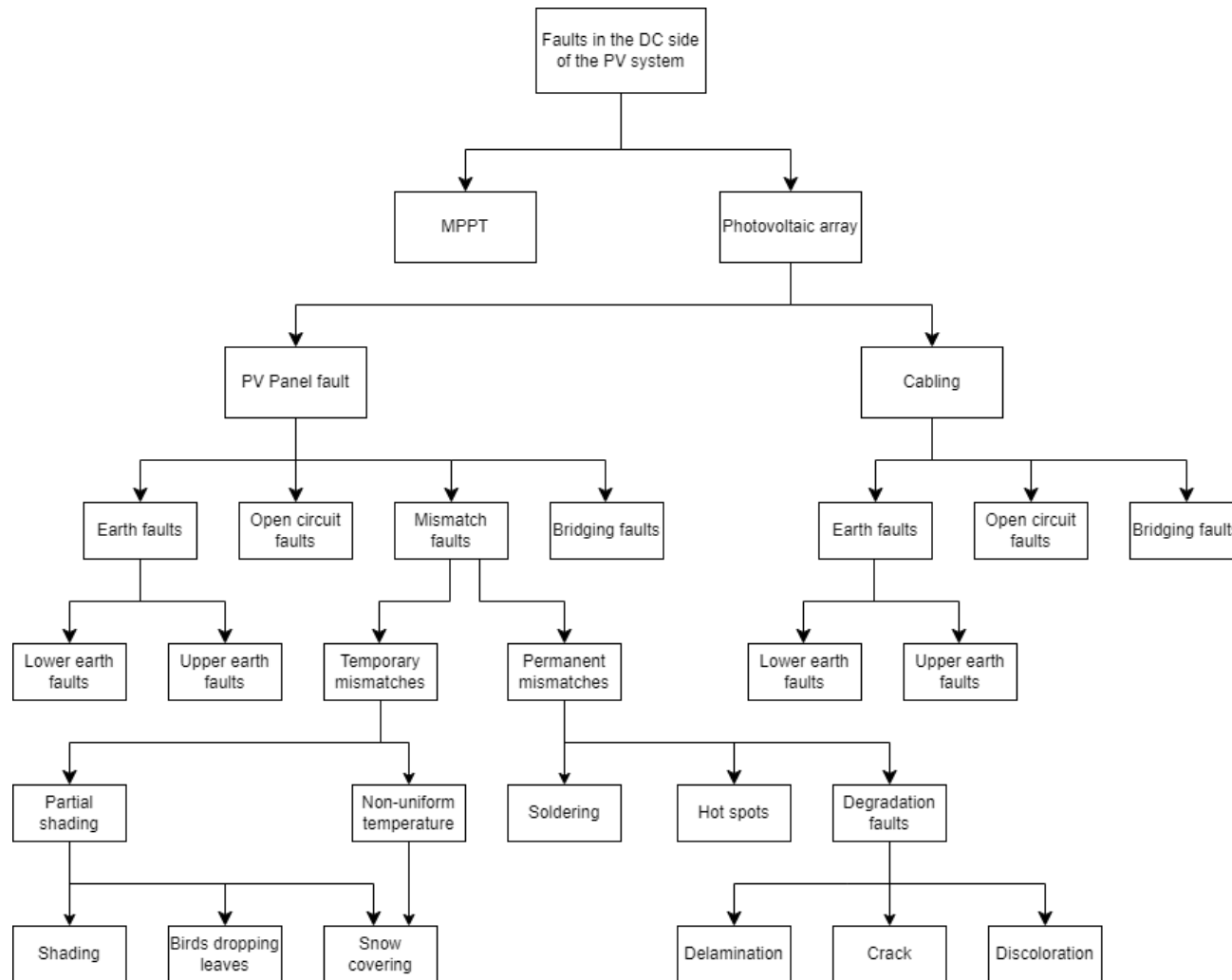


Figure 2.1: Location and structure-based DC side fault classification of PV system

The photovoltaic (PV) panels constitute a critical element of the PV system and are exposed to rigorous operational conditions. Failure to timely identify or predict potential faults in these panels can significantly impact the overall functionality and lifespan of the entire system. Previous research has introduced various fault detection techniques, with methods contingent upon discerning diverse faults occurring at different locations within the PV system. Some approaches focus on identifying faults on the direct current (DC) side, while others concentrate on faults occurring on the alternating current (AC) side of the system. An exhaustive examination of common faults specifically within the domain of the DC side of the PV system (PV panels) has been delineated in [26]. This examination encompasses fault types, causative factors, their ramifications on PV system performance, and potential methodologies for detection and prediction. The classification of faults takes into account their temporal characteristics, categorizing them as permanent, intermittent, or temporary. Additionally, a classification based on incipient faults has been established. The exploration of incipient faults assumes significance in proactively identifying issues at their nascent stages, thereby averting their progression into persistent faults.

2.3 Advanced Fault Identification Methods

Researchers have been investigating various approaches to identify and diagnose faults in PV systems. Techniques incorporating machine learning have been extensively examined as they provide an alternative approach to addressing intricate issues. Some of these methods focus on early fault detection, employing predictive measures to prevent significant power losses and damages to PV systems.

An extensive examination of electrical faults in the DC side of photovoltaic systems, focusing on voltage and current inspections has been conducted in [27]. The study employed a simplified hybrid model of photovoltaic panels in the MATLAB environment to classify, simulate, and discuss various fault types. It emphasized the significance of considering multiple parameters when evaluating photovoltaic module performance. The research underscored that faults in a photovoltaic system can occur on both the DC and AC sides, with the DC/AC inverter serving as the interface connected to the grid. The study also highlighted the necessity of employing an internal maximum power point tracker algorithm to enhance system efficiency.

A comprehensive review of challenges and limitations associated with fault diagnosis in solar modules [15]. The study proposed a monitoring tool utilizing thermography and artificial intelligence systems to detect various types of faults in photovoltaic modules. A neural network classifier was applied to the transfer characteristics (I-V data) of faulty modules, achieving efficient fault detection with an average detection time of less than 9 seconds. The developed algorithm demonstrated 100% accuracy when tested on a predetermined fault dataset. In [28] I-V curve analysis is carried out to identify and classify the nature of faults in the PV system

The diagnostic models based on machine learning (ML) can automatically identify structural damage. However, the extraction of characteristics in these models still relies on expert intervention, introducing associated empirical risks. The emergence of deep learning (DL) has revolutionized this field, offering notable advantages through the development of end-to-end diagnostic models that autonomously learn features from collected data and subsequently identify potential damage [29]. Nevertheless, these models necessitate a sufficient number of labelled samples, posing a substantial resource burden. Transfer learning (TL) provides a potential solution by reducing the cost of data collection. It achieves this by transferring previously acquired diagnostic knowledge from one domain to another [30].

A method employing two algorithms to detect faults in photovoltaic systems has been developed in [31]. The first algorithm compared measured output power to simulations in MATLAB/Simulink, identifying faults if the difference exceeded a specified threshold. The second algorithm, based on Radial Basis Function (RBF) neural networks, successfully diagnosed faults related to bypass diodes, short-circuit and open-circuit modules, and partial shading. The method was experimentally tested, demonstrating good accuracy, and was implemented into a Field Programmable Gate Array (FPGA) using Xilinx System Generator (XSG) and Integrated Software Environment (ISE).

An analytical model using equations for relative power to detect faults under open circuit and short circuit conditions in [32]. The diagnostic algorithm, requiring temperature and irradiance sensors, as well as a power meter by string, demonstrated the potential to diagnose faults based on the irradiance level, module temperature, and the number of PV modules in the string.

A fault diagnosis method to detect and isolate eight faults occurring in a photovoltaic array has been introduced in [33]. Two algorithms were employed for fault isolation and identification, with one algorithm detecting faults with different combinations of attributes and the other using an ANN to discriminate between faults with similar signatures. Simulation results confirmed the high accuracy of the proposed technique compared to other methods.

The monitoring and control of PV arrays can be done using advanced neural network algorithms. Studies have been conducted using neural networks for real-time monitoring, considering nine input features to identify faults in PV arrays. The developed algorithm demonstrated successful detection and identification of common faults and shading conditions, showing significant improvement in accuracy compared to traditional methods [34]. Experiments using real-time data are ongoing, further validating the algorithm's effectiveness.

A Back Propagation-Particle Swarm Optimization (BP-PSO) neural network algorithm is used for forecasting fault types in PV systems. The algorithm proposed in [35] exhibited the capability to intelligently forecast fault types in real-time without additional hardware support, contributing significantly to the system's lifetime, reliability, and safety functionality. Simulation results indicated improved convergence and higher forecast accuracy compared to the back-propagation algorithm.

A detailed comparative analysis of faults in various PV interconnection schemes, including Series-Parallel (SP), Honey-Comb (HC), and Total-cross-Tied (TCT) have been researched. The study investigated in [36] how TCT could enhance power generation under open circuits and severe shading faults due to its internal connections. It also compared monocrystalline and thin-film PV materials, finding that thin-film technology achieved higher peak power than monocrystalline in all developed faults. The results suggested the possibility of enhancing power generation and compensating for power loss through optimized interconnection topologies and materials in PV systems.

2.4 Machine Learning Approach Based Fault Diagnosis

The overview of the basic principles and structures of the most commonly used Artificial Neural Network (ANN) models in the area of fault diagnosis, in addition to their research progress in this area are discussed below.

2.4.1 Multi-Layer Neural Network (MNN)

A Multi-Layer Neural Network (MNN), often referred to as a neural network or artificial neural network, is a fundamental component of machine learning and deep learning systems. Unlike simple perceptron, which consist of a single layer of interconnected nodes, MNNs comprise multiple layers of nodes, each layer contributing to the network's ability to learn complex patterns and representations from data.

The basic building blocks of an MNN are neurons, or nodes, organized into layers: an input layer, one or more hidden layers, and an output layer. Information is processed through the network by transmitting signals between these layers. Each connection between nodes is associated with a weight, and the network learns by adjusting these weights during training based on the input data and the desired output.

The hidden layers of an MNN enable it to capture intricate relationships within the data, allowing it to learn and represent features that may be difficult for traditional algorithms to discern. This ability to automatically extract hierarchical features from data makes MNNs well-suited for tasks such as image recognition, natural language processing, and complex pattern recognition.

2.4.2 Radial Basis Function (RBF) Neural Network

A Radial Basis Function (RBF) Neural Network is a type of artificial neural network that distinguishes itself by its unique architecture and training methodology. The key feature of RBF networks lies in the radial basis functions within the hidden layer. These functions are responsible for transforming the input data into a high-dimensional space. Each radial basis function neuron computes its output based on the radial distance between the input and a center associated with the neuron. The closer the input is to the center, the higher the activation of the neuron. During the training phase, RBF networks undergo a two-step process. First, the centers of the radial basis functions are selected based on the input data. Common methods for center selection include clustering algorithms like k-means. Once the centers are established, the weights connecting the hidden layer to the output layer are adjusted using linear regression or other optimization techniques.

2.4.3 Probabilistic Neural Network (PNN)

The PNN operates based on the Bayesian minimum risk criterion, allowing it to classify datasets with fewer samples without the need for weight adjustments, resulting in faster training [37].

2.4.4 Deep Neural Networks (DNN)

In comparison to traditional ANN models widely employed in PV system fault diagnosis, DNNs show greater promise as PV systems expand in scale, accompanied by increased data volume and fault complexity. This section reviews several commonly employed DNN models in this field.

2.4.5 Other Neural Networks

Apart from the frequently used neural network models in PV system fault diagnosis, alternative neural network models have been applied for this purpose. An experimental study on the Detection Artificial Neural Network (DANN) with a substantial amount of healthy data demonstrated an impressive overall training and testing accuracy of 99.8%. Considering the challenge of obtaining labelled fault data from real on-site trials, the Kernel-Based Extreme Learning Machine (KELM) [38] emerges as a valuable tool for diagnosing PV system faults. Simulation results indicate the model's high accuracy and excellent generalization performance. Another approach involves determining the open-circuit voltage through the duty cycle, combined with the Multilayer Neural Network (MNN) and Adaptive Resonance Theory 2 Neural Network (ART2 NN) for PV panel fault diagnosis. This method eliminates the need for additional power calculations in the initial estimation of solar panel faults. Proposing a tree-like hierarchical structure for PV system modelling, a Fuzzy Nonlinear Autoregressive Network with External Inputs (NARX) is employed to identify precise PV system faults through three independent operations: diagnosing potential faults, classifying faults, and pinpointing the fault source. This method demonstrates high accuracy in identifying faulty PV panels and offers remote monitoring capabilities via Wi-Fi [39].

CHAPTER THREE: METHODOLOGY

This research introduces a fault detection approach for solar modules in a solar photovoltaic (PV) plant. The method identifies open-circuited or short-circuited (fault)PV modules, open-circuited PV strings, shaded PV modules, and MPPT faults. The proposed fault detection and classification method implements a Multilayer Neural Network (MNN) model and an analytical method. Initially, a Multilayer Neural Network is employed to estimate the optimal power considering different meteorological conditions such as irradiance and temperature. The MNN model is trained using a real-time dataset of the solar power plant located at the Time Pharmaceutical Factory in Gaidakot, Nawalpur, Nepal, which is collected from SOLARMAN PRO. Subsequently, the nature of the faults is determined using analytical equations. The effectiveness and accuracy of the proposed fault identification and diagnosis algorithm for the solar PV systems is verified using Simulink.

The following figure illustrates the overall methodology of the proposed research.

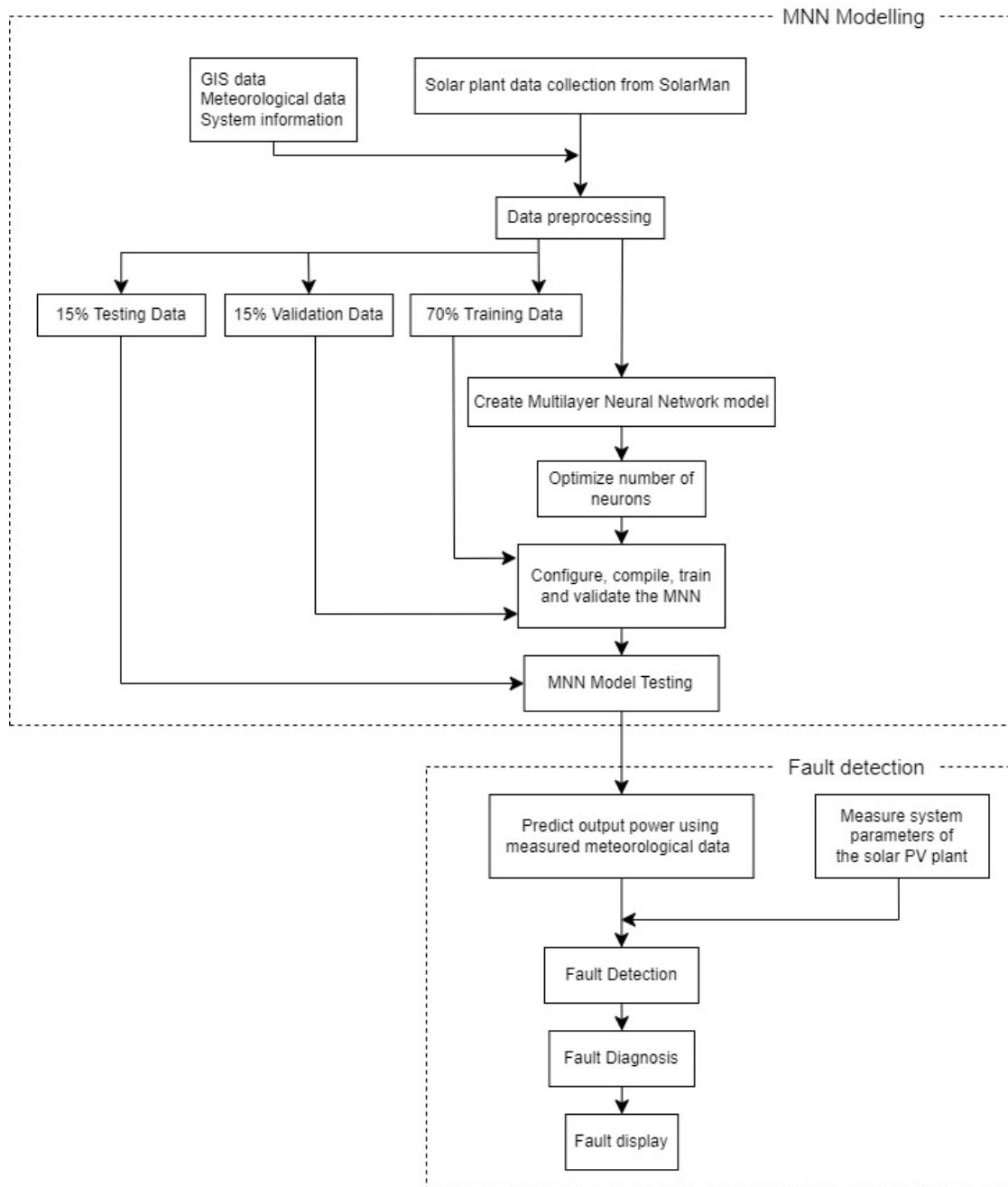


Figure 3.1: Research flowchart

3.1 System Description

A 120.25kWp solar PV plant is installed in the Time Pharmaceutical Factory in Gaindakot, Nawalpur, Nepal. This region has an interesting temperature and solar irradiance level. The plant consists of 370 (Eldora VSP.72.AAA.05) panels with monocrystalline silicon cells. The efficiency and peak power of each panel is 16.78% and 325Wp respectively.

In this grid-tied solar power plant, 20 PV strings are connected to the two grid-tied inverters named SoFar 60kW, i.e., 17 strings of 20 panels and 2 strings of 15 panels. Two number of grid-tied inverters named SoFar 60kW are installed. Each inverter has input power capability of 66kWp STC whereas the rated solar energy output of the inverter is 60kW. The Solar PV plant is installed on the roof and the gables of different buildings. Two office buildings have flat roofs; one gable has a tilt of 9° and another has a tilt of 10°. The PV plant was installed and commissioned on March 2021.



Figure 3.2: Google Earth map of solar PV plant installed in Time pharmaceutical factory

3.2 Data Collection

To prepare solar output power forecasting models, historical time series data are gathered either from ground-based stations (installed in the site or nearby area) or the data set that are based on satellite. Due to the limited availability of ground-based stations, a database with long term coverage, high accuracy and has open access, called NASA's POWER, is utilized for this project. Hourly data, including All Sky Surface Shortwave Downward Irradiance (Wh/m^2) and Temperature at 2 Meters ($^{\circ}\text{C}$) for every hour from May 1 to May 31, 2023, is collected from the POWER Data Access Viewer.

May is typically characterized by pleasantly warm weather in Nepal. The collected dataset extracted as an Excel file is subsequently processed in MATLAB. This is done by importing the necessary data as a CSV file.

Furthermore, the performance of the power plant throughout the years is monitored using the SOLARMAN PRO online portal. Through a combination of site visits and the online portal, detailed site information, energy generation data, and other technical details are collected. The relevant specification of the solar panels is summarized in the table below.

Table 3.1: Technical specifications of solar modules installed at site

Parameter	Value @ STC
Manufacturer	Vikram Solar
Model	Eldora VSP.72.AAA.05
Maximum Power, Pmax [Wp]	325 W
Maximum Voltage, Vmp [V]	37.8 V
Maximum Current, Imp [A]	8.61 A
Open circuit voltage, Voc [V]	46.2 V
Short circuit current, Isc [A]	9.13 A
Efficiency (%)	16.78%
No. of Cells	72
Temperature Coefficient of	
Isc	0.057%/°C
Voc	-0.29%/°C
Power	-0.38%/°C
Normal Operating Cell Temperature (NOCT)	-40°C ± 2°C

3.3 Data Preprocessing

Data preprocessing is crucial for examining and modifying input and output variables to reduce interference, accentuate crucial connections, and normalize the variable distribution. This ensures that the artificial neural network can effectively discern pertinent patterns. In practice, raw data collected for input and output variables is seldom directly inputted into the artificial neural network. For instance, the power

output data obtained from photovoltaic (PV) system inverters is initially in Watts (W) with 5-minute time intervals, but certain time series may contain observations. Consequently, the collected data undergoes several preprocessing steps.

3.3.1 Data cleaning

After importing the data, the data are pre-processed. The first stage involves the elimination of missing values and the exclusion of irrelevant columns. After removing the non-relevant columns, the next step involves merging the meteorological data with the solar output power data for the specified hour. Additionally, a preprocessing measure includes the exclusion of data between 6 pm and 6 am each day. As photovoltaic systems are unable to generate a substantial amount of energy during the night, resulting in computational values near zero, these hours are excluded.

3.3.2 Normalization

To finalize the data preprocessing, the time series are normalized within the range of 0 to 1, considering the varied magnitudes in each dataset. This normalization process aligns measured values with different scales, bringing the dataset to a standardized size [40]. The normalization is mathematically expressed by the equation given as follows:

$$x_{Normalized} = \frac{x - x_{min}}{x_{max} - x_{min}} \quad (1)$$

Where, x_{min} and x_{max} are the minimum and maximum values of the time series respectively.

This normalization of the data in the database served to streamline the information and diminish redundancy in relationships. It effectively eliminated unnecessary features such as duplication and the insertion or deletion of anomalies.

3.4 Multilayer Neural Network Model

An artificial neural network (ANN) is a structured system made up of numerous neuron models designed to simulate various fundamental functions of living organisms' nervous systems. Its primary purpose is to emulate multiple basic functions without the need for mathematical models, making it particularly well-suited for controlling intricate systems where nonlinear control is essential [41].

The Multilayer Neural Network (MNN) falls under the category of artificial neural networks, characterized by multiple interconnected layers of nodes or artificial neurons.

As a feedforward neural network, it processes information in a unidirectional manner—to the output layer from the input layer and through the hidden layer. MNNs find applications in various tasks, including pattern recognition, classification, and regression [42].

The structure of MNN consists of three main layers:

- i. **Input Layer:** Composed of nodes representing input features, each node corresponds to a specific feature in the dataset.
- ii. **Hidden Layers:** Located between the input and output layers, nodes in hidden layers are connected to every node in preceding and succeeding layers. The configuration of hidden layers and the number of nodes is adjustable based on the problem's complexity.
- iii. **Output Layer:** Produces the network's final result, with the number of nodes varying according to the nature of the task.

Each node in an MNN incorporates an activation function, such as the sigmoid, hyperbolic tangent (tanh), or Rectified Linear Unit (ReLU), governing its output based on the input.

The Node Output Equation with node i and output y_i in an MNN is given by:

$$y_i = f \left(\sum_{j=1}^n (w_{ij}x_j + b_i) \right) \quad (2)$$

where:

- f is the activation function,
- y_i is the node output
- x_j is the node j output in the prior layer,
- w_{ij} is the weight related with the connection between node i and j ,
- b_i is the bias term for node i , and
- n is the no. of nodes in the prior layer.

MNN training involves adjusting weights and biases to minimize the difference between forecasted and actual outputs, typically using optimization algorithms like gradient descent. The loss function quantifies the difference and aims to minimize it.

The loss function, L , measures the difference between actual and forecasted and outputs, so as to minimize:

$$L = \frac{1}{2} \left(\sum_{k=1}^n (y_k - \hat{y}_{ik})^2 \right) \quad (3)$$

where:

- N is no. of output nodes,
- \hat{y}_k is the actual output,
- y_k is the forecasted output.

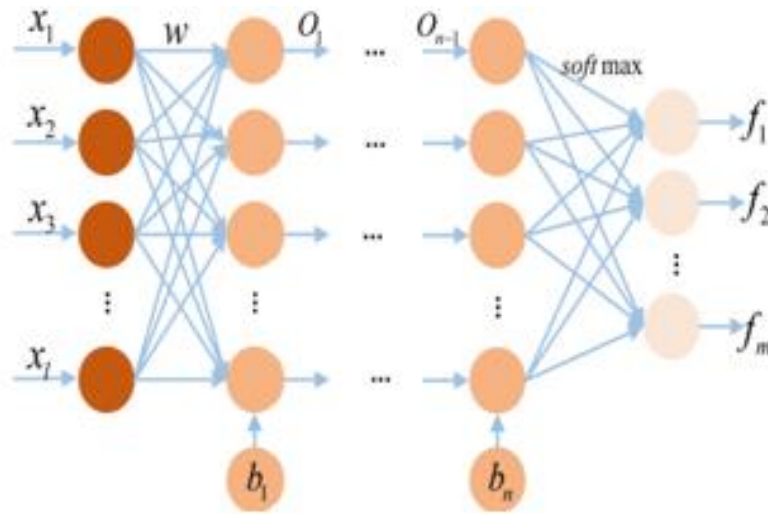


Figure 3.3: Architecture of MNN [39]

In this research, the dataset introduced for training the MNN model consists of 4468 individual data sets which belongs to the solar PV system data of every hour of May. The data hour is considered from 6 pm to 6 am. Every data set comprises 2 data points that belongs to the real time data collected from the site and are used in tbhe model to forecast the desired output. The pre-processed data is comprised of 240 input and output samples. The inputs to the proposed MNN model are the meteorological data i.e., ambient temperature and solar irradiance of the site of every hour of every day of May, 2023. This enables the model to replicate the actual system in various scenarios...

- Training set= 70%.
- Validation set= 15%.
- Testing set= 15%.
- No. of neurons in the hidden layer = 20

This approach enables the model to mimic real system behaviour across various scenarios, showcasing the versatility of MNNs in machine learning tasks. Careful hyperparameter adjustment and regularization techniques are crucial to prevent overfitting and enhance generalization.

3.5 Optimization

The Root Mean Square Error (RMSE) serves as a widely employed metric in statistical analyses and machine learning applications, assessing the accuracy of a model's forecasts by evaluating the average magnitude of errors [43]. This metric offers a comprehensive evaluation of the model's effectiveness, considering both the magnitude and direction of discrepancies.

The RMSE is calculated using the following expression:

$$RMSE = \frac{1}{N} \left(\sum_{i=1}^N (y_i - \hat{y}_i)^2 \right) \quad (4)$$

The RMSE is scaled in the same units as the target variable, allowing for straightforward interpretation within the problem's context. A lower RMSE indicates superior forecasted performance, with an RMSE of 0 signifying a perfect fit where forecasted values precisely match observed values.

The MNN is trained for different values of neurons in the hidden layer ranging from one to sixty, to ensure the accuracy of the forecast model. To analyse the neural network's performance, regression analysis is conducted between the network response and the corresponding targets. For each neuron count, the RMSE of the model is computed. The trained ANN with the lowest error for the given day is selected to forecast the progression of PV power for that specific day. The optimization of the number of neurons in the hidden layer is based on minimizing the RMSE. This ensures the high accuracy of the MNN model.

3.6 Multilayer Neural Network Training

Typically, a larger training set is employed to enable the model to learn patterns in the time series data. The testing set, constituting around 10% to 30% of the training set, is utilized to evaluate the generalization ability of the trained network. The final evaluation of the network's performance is conducted using the validation set, which

often includes the most recent observations to ensure sufficient data for both training and testing.

The Artificial Neural Network (ANN) model is trained with an optimal number of neurons in the hidden layer until the desired level of accuracy is attained. The model, using the measured PV output as a target, not only comprehends the impact of external parameters but also replicates the losses occurring in the power plant configuration with intricate details. Every aspect defining this configuration is incorporated into the machine-learning algorithm, considering variations over time such as solar radiation and temperature. The ANN maintains this temporal property, generating profiles that closely mimic the actual distribution in the case.

3.7 Fault Detection and Diagnosis

The diagram of a grid-tied PV system consists of the PV array, inverter, and the system load. The system load is connected to the PV array through an inverter, which can be either a single or two-stage type. Although not shown in the schematic, the inverter incorporates the MPPT algorithm. In the case of a stand-alone PV system, a preferred configuration involves a two-stage inverter with batteries added at the DC link to store excess power. The Multilayer Neural Network (MNN) serves as an estimator to predict the expected power based on the measured irradiance and temperature. By analyzing the difference between the estimated power (P_{pred}) and the measured power (P_{PV}), the fault detection process is initiated, and alarms are triggered based on the identified fault category.

In this proposed methodology, the process commences with the measurement of voltage and current output from the photovoltaic (PV) module, followed by power calculation. A critical aspect involves identifying Maximum Power Point Tracking (MPPT) problems, where continuous fluctuations in measured power without stabilization for an extended period indicate an MPPT problem. Once stability is achieved, an ANN-based estimator forecasts the anticipated power value using measured temperature and solar irradiance, facilitating the calculation of power differences. The detection algorithm then evaluates open circuit string and inverter issues based on power differences, conducting further checks for individual PV string currents and open circuit voltages to pinpoint faults. Non-uniform conditions are discerned when the open circuit voltage remains relatively constant, allowing differentiation between shading and

mismatch problems. Subsequently, relevant alarms are triggered. The entire process repeats at intervals of T_s , striking a balance between the update period's cost and the timing of fault detection to optimize system performance. The periodic execution of the algorithm ensures the system attains the Maximum Power Point (MPP) under prevailing irradiance conditions while minimizing power losses and potential risks associated with prolonged faults.

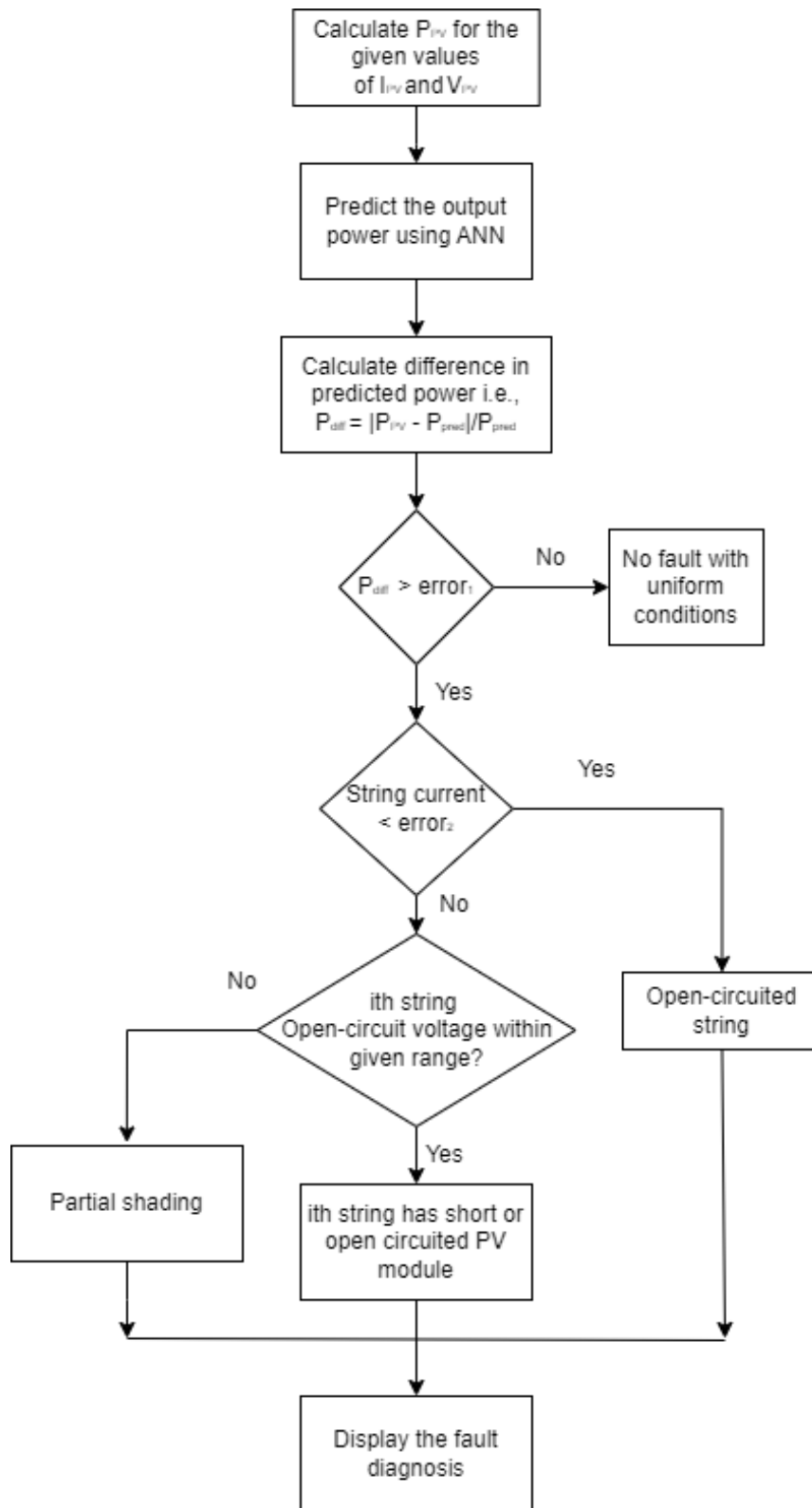


Figure 3.4: Fault detection and diagnosis model flowchart

CHAPTER FOUR: RESULTS AND DISCUSSION

4.1 Data Preprocessing

After filtering out the data, the input data are normalized from 0 to 1 in MATLAB along with the input data.

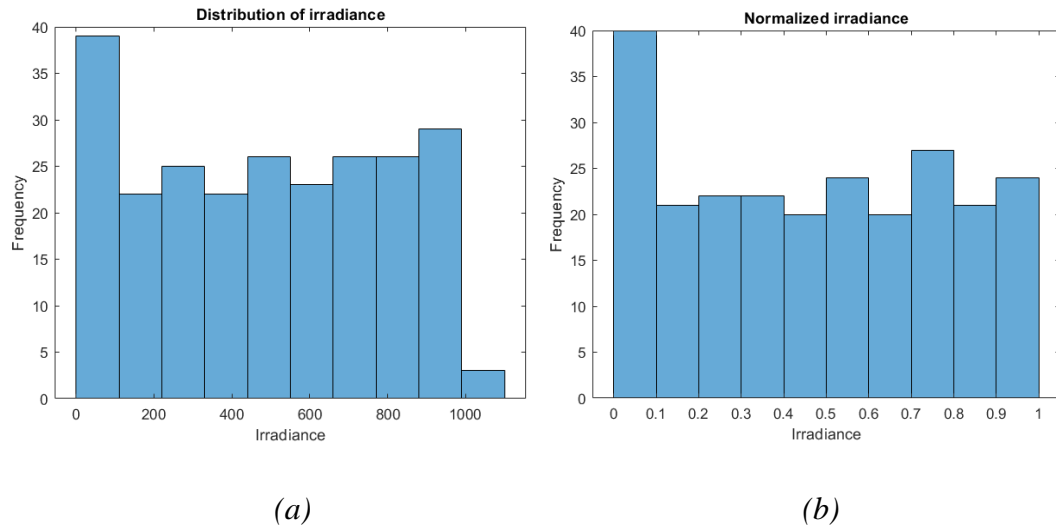


Figure 4.1: Solar irradiance normalization process (input data): (a) before normalization; (b) after normalization

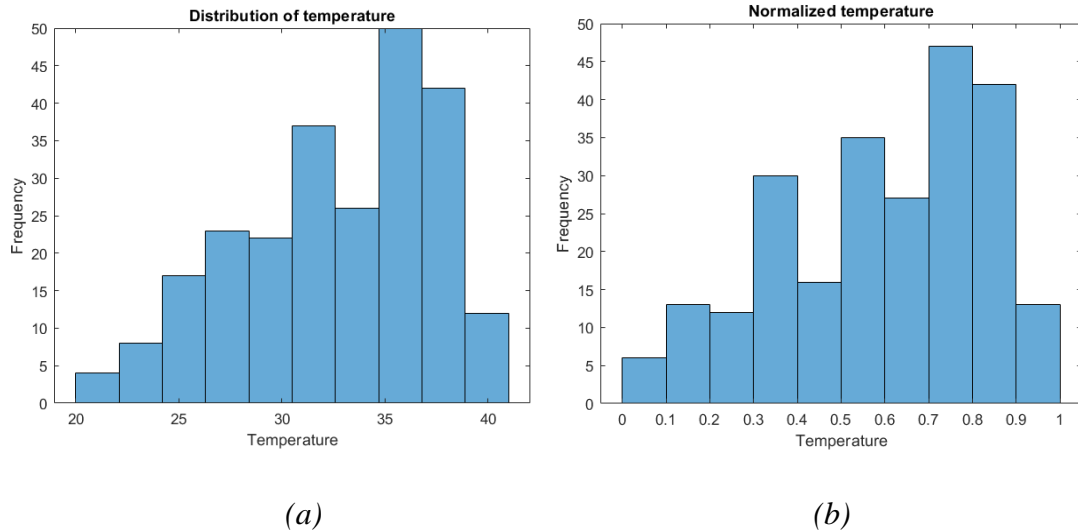


Figure 4.2: Ambient temperature normalization process (input data): (a) before normalization; (b) after normalization

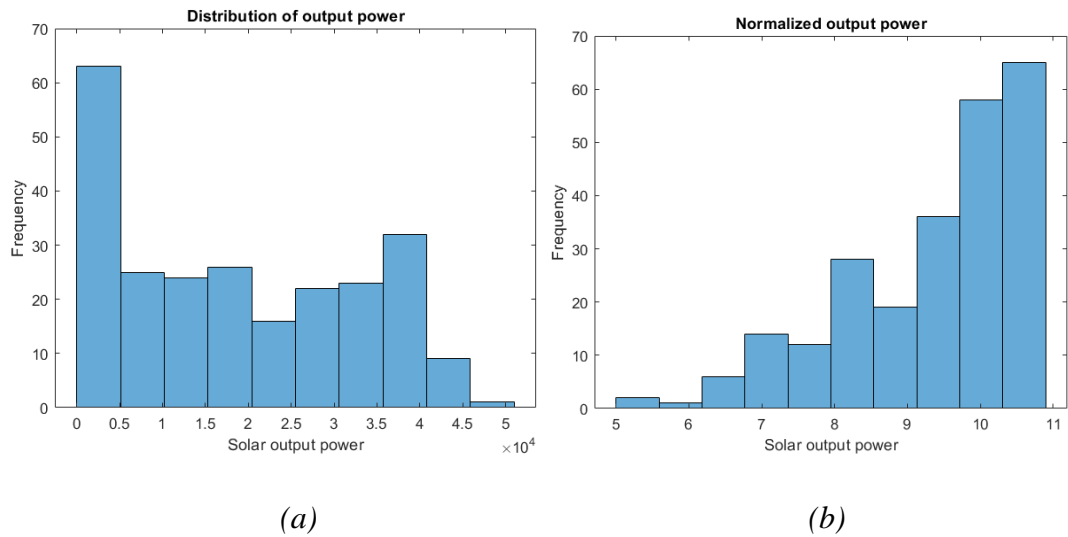


Figure 4.3: Solar PV output power normalization process (input data): (a) before normalization; (b) after normalization

Figures 4.1(a), 4.1(b), 4.2(a), 4.2(b), 4.3(a) and 4.3(b), illustrate the data both before and after normalization. The histograms created for the datasets offer a glimpse into the frequency of recorded samples and the prevailing values in each observation. These visual representations provide a distinct illustration of the measured values' spans and the gaps between successive measurements. Notably, in Figures 4.1(a), 4.2(a), and 4.3(a), it is apparent that the variables demonstrate a distribution that deviates from normal. Specifically, there are 240 irradiance samples ranging from 13.73 to 1022.89 W/m^2 , and the ambient temperature samples vary from 20.9 to 40.73°C.

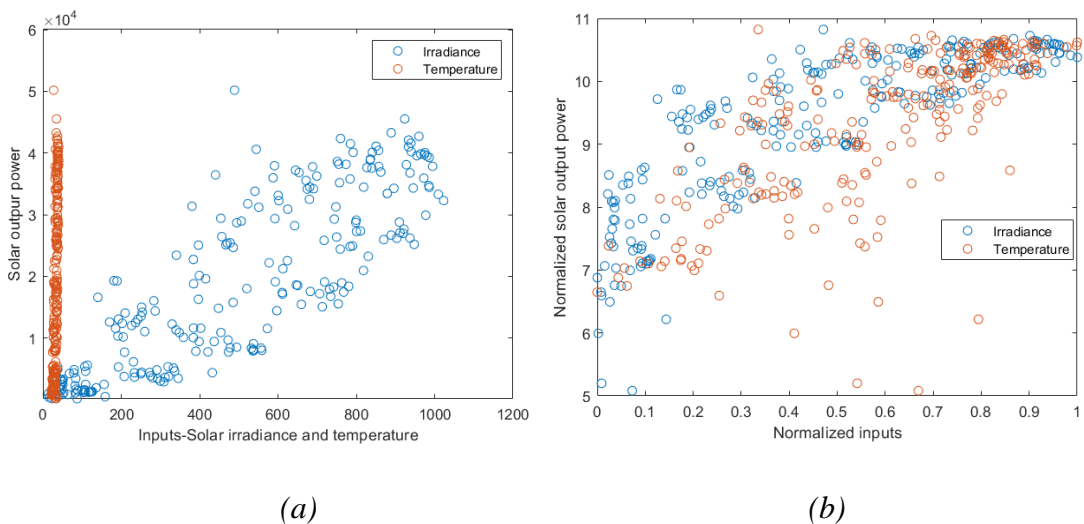


Figure 4.4: Correlation between inputs and output (a) before normalization; (b) after normalization

The Figure 4.4(a) and 4.4(b) illustrates the correlation between the inputs (irradiance and temperature) and solar output power both before and after normalization. It depicts how closely the variables move in tandem with each other. Before normalization, the inputs and outputs exhibit an uncorrelated relationship with the target, as illustrated in Figure 4.4(a). This scatter is influenced by factors like conversion losses, cable losses, inverter efficiency, and the energy management carried out by the inverter. However, post-normalization, the correlations among irradiance, temperature, and PV output power are very similar, sharing a profile resemblance, with the only distinction being in the slope.

4.2 Multilayer Neural Network-Based Solar PV System Modelling

The input to the MNN model is the pre-processed meteorological data and output solar power of the Time Pharmaceutical Factory in Gaidakot, Nepal for every hour from 6 am to 6 pm of May 1 to May 31, 2023. To configure the training parameters, the Levenberg-Marquardt algorithm is employed. The data sets are randomly divided into 70%, 15% and 15% for training, validation, and testing respectively. RMSE values are then calculated for both data sets used for training and validation to assess the model's suitability.

The ideal number of neurons is identified by minimizing both training and validation errors. In this assessment, a graph illustrating the Root Mean Squared Error (RMSE) of training versus the RMSE of validation is generated. This graph produces a series of points with coordinates denoting the errors. Employing this method enables the determination of the neuron combination that leads to the lowest error values for both training and validation sets. The index of one of these elements corresponds to the neuron combination that results in the minimum error value.

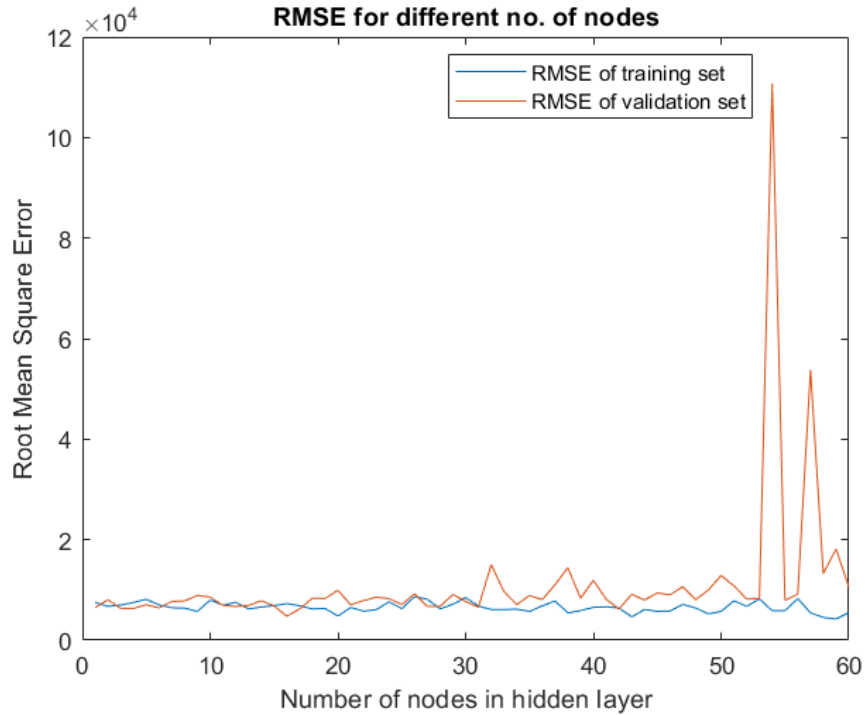


Figure 4.5: RMSE of training and validation sets for different no. of neurons

Table 4.1: MNN model result

S.N.	MNN Structure	Algorithm	Learning Rate	Train RMSE	Test RMSE
1	1 hidden layer (20 nodes)	Levenberg-Marquardt	DEFAULT VALUE	6.74	6.11

Figure 4.5 displays the plot generated following the model's training with one month of data. In this instance, the RMSE values for the validation sets were relatively large, ranging from 52 to 60 neurons. The minimum RMSE was identified for configurations with 20 and 42 neurons. Choosing a network with an excessively high number of neurons would result in undue complexity, while a network with too few neurons might oversimplify the representation of the studied phenomenon. Consequently, 20 neurons are selected for the hidden layer of the MNN model.

As depicted in Figure 4.5, when the RMSE of the training surpasses that of the validation, the MNN generates a model that is underfitting the data, indicating a lack of description of the relationship between inputs and the target. Conversely, if the RMSE of the validation exceeds that of the training, the model tends to overfit,

indicating high variance and poor interpolation of the data. The optimal scenario is when both errors are low, resulting in the algorithm providing accurate forecasts and interpolation for the given data.

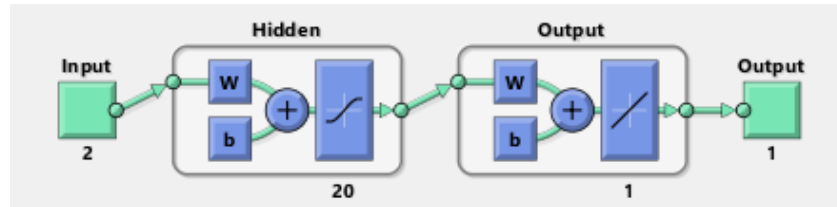


Figure 4.6: Final ANN architecture

After multiple rounds of training the model with different datasets, the optimal combination identified involved a network with one hidden layer comprising 20 neurons. This architecture, as illustrated in Figure 4.6, yields low error values for both the datasets used for training and validation of proposed MNN model.

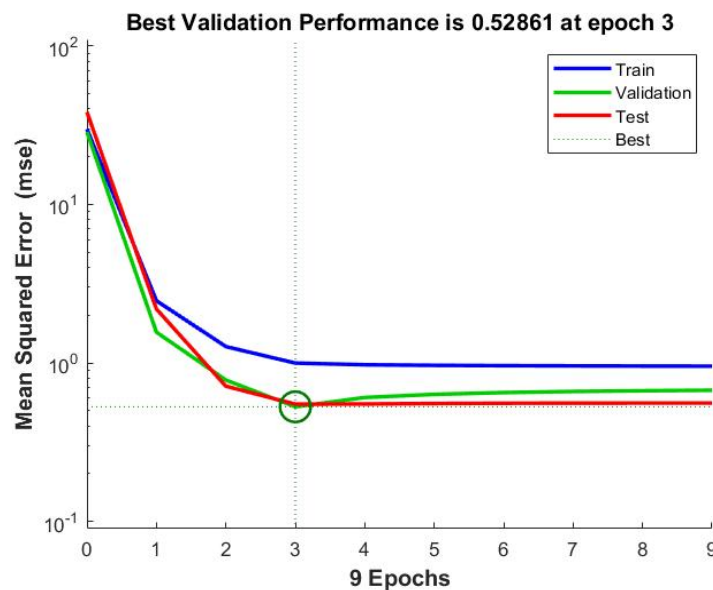


Figure 4.7: Best Performance of ANN

The trained MNN model exhibited optimal performance during different epochs across various techniques. Validation performance, indicative of consistent and accurate system operation across diverse characteristics, was assessed at different stages. Among the various models generated by the MNN with distinct feature sets, the most favorable epochs were identified at 3 epochs, yielding a value of 0.52861, as illustrated in Figure 4.7. These epochs are crucial for future use in constructing the model for forecasting solar PV output power.

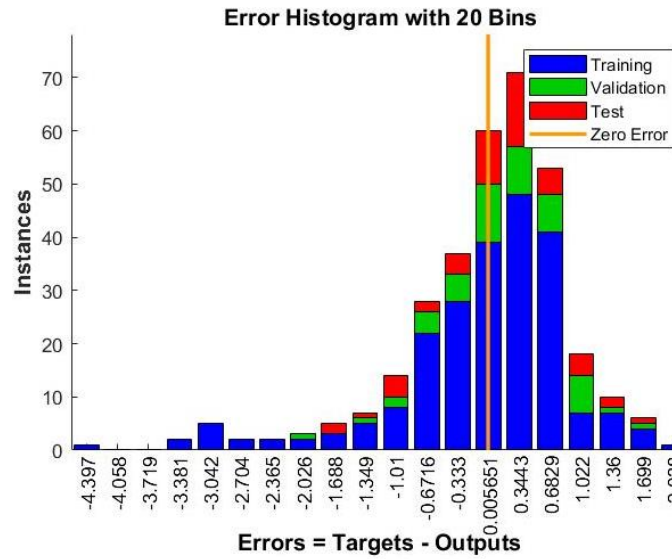


Figure 4.8: Neural network training error histogram

Figure 4.8 presents an error histogram, utilizing 20 bins to represent vertical bars in the graph, with each bin portraying the number of samples falling within a particular error range. The total error from each multi-layer neural network ranges from -4.397 to 2.038. Notably, over 80% of errors lie within +10 Watts, a benchmark suggesting that the algorithm can forecast the output accurately when the majority of errors fall within 10%.

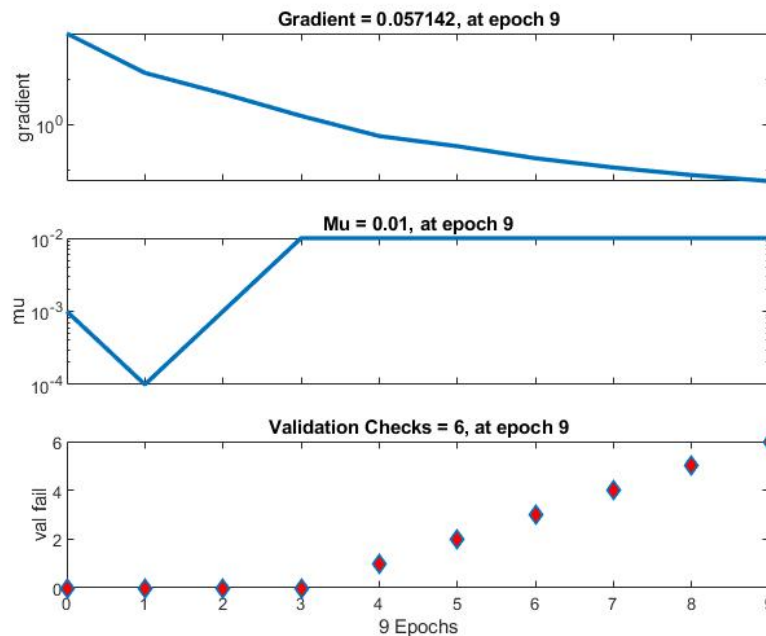


Figure 4.9: The gradient value, the Mu value, and the validation check value of the trained ANN model

At this stage, the main objective is to evaluate the accuracy and performance of the forecasting system. The training set, shown in Figure 4.9 consists of three different graphs: the gradient graph, whose gradient value epoch 9 is 0.057142. For the training, the errors were repeated 6 times and the test was stopped at epoch 9 with a gradient of 0.057142. The Mu graph has a Mu value of 0.001 at 9 epochs. The validation check graph is equal to 6 at epoch 9.

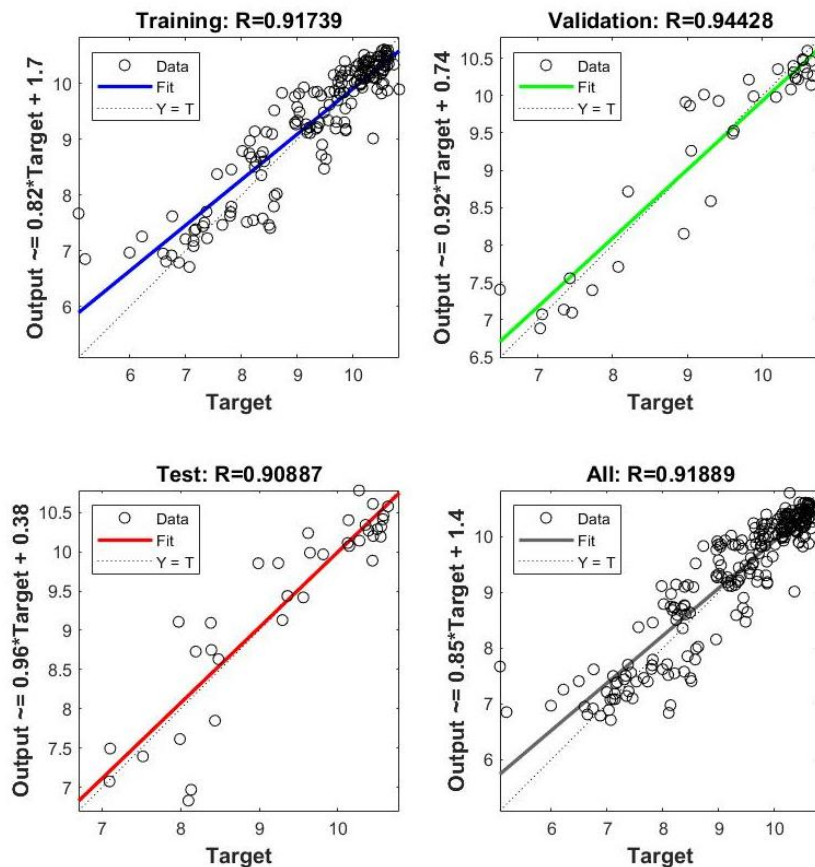


Figure 4.10: Neural network training regression

Figure 4.10 demonstrates the correlation between the initial power output and the predicted power output, employing the optimal epochs determined by the Multilayer Neural Network (MNN). The dots on the graph signify the original power output, while the blue, green, red, and brown lines represent the most accurate linearized forecast models generated by the MNN. The dashed line represents the most accurate linear relationship for the true target. It's worth noting that variations between the trend lines of the forecast model and the actual trend line were evident for all features, as depicted in Figure 4.10.

The monthly data used to train is also used to test and validate the performance of the proposed MNN model. The 240 output samples that were used to train the MNN model was compared with the forecasted results and the graph was plotted.

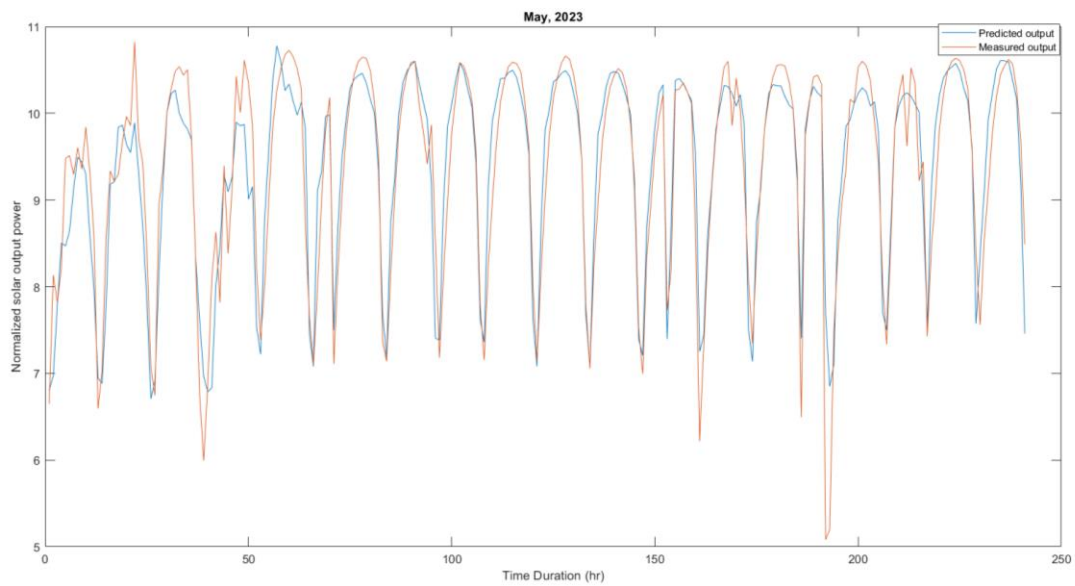


Figure 4.11: Full-month comparison between PV output forecasting using the MNN Model and measured PV output (May, 2023)

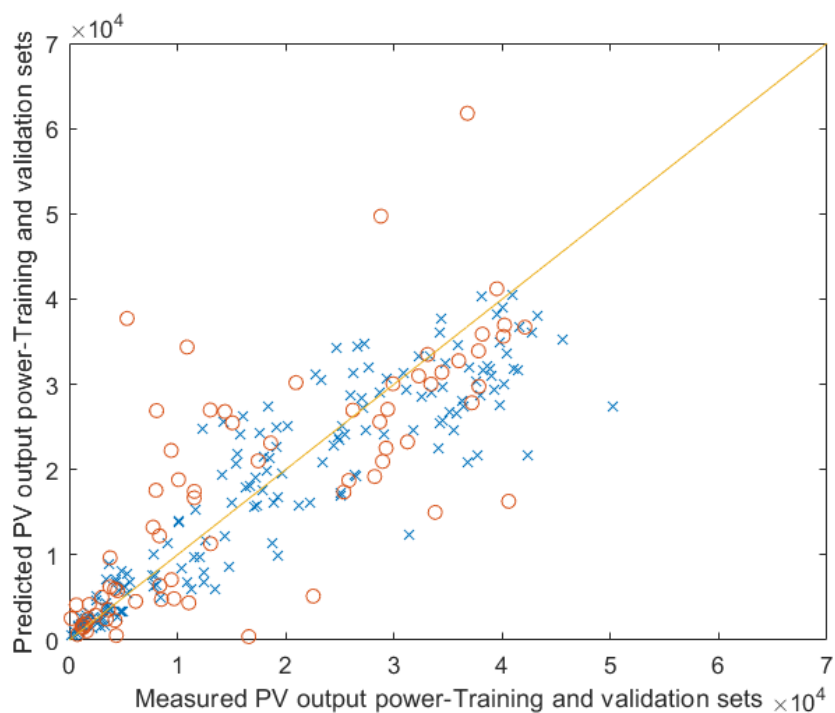


Figure 4.12: Correlation between forecasted and measured value for both training and validation sets

Throughout the training phase, as depicted in Fig. 4.11, the Multilayer Neural Network (MNN) was trained using 240 samples. The results exhibit a favourable pattern closely

resembling the actual values, indicating a robust profile for power production forecast. Both Fig. 4.11 and 4.12 illustrate the model's ability to forecast power production over an entire month, showcasing a consistent progression similar to the observed values. The obtained function effectively interpolates the target based solely on input values. Fig. 4.12 further demonstrates the correlation between forecasted and observed values for both training and validation sets, suggesting closer agreement if the error were smaller.

To validate the trained model, an independent test was conducted using a random month of observation, specifically June 2023, which was not part of the model's training/validation set.

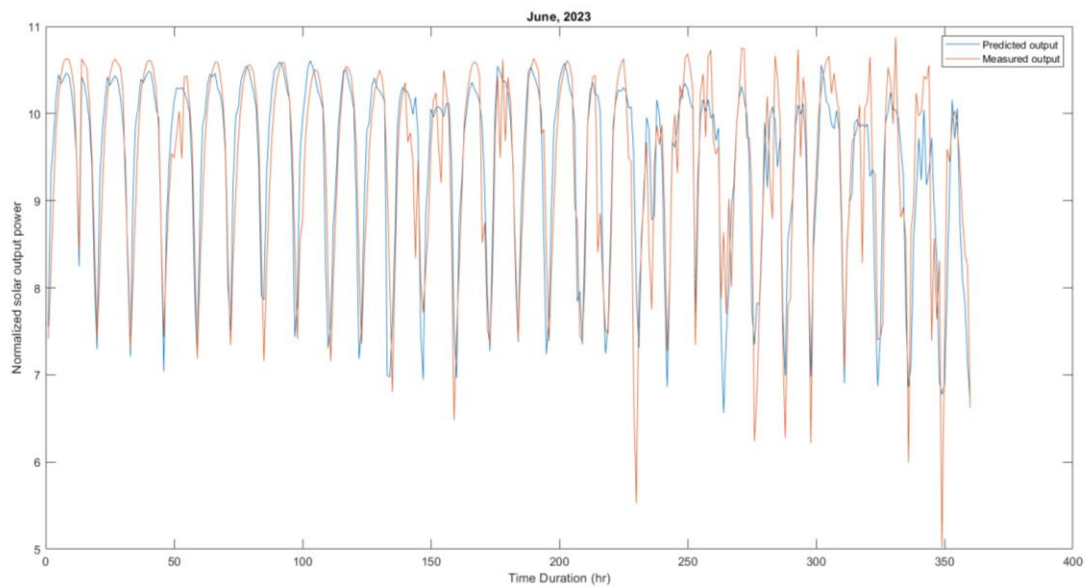


Figure 4.13: Full-month comparison between PV output forecasting using the MNN Model and measured PV output (June, 2023)

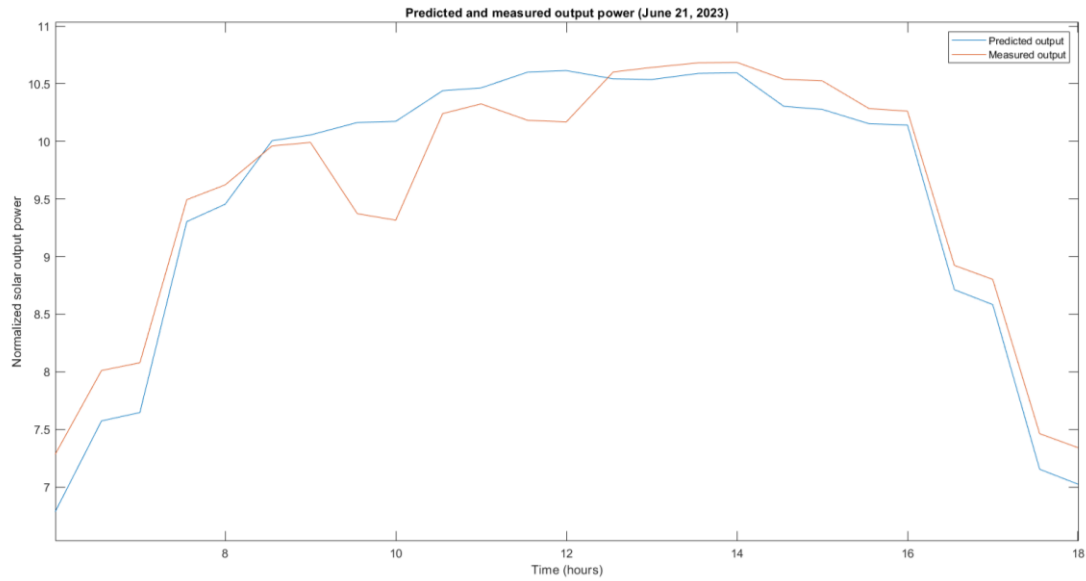


Figure 4.14: Zoom out of comparison between MNN model forecast and measured value over June 21,2023

The final results were highly promising, with the MNN providing accurate estimations of output power for the specified days, as evidenced by very low measured errors. It's noteworthy that the inputs introduced in the first case (Fig. 4.13) were entirely new to the model, not part of the training/validation set, yet the ANN successfully aligned with the measured values.

The root mean square error and percentage error for the full-month forecast are tabulated below.

Table 4.2: RMSE and accuracy of forecasted power

Month	RMSE	Accuracy (%)
May, 2023	0.48	96.1
June, 2023	0.62	94.86

4.3 Fault Detection and Diagnosis

Immediate fault detection mechanism is proposed to detect four possible faults, which are MPPT fault, open-circuited PV string, faulty (open-circuited/short-circuited) PV module and shaded solar module(s). Using the Simulink model, the fault detection and diagnosis algorithm were subjected to four different natures of faults occurring in the DC side of the PV system. Each fault results in a gradual percentual degradation in power. Each fault scenario introduced a gradual percentage degradation in power. The

algorithm relies on detecting changes in system parameters to classify and identify faults accurately.

Table 4.3: Tested fault cases

Cases	Fault Code	Fault type
Case 0	0	No fault
Case 1	1	MPPT fault
Case 2	2	Open-circuited string 1
Case 3	3	Open-circuited string 2
Case 4	4	Open-circuited/short-circuited module in string 1
Case 5	5	Open-circuited/short-circuited module in string 2
Case 6	6	Partial shading

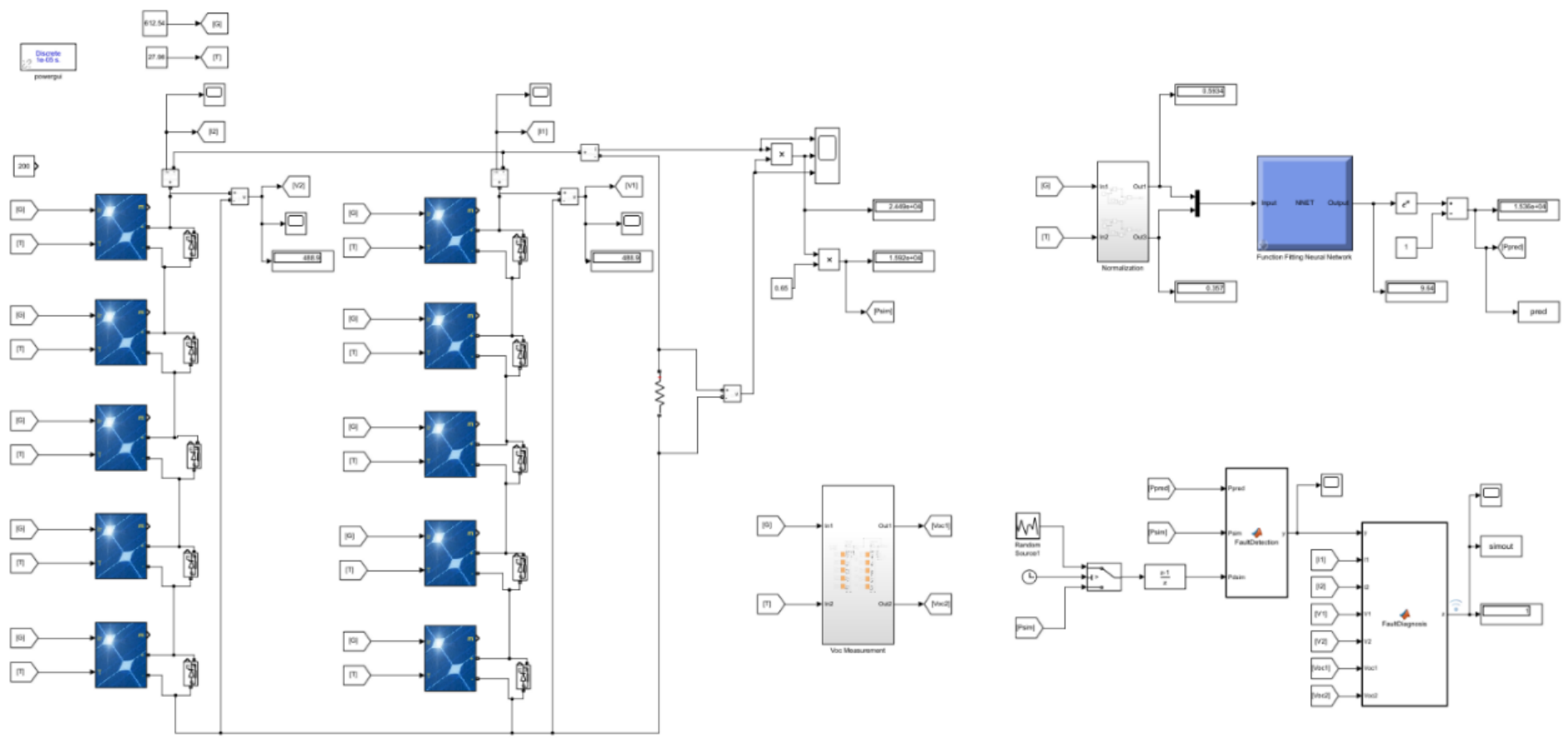


Figure 4.15: Fault detection and diagnosis model

Codes are assigned to the different types of PV modules faults as shown in the Table 4.3 such that the respective code is displayed in the output terminal. To test the proposed fault detection algorithm, a Simulink model with a capacity of 60kW is constructed. This model is designed based on the PV string configuration of a reference PV system installed in Time Pharmaceutical Factory, Gairidkot, Nawalpur, Nepal. For simplicity, the model represents the PV system connected to the 60kW inverter. It comprises a total of 180 solar modules, arranged with 20 panels in series and 9 strings in parallel. Additionally, the model incorporates a predefined threshold for the power difference between the measured and forecasted power. Moreover, specific error values are established for short-circuited, open-circuited, and MPPT faults.

The devised model is then subjected to simulations under various PV system fault scenarios, including a no-fault condition.

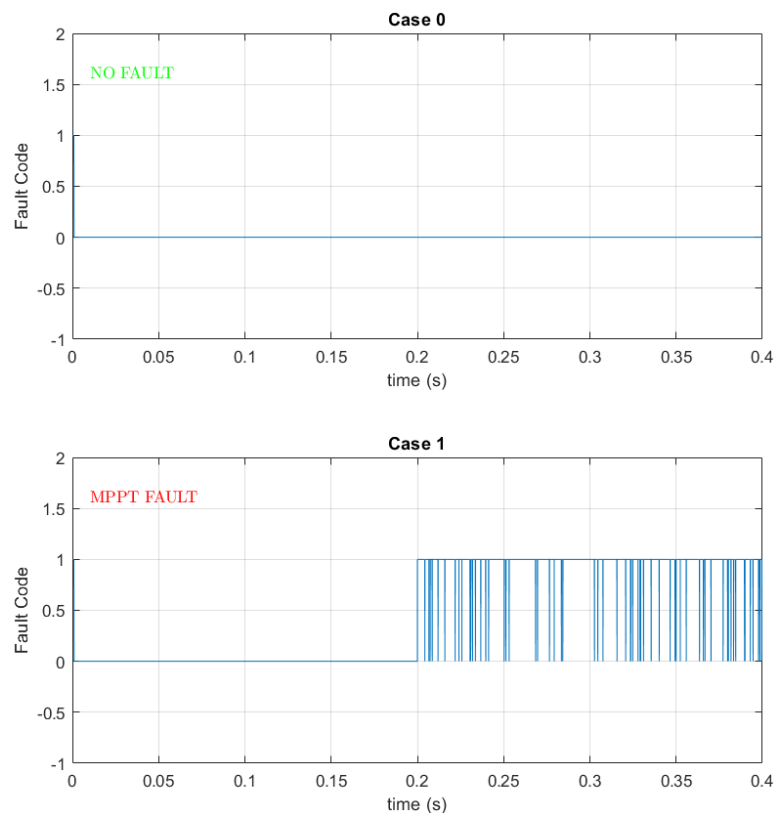


Figure 4.16: Fault indicator for normal condition and MPPT failure

For the given irradiance and temperature, the forecasted output power is used as a base to test the condition of the solar PV model undergoing different faults. For each case, the solar PV system is modelled to represent the respective fault. From the above simulation results, in Case 1, up to 0.2 sec, no fault is detected in the PV string but

during the time interval from 0.2 to 0.4, random output power is generated by the PV plant. As a result, MPPT fault is detected and respective fault code is displayed. However, when PV system is under no-fault the fault detection block doesn't send an alert signal to the fault diagnosis block, and displays no-fault condition.

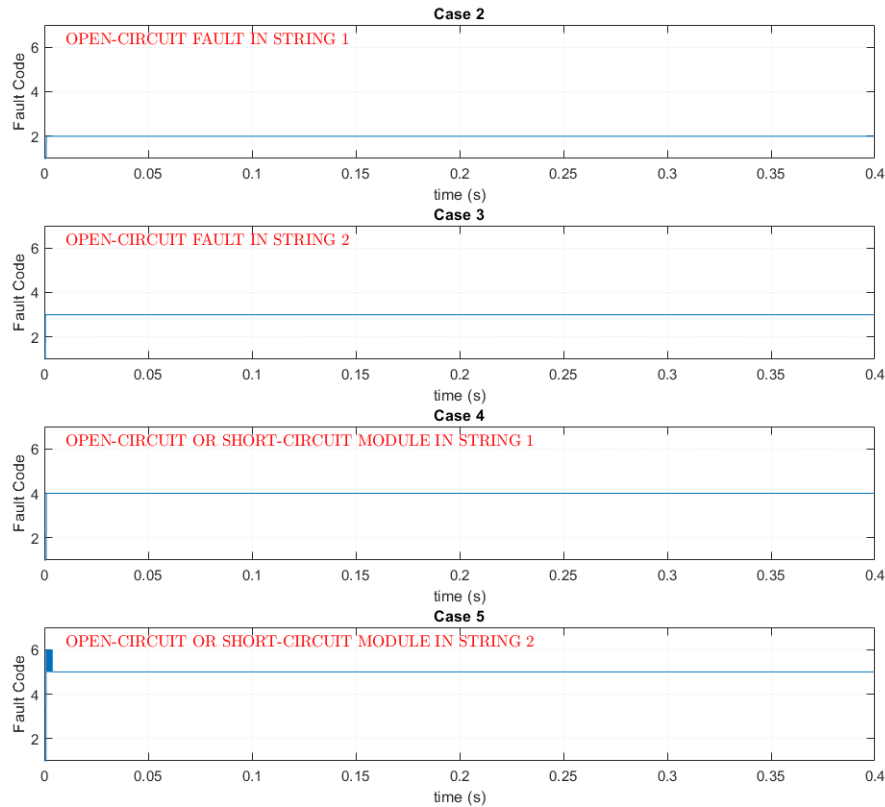


Figure 4.17: Fault indicators for open-circuited string and module fault

The fault classification algorithm is devised to pinpoint the specific string affected by a fault. In testing, identical faults are introduced simultaneously to different strings. The results demonstrate that the corresponding fault codes are accurately displayed for the respective strings experiencing faults, as illustrated in Cases 2 and 3 in the figure. Notably, when an open-circuit PV module or short-circuit PV module fault occurs, the affected strings exhibit similar string voltages. Consequently, a single fault code is displayed for both short-circuited and open-circuited PV module faults. However, for clarity regarding the string number experiencing the fault, distinct fault codes are assigned to individual strings, as depicted in the figure. Cases 4 and 5 specifically denote faulty PV modules in strings 1 and 2, respectively. This adaptable approach allows for the adjustment of fault codes for different numbers of strings, enabling the proposed system to accurately identify the precise string encountering a fault.

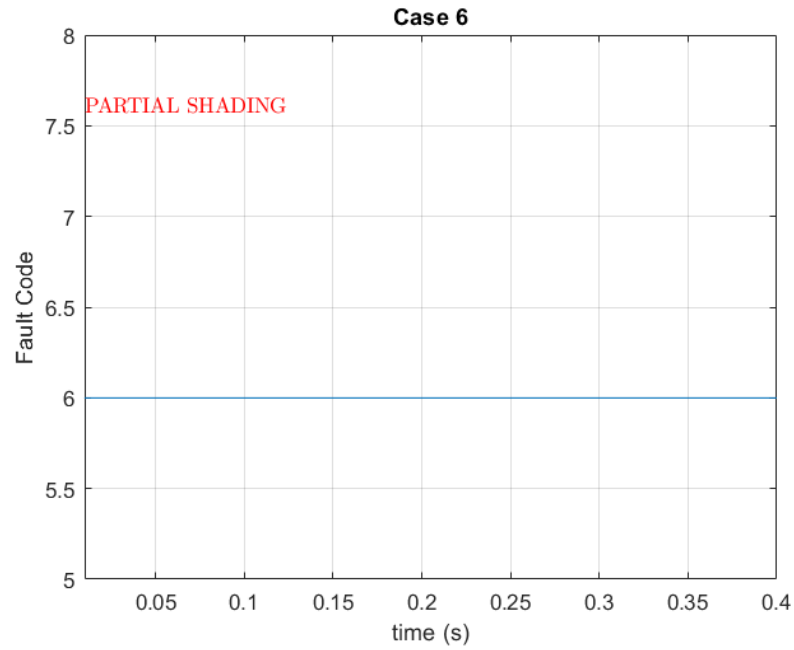


Figure 4.18: Fault indicator for MPPT fault

In instances where the fault detection model detects the fault but the fault classification algorithm encounters challenges in quantifying degradation in the system parameters corresponding to faults from Case 0 to Case 5, the system categorizes the fault under Case 6-specifically, a partial shading fault, as depicted in the figure. This fault is simulated by reducing the irradiance received by one of the PV modules to emulate a partially shaded condition.

From the results obtained, it is found that the proposed system can detect the fault and its type by using an artificial neural network. The system exhibits notable accuracy, swift fault detection, and overall efficiency.

CHAPTER FIVE: CONCLUSION AND RECOMMENDATION

5.1 Conclusion

As the renewable energy sector continues to expand, the importance of reliable fault detection mechanisms becomes crucial. The application of advanced machine learning approaches for fault detection represents a promising approach for optimizing the performance of solar energy systems. This study embarked on a fault detection mechanism of solar modules, employing Multilayer Neural Network as a powerful tool for enhancing the reliability and efficiency of solar energy systems. A large dataset from solar PV plant installed in Gaindakot, Nepal was extracted to train the algorithm after preprocessing. Total of 240 datasets were used to train, validate and test the MNN model and rigorous testing under varied meteorological conditions validated the model's effectiveness, demonstrated by its accurate output power predicting over the entire month. The accuracy of the trained model is found to be 96.1% and 94.9% for May and June respectively. The normal condition and four different fault conditions are defined for the designed PV module faults detection and classification algorithm. This study's findings underscore the potential of MNN-based fault detection systems in precisely identifying and categorizing diverse faults within solar modules. The swift detection and diagnosis ensure optimal energy generation, minimizes downtime and sustains the overall efficiency of solar PV systems.

5.2. Recommendation

A next step in this research could involve integrating the suggested mechanism into an experimental setup. While this study focuses on the occurrence and types of faults commonly found in PV strings, there is a need for more in-depth exploration of fault location and less common faults. Also, other neural network models can be studied for forecasting the solar PV output power more accurately.

REFERENCES

- [1] Y. Chouay and M. Ouassaid, “An intelligent method for fault diagnosis in photovoltaic systems.” Nov. 2017.
- [2] U. Kafle, T. Anderson, and S. P. Lohani, “The Potential for Rooftop Photovoltaic Systems in Nepal,” *Energies (Basel)*, vol. 16, no. 2, pp. 1–13, 2023, Accessed: Nov. 21, 2023. [Online]. Available: <https://ideas.repec.org/a/gam/jeners/v16y2023i2p747-d1029524.html>
- [3] “Annual Progress Report - AEPC.” Accessed: Dec. 08, 2023. [Online]. Available: <https://www.aepc.gov.np/documents/annual-progress-report-aepc>
- [4] “Energy consumption in Nepal.” Accessed: Dec. 08, 2023. [Online]. Available: <https://www.worlddata.info/asia/nepal/energy-consumption.php>
- [5] A. L. Bonkaney, S. Madougou, and R. Adamou, “Impact of Climatic Parameters on the Performance of Solar Photovoltaic (PV) Module in Niamey,” *Smart Grid and Renewable Energy*, vol. 08, no. 12, pp. 379–393, 2017, doi: 10.4236/SGRE.2017.812025.
- [6] N. Gokmen, E. Karatepe, S. Silvestre, B. Celik, and P. Ortega, “An efficient fault diagnosis method for PV systems based on operating voltage-window,” *Energy Convers Manag*, vol. 73, pp. 350–360, 2013, doi: 10.1016/J.ENCONMAN.2013.05.015.
- [7] T. Rahman *et al.*, “Investigation of Degradation of Solar Photovoltaics: A Review of Aging Factors, Impacts, and Future Directions toward Sustainable Energy Management,” *Energies 2023, Vol. 16, Page 3706*, vol. 16, no. 9, p. 3706, Apr. 2023, doi: 10.3390/EN16093706.
- [8] S. R. Madeti and S. N. Singh, “A comprehensive study on different types of faults and detection techniques for solar photovoltaic system,” *Solar Energy*, vol. 158, pp. 161–185, Dec. 2017, doi: 10.1016/J.SOLENER.2017.08.069.
- [9] A. Alcañiz, M. M. Nikam, Y. Snow, O. Isabella, and H. Ziar, “Photovoltaic system monitoring and fault detection using peer systems,” *Progress in Photovoltaics: Research and Applications*, vol. 30, no. 9, pp. 1072–1086, Sep. 2022, doi: 10.1002/PIP.3558.

- [10] C. E. Packard, J. H. Wohlgemuth, and S. R. Kurtz, “Development of a Visual Inspection Data Collection Tool for Evaluation of Fielded PV Module Condition,” Aug. 2012, doi: 10.2172/1050110.
- [11] J. A. Tsanakas, D. Chrysostomou, P. N. Botsaris, and A. Gasteratos, “Fault diagnosis of photovoltaic modules through image processing and Canny edge detection on field thermographic measurements,” *International Journal of Sustainable Energy*, vol. 34, no. 6, pp. 351–372, Jul. 2015, doi: 10.1080/14786451.2013.826223.
- [12] S. R. Madeti and S. N. Singh, “Monitoring system for photovoltaic plants: A review,” *Renewable and Sustainable Energy Reviews*, vol. 67, pp. 1180–1207, Jan. 2017, doi: 10.1016/j.rser.2016.09.088.
- [13] “Technology Roadmap - Solar Photovoltaic Energy 2014 – Analysis - IEA.” Accessed: Dec. 08, 2023. [Online]. Available: <https://www.iea.org/reports/technology-roadmap-solar-photovoltaic-energy-2014>
- [14] S. Firth, K. J. Lomas, and S. Rees, “A simple model of PV system performance and its use in fault detection,” vol. 624–635. Apr. 2010.
- [15] A. Haque, K. V. S. Bharath, M. A. Khan, I. Khan, and Z. A. Jaffery, “Fault diagnosis of Photovoltaic Modules,” *Energy Sci Eng*, vol. 7, no. 3, pp. 622–644, Mar. 2019.
- [16] D. S. Pillai and N. Rajasekar, “A comprehensive review on protection challenges and fault diagnosis in PV systems,” *Renewable and Sustainable Energy Reviews*, vol. 91, pp. 18–40, Aug. 2018, doi: 10.1016/j.rser.2018.03.082.
- [17] D. Gielen, F. Boshell, D. Saygin, M. D. Bazilian, N. Wagner, and R. Gorini, “The role of renewable energy in the global energy transformation,” *Energy Strategy Reviews*, vol. 24, pp. 38–50, Nov. 2019.
- [18] “NEPAL ELECTRICITY AUTHORITY.” Accessed: Nov. 21, 2023. [Online]. Available: https://www.nea.org.np/annual_report
- [19] “Nepal Hydropower Development Program | Fact Sheet | Nepal | Archive - U.S. Agency for International Development.” Accessed: Nov. 21, 2023. [Online].

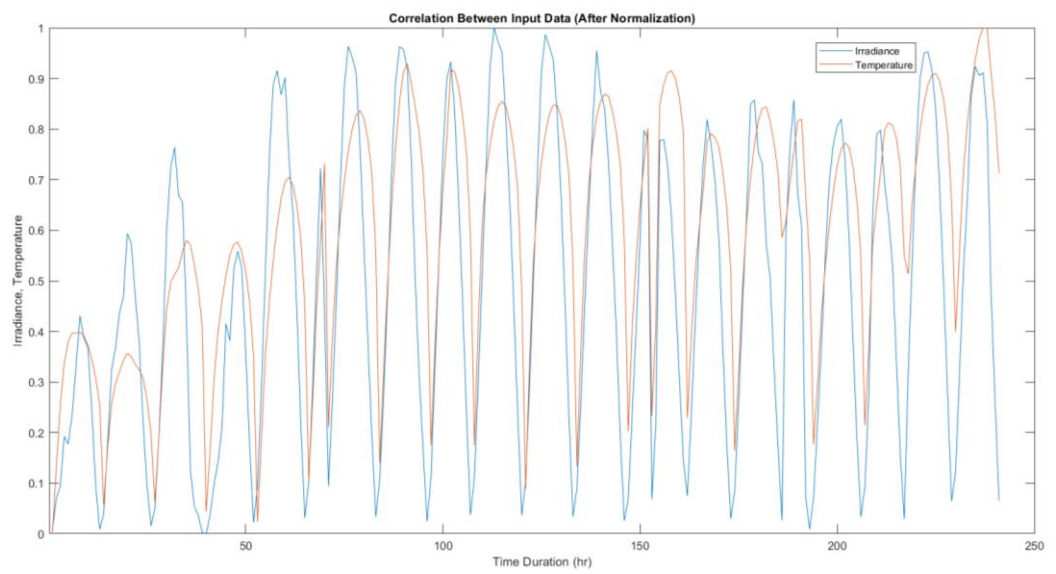
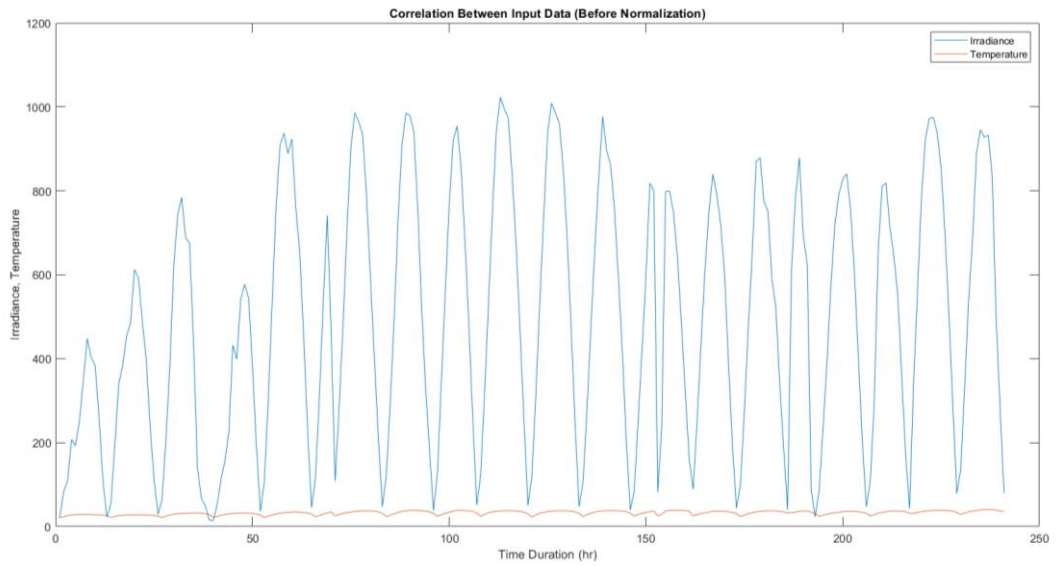
Available: <https://2017-2020.usaid.gov/nepal/fact-sheets/nepal-hydropower-development-program>

- [20] “Solar energy for household consumption: Its financial feasibility - The Himalayan Times - Nepal’s No.1 English Daily Newspaper | Nepal News, Latest Politics, Business, World, Sports, Entertainment, Travel, Life Style News.” Accessed: Dec. 09, 2023. [Online]. Available: <https://thehimalayantimes.com/opinion/solar-energy-for-household-consumption-its-financial-feasibility>
- [21] “Solar energy with pumped storage hydro in Nepal.” Accessed: Dec. 09, 2023. [Online]. Available: <https://www.hydropower.org/blog/solar-energy-with-pumped-storage-hydro-in-nepal>
- [22] L. D. Jathar *et al.*, “Comprehensive review of environmental factors influencing the performance of photovoltaic panels: Concern over emissions at various phases throughout the lifecycle,” vol. 121474. Jun. 2023.
- [23] G. M. El-Banby, N. M. Moawad, B. A. Abouzalm, W. F. Abouzaid, and E. A. Ramadan, “Photovoltaic system fault detection techniques: a review,” *Neural Comput Appl*, vol. 35, no. 35, pp. 24829–24842, Oct. 2023.
- [24] I. U. Khalil *et al.*, “Comparative Analysis of Photovoltaic Faults and Performance Evaluation of its Detection Techniques,” *IEEE Access*, vol. 8, pp. 26676–26700, 2020, doi: 10.1109/ACCESS.2020.2970531.
- [25] V. S. B. Kurukuru, A. Haque, M. A. Khan, S. Sahoo, A. Malik, and F. Blaabjerg, “A Review on Artificial Intelligence Applications for Grid-Connected Solar Photovoltaic Systems,” *Energies 2021, Vol. 14, Page 4690*, vol. 14, no. 15, p. 4690, Aug. 2021, doi: 10.3390/EN14154690.
- [26] K. Abdulmawjood, S. S. Refaat, and W. G. Morsi, “Detection and prediction of faults in photovoltaic arrays: A review,” *Proceedings - 2018 IEEE 12th International Conference on Compatibility, Power Electronics and Power Engineering, CPE-POWERENG 2018*, pp. 1–8, Jun. 2018, doi: 10.1109/CPE.2018.8372609.

- [27] M. Davarifar, A. Rabhi, and A. E. Hajjaji, "Comprehensive Modulation and Classification of Faults and Analysis Their Effect in DC Side of Photovoltaic System," *Energy Power Eng*, vol. 05, no. 04, pp. 230–236, 2013.
- [28] B. Zbib and H. Al Sheikh, "Fault Detection and Diagnosis of Photovoltaic Systems through I-V Curve Analysis," *2nd International Conference on Electrical, Communication and Computer Engineering, ICECCE 2020*, Jun. 2020, doi: 10.1109/ICECCE49384.2020.9179390.
- [29] X. Luo, D. Zhang, and X. Zhu, "Deep learning based forecasting of photovoltaic power generation by incorporating domain knowledge," *Energy*, vol. 225, p. 120240, Jun. 2021, doi: 10.1016/J.ENERGY.2021.120240.
- [30] G. Ciaburro, "Machine fault detection methods based on machine learning algorithms: A review," *Mathematical Biosciences and Engineering*, vol. 19, no. 11, pp. 11453–11490, 2022, doi: 10.3934/MBE.2022534.
- [31] W. Chine, A. Mellit, V. Lughi, A. Malek, G. Sulligoi, and A. Pavan, "A novel fault diagnosis technique for photovoltaic systems based on artificial neural networks," vol. 501–512. May 2016.
- [32] N. Gökmen, E. Karatepe, B. Celik, and S. Silvestre, "Simple diagnostic approach for determining of faulted PV modules in string based PV arrays," vol. 3364–3377. Nov. 2012.
- [33] Y. Chouay and M. Ouassaid, "An intelligent method for fault diagnosis in photovoltaic systems." Nov. 2017.
- [34] S. Rao, A. Spanias, and C. Tepedelenlioglu, "Solar Array Fault Detection using Neural Networks," *2019 IEEE International Conference on Industrial Cyber Physical Systems (ICPS)*, Nov. 2019.
- [35] G. S. Eldeghady, H. A. Kamal, and M. A. M. Hassan, "Fault diagnosis for PV system using a deep learning optimized via PSO heuristic combination technique," *Electrical Engineering*, vol. 105, no. 4, pp. 2287–2301, Mar. 2023.
- [36] S. Gul, A. Ul Haq, M. Jalal, A. Anjum, and I. U. Khalil, "A Unified Approach for Analysis of Faults in Different Configurations of PV Arrays and Its Impact on Power Grid," *Energies (Basel)*, vol. 13, no. 1, p. 156, Dec. 2019.

- [37] H. Zhu, L. Lu, J. Yao, S. Dai, and Y. Hu, "Fault diagnosis approach for photovoltaic arrays based on unsupervised sample clustering and probabilistic neural network model," *Solar Energy*, vol. 176, pp. 395–405, Dec. 2018, doi: 10.1016/J.SOLENER.2018.10.054.
- [38] F. Harrou, A. Saidi, Y. Sun, and S. Khadraoui, "Monitoring of photovoltaic systems using improved kernel-based learning schemes," *IEEE J Photovolt*, vol. 11, no. 3, pp. 806–818, May 2021, doi: 10.1109/JPHOTOV.2021.3057169.
- [39] Z. Yuan, G. Xiong, and X. Fu, "Artificial Neural Network for Fault Diagnosis of Solar Photovoltaic Systems: A Survey," *Energies 2022, Vol. 15, Page 8693*, vol. 15, no. 22, p. 8693, Nov. 2022, doi: 10.3390/EN15228693.
- [40] P. J. M. Ali, R. H. Faraj, E. Koya, P. J. M. Ali, and R. H. Faraj, "Data normalization and standardization: a technical report," *Mach Learn Tech Rep*, vol. 1, no. 1, pp. 1–6, 2014.
- [41] J. Sun and Q. Tang, "Artificial Neural Network and its Application Research Progress in Distillation," Oct. 2021, Accessed: Nov. 28, 2023. [Online]. Available: <https://arxiv.org/abs/2110.01449v1>
- [42] K. El Bouchefry and R. S. de Souza, "Learning in Big Data: Introduction to Machine Learning," *Knowledge Discovery in Big Data from Astronomy and Earth Observation: Astrogeoinformatics*, pp. 225–249, Apr. 2020, doi: 10.1016/B978-0-12-819154-5.00023-0.
- [43] E. I. Georga, D. I. Fotiadis, and S. K. Tigas, "Nonlinear Models of Glucose Concentration," *Personalized Predictive Modeling in Type 1 Diabetes*, pp. 131–151, 2018, doi: 10.1016/B978-0-12-804831-3.00006-6.

Appendix A: Correlation Between Irradiance and Temperature Before and After Normalization



Appendix B: Error Comparison Power Data Sheet

Date	Time	Normalized		Percentage Error (%)	Error/Difference
		Output Power (W)	Predicted Output Power (W)		
5/1/23	6:02	6.8064	6.6477	2.33	0.1587
5/1/23	7:03	6.9728	8.1348	16.66	-1.162
5/1/23	8:04	7.7896	7.8164	0.34	-0.0268
5/1/23	9:02	8.5032	8.2351	3.15	0.2681
5/1/23	10:03	8.4685	9.4782	11.92	-1.0097
5/1/23	11:04	8.642	9.512	10.06	-0.87
5/1/23	12:02	9.13	9.2948	1.8	-0.1648
5/1/23	13:04	9.4933	9.6038	1.16	-0.1105
5/1/23	14:00	9.4371	9.358	0.83	0.0791
5/1/23	15:02	9.2996	9.8417	5.82	-0.5421
5/1/23	16:09	8.5877	9.3103	8.41	-0.7226
5/1/23	17:06	7.984	8.5906	7.59	-0.6066
5/1/23	18:03	6.9462	6.5944	5.06	0.3518
5/2/23	6:02	6.8854	7.0309	2.11	-0.1455
5/2/23	7:04	7.7915	8.5775	10.08	-0.786
5/2/23	8:00	9.1834	9.3344	1.64	-0.151
5/2/23	9:03	9.209	9.2164	0.08	-0.0074
5/2/23	10:00	9.8399	9.2957	5.53	0.5442
5/2/23	11:01	9.8633	9.6653	2	0.198
5/2/23	12:03	9.6396	9.9637	3.36	-0.3241
5/2/23	13:05	9.5471	9.8585	3.26	-0.3114
5/2/23	14:01	9.8903	10.8234	9.43	-0.9331
5/2/23	15:03	9.3081	9.6978	4.18	-0.3897
5/2/23	16:00	8.7127	9.432	8.25	-0.7193
5/2/23	17:01	7.8515	8.4384	7.47	-0.5869
5/2/23	18:03	6.7065	7.0656	5.35	-0.3591
5/3/23	6:01	6.9133	6.7464	2.41	0.1669
5/3/23	7:02	8.1517	8.9504	9.79	-0.7987
5/3/23	8:04	9.21	9.3606	1.63	-0.1506
5/3/23	9:01	10.0197	10.0231	0.03	-0.0034
5/3/23	10:02	10.2266	10.2844	0.56	-0.0578
5/3/23	11:00	10.2677	10.4855	2.12	-0.2178
5/3/23	12:04	10.0016	10.539	5.37	-0.5374
5/3/23	13:00	9.8861	10.4385	5.58	-0.5524
5/3/23	14:02	9.8181	10.5034	6.97	-0.6853
5/3/23	15:04	9.6956	9.7166	0.21	-0.021
5/3/23	16:00	8.3514	8.3526	0.01	-0.0012
5/3/23	17:01	7.6155	6.7581	11.25	0.8574
5/3/23	18:04	6.9645	5.994	13.93	0.9705

5/4/23	6:00	6.7855	6.8783	1.36	-0.0928
5/4/23	7:02	6.8353	8.102	18.53	-1.2667
5/4/23	8:04	8.0202	8.6307	7.61	-0.6105
5/4/23	9:00	8.4542	7.8164	7.54	0.6378
5/4/23	10:01	9.29	9.3952	1.13	-0.1052
5/4/23	11:03	9.0946	8.385	7.8	0.7096
5/4/23	12:04	9.2672	9.1507	1.25	0.1165
5/4/23	13:01	9.8972	10.4282	5.36	-0.531
5/4/23	14:03	9.8555	10.0079	1.54	-0.1524
5/4/23	15:05	9.8715	10.6113	7.49	-0.7398
5/4/23	16:01	9.0102	10.3533	14.9	-1.3431
5/4/23	17:03	9.1534	9.8653	7.77	-0.7119
5/4/23	18:05	7.5444	8.2082	8.79	-0.6638
5/5/23	6:04	7.2211	7.3846	2.26	-0.1635
5/5/23	7:00	8.786	8.0133	8.79	0.7727
5/5/23	8:02	9.5738	8.996	6.03	0.5778
5/5/23	9:04	10.3909	9.8491	5.21	0.5418
5/5/23	10:01	10.779	10.2678	4.74	0.5112
5/5/23	11:02	10.5891	10.5127	0.72	0.0764
5/5/23	12:04	10.2626	10.6752	4.02	-0.4126
5/5/23	13:01	10.3363	10.7259	3.76	-0.3896
5/5/23	14:03	10.1422	10.6535	5.04	-0.5113
5/5/23	15:05	9.979	10.5141	5.36	-0.5351
5/5/23	16:01	10.1242	10.2895	1.63	-0.1653
5/5/23	17:13	9.8275	8.7227	11.24	1.1048
5/5/23	18:00	7.4609	7.6549	2.6	-0.194
5/6/23	6:04	7.0791	7.0992	0.28	-0.0201
5/6/23	7:01	9.1083	7.9763	12.42	1.132
5/6/23	8:02	9.3321	9.001	3.54	0.3311
5/6/23	9:05	9.9662	9.8131	1.53	0.1531
5/6/23	16:04	9.9804	10.1827	2.02	-0.2023
5/7/23	6:04	7.4968	7.1074	5.19	0.3894
5/7/23	7:00	8.6753	8.1722	5.79	0.5031
5/7/23	8:02	9.4802	9.0373	4.67	0.4429
5/7/23	9:03	9.9241	9.7521	1.73	0.172
5/7/23	10:02	10.2891	10.1724	1.13	0.1167
5/7/23	11:04	10.391	10.4464	0.53	-0.0554
5/7/23	12:02	10.4346	10.5924	1.51	-0.1578
5/7/23	13:04	10.461	10.6476	1.78	-0.1866
5/7/23	14:01	10.3507	10.6332	2.72	-0.2825
5/7/23	15:03	10.1615	10.4907	3.23	-0.3292
5/7/23	16:03	10.0023	10.1287	1.26	-0.1264
5/7/23	17:05	9.3363	9.5512	2.3	-0.2149
5/7/23	18:02	7.6981	7.3721	4.23	0.326
5/8/23	6:03	7.1751	7.1397	0.49	0.0354
5/8/23	7:04	8.7425	8.1377	6.91	0.6048

5/8/23	8:03	9.2621	9.0491	2.29	0.213
5/8/23	9:03	10.001	9.7926	2.08	0.2084
5/8/23	10:01	10.3539	10.207	1.41	0.1469
5/8/23	11:02	10.4863	10.4545	0.3	0.0318
5/8/23	12:03	10.5608	10.5841	0.22	-0.0233
5/8/23	13:04	10.6001	10.6019	0.01	-0.0018
5/8/23	14:00	10.3517	10.1032	2.4	0.2485
5/8/23	15:02	10.1357	9.7987	3.32	0.337
5/8/23	16:03	9.9287	9.415	5.17	0.5137
5/8/23	17:04	9.1797	9.8674	7.49	-0.6877
5/8/23	18:01	7.4048	8.5114	14.94	-1.1066
5/9/23	6:02	7.3836	7.1785	2.77	0.2051
5/9/23	7:04	8.9682	8.1464	9.16	0.8218
5/9/23	8:00	9.8527	8.9886	8.77	0.8641
5/9/23	9:02	10.1011	9.7672	3.3	0.3339
5/9/23	10:03	10.3844	10.2025	1.75	0.1819
5/9/23	13:31	10.5855	10.5853	0	0.0002
5/9/23	14:00	10.4866	10.5404	0.51	-0.0538
5/9/23	15:02	10.2673	10.3887	1.18	-0.1214
5/9/23	16:04	10.0721	10.1437	0.71	-0.0716
5/9/23	17:02	9.4184	9.5604	1.5	-0.142
5/9/23	18:04	7.6225	7.7919	2.22	-0.1694
5/10/23	6:03	7.3609	7.1554	2.79	0.2055
5/10/23	7:04	9.1373	8.2351	9.87	0.9022
5/10/23	8:01	9.9114	8.9735	9.46	0.9379
5/10/23	9:03	10.1511	9.6512	4.92	0.4999
5/10/23	10:04	10.4004	10.1338	2.56	0.2666
5/10/23	11:01	10.4044	10.3822	0.21	0.0222
5/10/23	12:04	10.4708	10.5411	0.67	-0.0703
5/10/23	13:03	10.4966	10.5899	0.88	-0.0933
5/10/23	14:00	10.4129	10.5716	1.52	-0.1587
5/10/23	15:02	10.2162	10.4784	2.56	-0.2622
5/10/23	16:04	9.9712	10.1307	1.59	-0.1595
5/10/23	17:02	9.5287	9.6165	0.92	-0.0878
5/10/23	18:03	7.6174	7.9933	4.93	-0.3759
5/11/23	6:01	7.0805	7.1397	0.83	-0.0592
5/11/23	7:03	8.7302	8.1945	6.13	0.5357
5/11/23	8:04	9.8154	9.0289	8.01	0.7865
5/11/23	9:01	10.0326	9.7262	3.05	0.3064
5/11/23	10:04	10.3629	10.1736	1.82	0.1893
5/11/23	11:02	10.3964	10.4133	0.16	-0.0169
5/11/23	12:01	10.4603	10.5782	1.12	-0.1179
5/11/23	13:03	10.4924	10.662	1.61	-0.1696
5/11/23	14:01	10.4284	10.6235	1.87	-0.1951
5/11/23	15:02	10.234	10.4482	2.09	-0.2142
5/11/23	16:04	9.9908	10.1414	1.5	-0.1506

5/11/23	17:00	9.4778	9.4751	0.02	0.0027
5/11/23	18:01	7.6879	7.8043	1.51	-0.1164
5/12/23	6:03	7.0731	7.057	0.22	0.0161
5/12/23	7:04	8.5888	8.2587	3.84	0.3301
5/12/23	8:00	9.76	8.9543	8.25	0.8057
5/12/23	9:03	9.987	9.6454	3.42	0.3416
5/12/23	10:04	10.3048	10.0541	2.43	0.2507
5/12/23	11:01	10.4603	10.306	1.47	0.1543
5/12/23	12:03	10.4806	10.4421	0.36	0.0385
5/12/23	13:05	10.464	10.5165	0.5	-0.0525
5/12/23	14:01	10.3374	10.4683	1.26	-0.1309
5/12/23	15:00	10.1831	10.2874	1.02	-0.1043
5/12/23	16:01	9.9897	9.8833	1.06	0.1064
5/12/23	17:03	9.1066	9.2283	1.33	-0.1217
5/12/23	18:05	7.397	7.5235	1.71	-0.1265
5/13/23	6:03	7.2075	6.9948	2.95	0.2127
5/13/23	7:04	8.6964	8.3431	4.06	0.3533
5/13/23	8:00	9.293	8.9556	3.63	0.3374
5/13/23	9:03	9.8453	9.5764	2.73	0.2689
5/13/23	10:00	10.2346	9.9499	2.78	0.2847
5/13/23	11:01	10.3291	10.2136	1.11	0.1155
5/14/23	6:33	7.3964	7.728	4.48	-0.3316
5/14/23	7:01	8.7164	8.2055	5.86	0.5109
5/14/23	11:46	10.3762	10.2661	1.06	0.1101
5/14/23	12:01	10.4024	10.2782	1.19	0.1242
5/14/23	13:02	10.3413	10.3498	0.08	-0.0085
5/14/23	14:03	10.2434	10.2475	0.04	-0.0041
5/14/23	15:04	10.1487	10.1142	0.33	0.0345
5/14/23	16:00	9.5144	8.585	9.76	0.9294
5/14/23	17:02	7.2524	6.2166	14.28	1.0358
5/15/23	6:03	7.4347	7.3072	1.71	0.1275
5/15/23	7:05	8.6009	8.4031	2.29	0.1978
5/15/23	8:02	9.1765	9.1528	0.25	0.0237
5/15/23	9:00	9.8169	9.7637	0.54	0.0532
5/15/23	10:02	10.0786	10.18	1	-0.1014
5/15/23	12:04	10.3215	10.5329	2.04	-0.2114
5/15/23	13:01	10.308	10.5992	2.82	-0.2912
5/15/23	14:02	10.225	9.8575	3.59	0.3675
5/15/23	15:01	10.0823	10.4076	3.22	-0.3253
5/15/23	16:01	10.2148	10.0315	1.79	0.1833
5/15/23	17:13	9.8548	9.2429	6.2	0.6119
5/15/23	18:00	7.5138	8.0929	7.7	-0.5791
5/16/23	6:04	7.1374	7.3467	2.93	-0.2093
5/16/23	7:00	8.7506	8.3919	4.09	0.3587
5/16/23	8:02	9.1146	9.1779	0.69	-0.0633
5/16/23	9:04	9.8346	9.8315	0.03	0.0031

5/16/23	10:00	10.2262	10.164	0.6	0.0622
5/16/23	11:01	10.3304	10.4169	0.83	-0.0865
5/16/23	12:03	10.3185	10.5496	2.23	-0.2311
5/16/23	13:00	10.3145	10.5616	2.39	-0.2471
5/16/23	14:01	10.191	10.5435	3.45	-0.3525
5/16/23	15:03	10.0972	10.3663	2.66	-0.2691
5/16/23	16:00	10.0519	10.0618	0.09	-0.0099
5/16/23	17:02	9.2134	9.3554	1.54	-0.142
5/16/23	18:04	7.4041	6.4938	12.29	0.9103
5/17/23	9:03	9.8204	9.7486	0.73	0.0718
5/17/23	10:00	10.1424	10.1198	0.22	0.0226
5/17/23	11:02	10.3094	10.4175	1.04	-0.1081
5/17/23	13:37	10.2361	10.44	1.99	-0.2039
5/17/23	14:04	10.1894	10.3382	1.46	-0.1488
5/17/23	17:00	7.6661	5.0814	33.71	2.5847
5/17/23	18:02	6.8486	5.1985	24.09	1.6501
5/18/23	6:05	7.0956	7.4565	5.08	-0.3609
5/18/23	7:01	8.7661	8.3805	4.39	0.3856
5/18/23	8:03	9.2628	8.9697	3.16	0.2931
5/18/23	9:01	9.8496	9.3545	5.02	0.4951
5/18/23	10:03	9.924	10.1593	2.37	-0.2353
5/18/23	11:00	10.1101	10.1239	0.13	-0.0138
5/18/23	12:01	10.2289	10.5353	2.99	-0.3064
5/18/23	13:03	10.2953	10.5997	2.95	-0.3044
5/18/23	14:04	10.2476	10.5504	2.95	-0.3028
5/18/23	15:01	10.083	10.3813	2.95	-0.2983
5/18/23	16:18	10.1335	9.91	2.2	0.2235
5/18/23	17:00	9.7806	9.4247	3.63	0.3559
5/18/23	18:01	7.7087	8.0743	4.74	-0.3656
5/19/23	6:00	7.4997	7.3337	2.21	0.166
5/19/23	7:01	8.6336	8.4828	1.74	0.1508
5/19/23	9:02	9.8371	9.8261	0.11	0.011
5/19/23	10:04	10.0871	10.2169	1.28	-0.1298
5/19/23	11:00	10.2009	10.4476	2.41	-0.2467
5/19/23	13:05	10.2369	9.6212	6.01	0.6157
5/19/23	14:51	10.1971	10.5241	3.2	-0.327
5/19/23	15:03	10.1096	10.3479	2.35	-0.2383
5/19/23	16:04	10.0131	9.2204	7.91	0.7927
5/19/23	17:01	8.8994	9.4415	6.09	-0.5421
5/19/23	18:00	7.5559	7.4271	1.7	0.1288
5/30/23	7:27	9.1267	8.4448	7.47	0.6819
5/30/23	8:01	9.8642	9.0325	8.43	0.8317
5/30/23	9:04	10.2134	9.8191	3.86	0.3943
5/30/23	10:00	10.4122	10.2274	1.77	0.1848
5/30/23	11:05	10.4925	10.4894	0.02	0.0031
5/30/23	12:01	10.5346	10.5979	0.6	-0.0633

5/30/23	13:03	10.5755	10.6356	0.56	-0.0601
5/30/23	14:05	10.4848	10.6069	1.16	-0.1221
5/30/23	15:04	10.2849	10.4982	2.07	-0.2133
5/30/23	16:06	10.1399	10.2734	1.31	-0.1335
5/30/23	17:01	9.6141	9.5737	0.42	0.0404
5/30/23	18:09	7.5741	8.3782	10.61	-0.8041
5/31/23	6:03	8.3721	7.5606	9.69	0.8115
5/31/23	7:04	9.0911	8.545	6	0.5461
5/31/23	8:05	9.927	9.1139	8.19	0.8131
5/31/23	9:04	10.2248	9.7729	4.41	0.4519
5/31/23	10:05	10.5089	10.1917	3.01	0.3172
5/31/23	11:03	10.6079	10.4435	1.54	0.1644
5/31/23	12:03	10.6049	10.548	0.53	0.0569
5/31/23	13:02	10.5917	10.6209	0.27	-0.0292
5/31/23	14:01	10.378	10.5672	1.82	-0.1892
5/31/23	16:03	10.157	10.2643	1.05	-0.1073
5/31/23	17:00	9.1884	9.6835	5.38	-0.4951
5/31/23	18:02	7.4594	8.489	13.8	-1.0296
6/1/2023	6:04	7.4151751	7.556996404	1.91	-0.141821295
6/1/2023	7:00	8.152198	9.282557256	13.86	-1.13035924
6/1/2023	8:02	9.0408561	9.677346829	7.04	-0.636490765
6/1/2023	9:03	9.8009564	10.16441201	3.7	-0.363455647
6/1/2023	10:00	10.20029	10.44743491	2.42	-0.247144511
6/1/2023	11:01	10.443513	10.34492605	0.94	0.098586639
6/1/2023	12:04	10.598159	10.40119576	1.85	0.196962811
6/1/2023	13:00	10.631543	10.46296913	1.58	0.168574151
6/1/2023	2:01	10.621596	10.44060966	1.7	0.180985946
6/1/2023	3:09	10.501802	10.26027727	2.29	0.241524666
6/1/2023	4:00	10.307986	9.977958658	3.2	0.330026868
6/1/2023	5:23	9.5030846	9.519050954	0.16	-0.015966344
6/1/2023	6:04	8.4274873	8.245452641	2.16	0.182034637
6/2/2023	1:20	10.628642	10.419822	1.96	0.208819994
6/2/2023	2:00	10.573136	10.34115307	2.19	0.231982713
6/2/2023	3:02	10.52113	10.17028814	3.33	0.350841492
6/2/2023	4:17	10.138599	9.919682177	2.15	0.218917023
6/2/2023	5:19	9.497097	9.386618484	1.16	0.110478532
6/2/2023	6:00	8.4661104	8.066013876	4.72	0.400096525
6/3/2023	6:01	7.4271441	7.295590473	1.77	0.13155366
6/3/2023	7:02	8.1777967	9.176290518	12.2	-0.998493835
6/3/2023	8:04	9.0860235	9.769378963	7.52	-0.683355425
6/3/2023	9:01	9.7660055	10.11208687	3.54	-0.346081358
6/3/2023	10:04	10.190582	10.42053247	2.25	-0.229950515
6/3/2023	11:05	10.447003	10.32558113	1.16	0.12142186
6/3/2023	12:02	10.573136	10.38197538	1.8	0.191160406
6/3/2023	1:03	10.62646	10.43528402	1.79	0.191176466
6/3/2023	2:04	10.577477	10.38584989	1.81	0.191627505

6/3/2023	3:00	10.53638	10.20983268	3.09	0.326547675
6/3/2023	4:02	10.307318	9.939807171	3.56	0.367510821
6/3/2023	5:40	9.2174153	9.461645181	2.64	-0.244229896
6/3/2023	6:11	8.3572592	8.223508072	1.6	0.133751082
6/4/2023	6:02	7.3138868	7.207843002	1.44	0.10604383
6/4/2023	7:03	8.0989467	9.071210967	12	-0.972264218
6/4/2023	8:00	8.9373498	9.881157442	10.56	-0.943807594
6/4/2023	9:02	9.7250186	10.0639135	3.48	-0.338894937
6/4/2023	10:08	10.199547	10.39357146	1.9	-0.194024525
6/4/2023	11:00	10.413643	10.35238059	0.58	0.061262366
6/4/2023	12:08	10.555057	10.42612264	1.22	0.128934602
6/4/2023	1:14	10.610562	10.48432077	1.18	0.126241519
6/4/2023	2:00	10.603635	10.46984703	1.26	0.133788138
6/4/2023	3:06	10.50345	10.28733082	2.05	0.216118976
6/4/2023	4:04	10.261197	10.05950578	1.96	0.201691185
6/4/2023	5:00	9.8163489	9.941115472	1.27	-0.124766577
6/4/2023	6:01	8.6145014	8.605428157	0.1	0.009073217
6/5/2023	6:04	7.4389716	7.036432009	5.41	0.402539583
6/5/2023	7:00	8.37586	8.733573726	4.27	-0.357713711
6/5/2023	8:02	9.0491147	9.401580971	3.89	-0.352466247
6/5/2023	9:04	9.5411538	9.859496494	3.33	-0.318342724
6/5/2023	10:00	9.4933365	10.14256561	6.83	-0.649229126
6/5/2023	11:03	9.753304	10.29710843	5.57	-0.543804438
6/5/2023	12:04	10.028401	10.28144004	2.52	-0.253039375
6/5/2023	1:00	9.4789161	10.30096538	8.67	-0.822049307
6/5/2023	2:02	10.419927	10.24454832	1.68	0.175379065
6/5/2023	3:00	10.427654	10.15436831	2.62	0.273285481
6/5/2023	4:01	10.106469	10.01086265	0.94	0.095606566
6/5/2023	5:04	9.6797813	9.363708141	3.26	0.316073202
6/5/2023	6:01	8.4252972	7.945284203	5.69	0.480012974
6/6/2023	6:03	7.1861443	7.211253385	0.34	-0.02510908
6/6/2023	7:04	8.1550749	8.729146714	7.03	-0.574071827
6/6/2023	8:01	8.9241239	9.844474569	10.31	-0.920350677
6/6/2023	9:03	9.6709879	9.986780092	3.26	-0.315792223
6/6/2023	10:04	10.094562	10.32653386	2.29	-0.231971504
6/6/2023	11:01	10.347885	10.45494565	1.03	-0.107060784
6/6/2023	12:02	10.500151	10.42270981	0.73	0.077441559
6/6/2023	1:04	10.591899	10.46034484	1.24	0.131553693
6/6/2023	2:00	10.586862	10.28609455	2.84	0.300767587
6/6/2023	3:01	10.437961	10.22543741	2.03	0.212523931
6/6/2023	4:02	10.160491	10.02323107	1.35	0.137260254
6/6/2023	5:00	9.6078405	9.544618736	0.65	0.063221775
6/6/2023	6:01	8.2403851	8.012295293	2.76	0.228089822
6/7/2023	6:02	7.3401868	7.499496241	2.17	-0.159309406
6/7/2023	7:04	8.3804567	9.199823919	9.77	-0.819367251
6/7/2023	8:00	9.0479391	9.966689469	10.15	-0.918750386

6/7/2023	9:03	9.6983681	10.06620493	3.79	-0.36783684
6/7/2023	10:00	10.089594	10.37426591	2.82	-0.2846723
6/7/2023	11:02	10.362525	10.46879365	1.02	-0.106268623
6/7/2023	12:03	10.493799	10.54351774	0.47	-0.049718929
6/7/2023	13:00	10.561033	10.51180268	0.46	0.049230786
6/7/2023	2:01	10.545105	10.37162458	1.64	0.173479993
6/7/2023	3:03	10.462274	10.23799158	2.14	0.224282845
6/7/2023	4:00	10.188704	10.06645839	1.19	0.122245698
6/7/2023	5:01	9.6971397	9.388557535	3.18	0.308582126
6/7/2023	6:03	8.3501937	7.910213472	5.26	0.439980178
6/8/2023	6:02	7.1553963	7.861543536	9.86	-0.706147234
6/8/2023	7:03	8.1833974	9.281176327	13.41	-1.097778957
6/8/2023	8:04	9.0083466	9.871958363	9.58	-0.863611783
6/8/2023	9:02	9.6804065	10.24364394	5.81	-0.563237442
6/8/2023	10:05	10.112573	10.49324479	3.76	-0.380672047
6/8/2023	11:01	10.371333	10.53223551	1.55	-0.160902905
6/8/2023	12:02	10.516265	10.5908533	0.7	-0.074588409
6/8/2023	1:04	10.588376	10.56508362	0.21	0.023292104
6/8/2023	2:01	10.580531	10.42673308	1.45	0.15379768
6/8/2023	3:00	10.377577	10.26444834	1.09	0.113128234
6/8/2023	4:02	10.139784	10.15728878	0.17	-0.017504556
6/8/2023	5:04	9.6125335	9.251418865	3.75	0.361114601
6/8/2023	6:00	8.5153916	7.437242757	12.66	1.078148813
6/9/2023	6:02	7.4151751	7.821549069	5.48	-0.406373959
6/9/2023	7:04	8.5233741	9.507807187	11.54	-0.984433136
6/9/2023	8:01	8.7704391	9.934836908	13.27	-1.164397822
6/9/2023	9:03	9.6363268	10.20558648	5.9	-0.569259679
6/9/2023	10:00	10.023091	10.51097114	4.86	-0.487879989
6/9/2023	11:01	10.280587	10.60931118	3.19	-0.328723697
6/9/2023	12:02	10.446422	10.53585089	0.85	-0.089428768
6/9/2023	1:03	10.506464	10.40936492	0.92	0.097098905
6/9/2023	2:01	10.474213	10.25487126	2.09	0.219341569
6/9/2023	3:02	10.318276	10.17007298	1.43	0.148202753
6/9/2023	4:00	10.089178	10.05430593	0.34	0.034872498
6/9/2023	5:01	9.5119993	8.274842426	13	1.237156885
6/9/2023	6:04	8.0680896	7.306858668	9.43	0.761230959
6/10/2023	6:02	7.1553963	7.590746525	6.08	-0.435350223
6/10/2023	7:04	8.1140254	8.710664747	7.35	-0.596639304
6/10/2023	8:00	8.8861326	9.192401281	3.44	-0.306268663
6/10/2023	9:03	9.6343655	9.883023909	2.58	-0.248658403
6/10/2023	10:04	10.060534	10.22244384	1.6	-0.161909808
6/10/2023	12:00	10.45077	10.49238686	0.39	-0.041616398
6/10/2023	1:01	10.544578	10.50322366	0.39	0.041354328
6/10/2023	2:03	10.512737	10.35917513	1.46	0.153561555
6/10/2023	3:00	10.423501	10.2324866	1.83	0.191014237
6/10/2023	4:01	10.12827	10.05300001	0.74	0.075269749

6/10/2023	5:03	9.5701803	8.921148917	6.78	0.649031385
6/10/2023	6:00	8.3335107	7.180713586	13.83	1.152797123
6/11/2023	6:04	7.3530819	7.533326724	2.45	-0.180244804
6/11/2023	7:00	8.274102	8.930238226	7.92	-0.656136223
6/11/2023	8:02	8.9360351	9.792184556	9.58	-0.856149459
6/11/2023	9:04	9.5874746	9.909771038	3.36	-0.322296448
6/11/2023	10:01	9.9763197	10.31046909	3.34	-0.334149379
6/11/2023	11:03	10.227417	10.40934003	1.77	-0.181922855
6/11/2023	12:05	10.380994	10.29777449	0.8	0.083219725
6/11/2023	1:01	10.501802	10.26037235	2.29	0.241429592
6/11/2023	2:02	10.412441	10.20512608	1.99	0.207315344
6/11/2023	3:00	10.098684	10.15328927	0.54	-0.054605073
6/11/2023	5:00	9.1963429	6.993215687	23.95	2.203127175
6/11/2023	6:01	8.0426995	6.97677175	13.25	1.065927747
6/12/2023	6:01	6.8035053	7.59089989	11.57	-0.787394632
6/12/2023	7:02	8.2027564	8.550149005	4.23	-0.347392624
6/12/2023	9:04	9.4857727	9.869025661	4.04	-0.383252939
6/12/2023	10:01	9.9938309	10.19473052	2.01	-0.200899643
6/12/2023	11:00	10.227779	10.30343715	0.73	-0.07565839
6/12/2023	12:04	10.358726	10.26051361	0.94	0.098212862
6/12/2023	1:00	9.6728787	10.24820953	5.94	-0.575330823
6/12/2023	2:02	9.7808113	10.14359635	3.7	-0.362785032
6/12/2023	3:04	9.4391479	9.990409656	5.84	-0.551261803
6/12/2023	4:04	8.3406946	10.1907108	22.18	-1.850016156
6/12/2023	5:00	9.453365	9.755085823	3.19	-0.301720844
6/12/2023	6:02	8.0680896	7.507532734	6.94	0.560556893
6/13/2023	6:03	7.7146775	6.944088969	9.98	0.770588505
6/13/2023	7:04	8.2244316	8.817456789	7.21	-0.593025216
6/13/2023	8:00	8.6896327	9.33932864	7.47	-0.649695892
6/13/2023	9:05	9.6165385	10.05381666	4.54	-0.437278117
6/13/2023	10:28	10.146865	9.961468129	1.82	0.185396882
6/13/2023	11:00	10.238924	10.06678417	1.68	0.172139365
6/13/2023	12:01	9.6191997	10.0802176	4.79	-0.461017891
6/13/2023	1:03	9.2064327	10.04223365	9.07	-0.8358009
6/13/2023	2:00	10.494907	9.96709049	5.02	0.527816012
6/13/2023	3:01	10.283669	10.11507905	1.63	0.168589993
6/13/2023	4:03	9.9456367	10.11445941	1.69	-0.168822748
6/13/2023	5:04	8.7013464	9.469884118	8.83	-0.768537715
6/13/2023	6:01	6.4785096	7.559564376	16.68	-1.081054734
6/14/2023	6:04	7.4271441	6.961686856	6.26	0.465457278
6/14/2023	7:00	8.2217477	8.767342133	6.63	-0.545594405
6/14/2023	8:02	9.0372957	9.208135467	1.89	-0.170839815
6/14/2023	9:03	9.8985253	9.796327865	1.03	0.102197396
6/14/2023	10:04	10.197313	10.04642877	1.47	0.150884441
6/14/2023	11:01	10.414843	10.27535914	1.33	0.139483896
6/14/2023	12:03	10.55297	10.360225	1.82	0.19274516

6/14/2023	1:04	10.594658	10.27679415	3	0.317863629
6/14/2023	2:00	10.566459	10.22858305	3.19	0.337875938
6/14/2023	3:03	10.42112	10.12991828	2.79	0.291201678
6/14/2023	4:00	8.5153916	9.849416583	15.66	-1.334025013
6/14/2023	5:02	8.7484636	9.094168753	3.95	-0.345705123
6/14/2023	6:03	7.5288693	7.92149361	5.21	-0.392624353
6/15/2023	6:03	7.3594676	7.276144567	1.13	0.083323072
6/15/2023	7:00	8.1693364	8.578393995	5	-0.409057599
6/15/2023	9:01	9.7509772	10.01426375	2.7	-0.263286552
6/15/2023	11:02	10.4312	10.54244088	1.06	-0.111241088
6/15/2023	12:03	9.4940897	10.47039737	10.28	-0.976307648
6/15/2023	13:00	10.623788	10.36735723	2.41	0.256430499
6/15/2023	2:02	9.6829032	10.36959581	7.09	-0.686692587
6/15/2023	3:04	10.417538	10.2421661	1.68	0.175371866
6/15/2023	4:00	10.142544	9.948608647	1.91	0.193935176
6/15/2023	5:02	9.3484488	9.393572141	0.48	-0.045123367
6/15/2023	6:04	8.3017698	8.109008159	2.32	0.192761604
6/16/2023	6:03	7.4091364	7.376532774	0.44	0.03260367
6/16/2023	7:04	8.3335107	8.744484663	4.93	-0.410973954
6/16/2023	8:00	9.0301366	9.44949259	4.64	-0.419356019
6/16/2023	9:03	9.733944	10.01046024	2.84	-0.27651623
6/16/2023	11:02	10.412141	10.48514339	0.7	-0.073002567
6/16/2023	12:04	10.522207	10.53331093	0.1	-0.011103454
6/16/2023	13:00	10.63275	10.4421899	1.79	0.190559767
6/16/2023	2:02	10.568518	10.36292757	1.94	0.205590572
6/16/2023	3:04	10.472516	10.25082812	2.11	0.221687928
6/16/2023	4:00	9.7648575	10.0041361	2.45	-0.239278627
6/16/2023	5:02	9.8179841	8.521938283	13.2	1.296045846
6/16/2023	6:04	8.3895871	7.237267191	13.73	1.152319876
6/17/2023	6:03	7.3846104	7.67709361	3.96	-0.292483227
6/17/2023	7:04	8.2689882	8.954844815	8.29	-0.685856605
6/17/2023	8:00	9.01323	9.88830212	9.7	-0.875072122
6/17/2023	9:03	9.748645	10.08028488	3.4	-0.331639917
6/17/2023	10:04	10.162809	10.37734834	2.11	-0.214539608
6/17/2023	11:00	10.370393	10.50293559	1.27	-0.132542953
6/17/2023	12:03	10.514367	10.57919567	0.61	-0.064829039
6/17/2023	1:04	10.60661	10.47096797	1.27	0.13564185
6/17/2023	2:00	10.564912	10.29130551	2.58	0.273606332
6/17/2023	3:03	10.410937	10.1922434	2.1	0.218694084
6/17/2023	4:04	8.9594401	9.856213644	10	-0.896773501
6/17/2023	5:01	8.7436911	7.841105563	10.32	0.902585548
6/17/2023	6:03	7.4448333	7.955341356	6.85	-0.510508083
6/18/2023	6:04	7.3907985	7.348029445	0.57	0.042769077
6/18/2023	7:00	8.1550749	8.602574593	5.48	-0.447499706
6/18/2023	9:18	9.8679122	9.864223601	0.03	0.003688586
6/18/2023	10:02	10.144903	10.25973275	1.13	-0.114829604

6/18/2023	11:04	10.414843	10.35485665	0.57	0.059986381
6/18/2023	1:04	10.437375	10.21785638	2.1	0.219518812
6/18/2023	2:01	8.4053674	10.21154843	21.48	-1.806181059
6/18/2023	3:04	8.8509475	10.01752428	13.18	-1.166576826
6/18/2023	4:00	8.0394799	8.12775683	1.09	-0.088276911
6/18/2023	6:03	7.5071411	7.245008679	3.49	0.262132401
6/19/2023	6:02	7.4736371	7.561620254	1.17	-0.087983145
6/19/2023	7:03	8.3986349	8.618841011	2.62	-0.220206155
6/19/2023	9:04	9.791494	9.886240603	0.96	-0.094746627
6/19/2023	10:00	10.206957	10.14328582	0.62	0.063671031
6/19/2023	11:02	10.441763	10.27070749	1.63	0.171055468
6/19/2023	12:04	10.563362	10.25418365	2.92	0.309178645
6/19/2023	1:00	10.629368	10.29773338	3.11	0.331634726
6/19/2023	2:02	10.26608	10.24933746	0.16	0.016742496
6/19/2023	3:04	9.4865317	10.06418308	6.08	-0.577651398
6/19/2023	4:00	9.4486484	10.07795358	6.66	-0.629305218
6/19/2023	5:02	6.7464121	9.498948741	40.8	-2.752536613
6/19/2023	6:04	5.5254529	7.953646788	43.94	-2.428193849
6/20/2023	6:03	7.9124231	7.311465385	7.59	0.600957737
6/20/2023	7:05	8.4597759	8.592681428	1.57	-0.132905508
6/20/2023	8:00	9.1685804	9.035021112	1.45	0.133559326
6/20/2023	9:01	9.6735082	9.955228055	2.91	-0.281719865
6/20/2023	10:00	8.3895871	9.812377799	16.95	-1.422790732
6/20/2023	11:00	7.7497534	8.77900428	13.28	-1.029250874
6/20/2023	12:03	9.4059894	8.822107124	6.2	0.583882265
6/20/2023	3:03	9.8601102	10.15735197	3.01	-0.297241761
6/20/2023	4:00	9.6434855	9.988613934	3.57	-0.345128438
6/20/2023	5:02	9.8704994	9.506907397	3.68	0.36359198
6/20/2023	6:00	8.8819752	8.110777063	8.68	0.771198121
6/21/2023	6:04	7.2730926	6.862651504	5.64	0.410441092
6/21/2023	7:01	8.0774471	8.053686017	0.29	0.023761132
6/21/2023	8:02	9.621191	9.669355954	0.5	-0.048165001
6/21/2023	9:00	9.9897111	9.61442351	3.75	0.375287609
6/21/2023	10:01	9.3147905	9.884024025	6.11	-0.569233552
6/21/2023	11:04	10.323874	10.12751624	1.9	0.19635787
6/21/2023	12:00	10.167811	10.27343058	1.03	-0.105619142
6/21/2023	1:02	10.640197	10.34704596	2.75	0.293151006
6/21/2023	2:03	10.68444	10.27989853	3.78	0.404541012
6/21/2023	3:00	10.52436	10.12378268	3.8	0.400577014
6/21/2023	4:01	10.261197	10.05140289	2.04	0.209794072
6/21/2023	6:02	7.3401868	7.704493219	4.96	-0.364306384
6/22/2023	8:00	9.0107913	9.292505107	3.12	-0.281713837
6/22/2023	10:00	10.245693	9.977402114	2.61	0.268291207
6/22/2023	11:00	10.457401	10.15956125	2.84	0.297840153
6/22/2023	12:03	9.7297887	10.02560959	3.04	-0.295820876
6/22/2023	1:02	10.653275	10.16245703	4.6	0.490817928

6/22/2023	2:03	10.729438	9.947708825	7.28	0.78172891
6/22/2023	3:03	9.6891179	9.995401367	3.16	-0.306283469
6/22/2023	4:00	9.5332207	9.688856505	1.63	-0.155635849
6/22/2023	5:02	9.614538	9.835095272	2.29	-0.220557261
6/22/2023	6:03	7.8713112	7.499701202	4.72	0.371610001
6/23/2023	6:01	8.6378166	6.564019599	24	2.073797035
6/23/2023	7:02	7.6966671	7.427524719	3.49	0.269142362
6/23/2023	8:03	9.021719	7.980054675	11.54	1.041664338
6/23/2023	9:01	8.0067008	8.909419979	11.27	-0.902719134
6/23/2023	10:00	9.0757799	9.195559255	1.31	-0.119779377
6/23/2023	11:02	9.847499	9.847981578	0	-0.000482535
6/23/2023	12:02	10.196194	10.17902029	0.16	0.017174185
6/23/2023	1:04	10.753019	10.31186802	4.1	0.441150616
6/23/2023	3:00	10.743998	10.16659493	5.37	0.57740322
6/23/2023	4:02	9.7244207	9.987126927	2.7	-0.262706233
6/23/2023	5:04	9.7172182	9.441990601	2.83	0.275227613
6/23/2023	6:00	9.0995205	7.738275278	14.95	1.361245259
6/24/2023	7:01	6.2363696	7.344474557	17.76	-1.108104967
6/24/2023	8:03	6.7810576	7.82740611	15.43	-1.046348484
6/24/2023	9:04	7.8442407	7.805293969	0.49	0.038946749
6/24/2023	10:03	8.7145676	8.608543856	1.21	0.106023695
6/24/2023	11:05	9.5259537	9.891735599	3.83	-0.36578189
6/24/2023	12:01	10.197313	9.151866969	10.25	1.045446245
6/24/2023	1:03	9.2399963	9.938480934	7.55	-0.698484677
6/24/2023	2:00	8.7949764	10.08022489	14.61	-1.285248454
6/24/2023	3:01	10.663382	9.920468324	6.96	0.742913428
6/24/2023	4:01	10.40611	9.384771812	9.81	1.021337807
6/24/2023	5:02	9.8858835	9.722941086	1.64	0.16294242
6/24/2023	6:04	7.4271441	7.72504672	4.01	-0.297902586
6/25/2023	6:02	6.274762	6.989814947	11.39	-0.715052926
6/25/2023	7:03	7.7710671	8.553913522	10.07	-0.782846436
6/25/2023	8:00	7.8789129	8.770203872	11.31	-0.891290959
6/25/2023	9:02	9.1892189	9.089519009	1.08	0.099699866
6/25/2023	10:05	9.9532772	9.864546549	0.89	0.088730668
6/25/2023	2:04	10.734242	10.0966257	5.94	0.637616487
6/25/2023	3:02	9.4993466	9.992297332	5.18	-0.492950765
6/25/2023	4:04	10.418136	10.11310887	2.92	0.305026989
6/25/2023	5:00	10.109729	9.625652002	4.78	0.484077064
6/25/2023	6:02	8.3262748	8.231564681	1.13	0.094710107
6/26/2023	6:01	6.2166061	6.984091671	12.34	-0.767485569
6/26/2023	7:02	8.6929935	8.459402919	2.68	0.233590613
6/26/2023	8:04	9.2780925	9.01739456	2.8	0.260697914
6/26/2023	9:00	9.9860348	9.641854599	3.44	0.344180214
6/26/2023	10:02	10.282643	10.55571033	2.65	-0.273067425
6/26/2023	11:03	10.478724	10.41774474	0.58	0.060978824
6/26/2023	12:01	10.601647	10.14140518	4.34	0.460241971

6/26/2023	1:02	10.660337	10.09115703	5.33	0.569179936
6/26/2023	2:04	10.231027	9.877847401	3.45	0.353179754
6/26/2023	3:01	10.459984	9.824228476	6.07	0.635755719
6/26/2023	4:02	10.186446	10.0376129	1.46	0.148833089
6/26/2023	5:03	10.012387	9.811790521	2	0.200596278
6/26/2023	6:04	8.7178457	8.564451274	1.75	0.153394431
6/27/2023	6:04	7.0656134	6.903594569	2.29	0.162018795
6/27/2023	7:00	8.4597759	8.419525549	0.47	0.040250372
6/27/2023	8:02	8.9399742	8.973569749	0.37	-0.033595571
6/27/2023	9:04	9.6602051	9.087713447	5.92	0.57249162
6/27/2023	10:00	9.7410274	9.883152936	1.45	-0.142125491
6/27/2023	11:02	9.8298948	9.931417637	1.03	-0.101522804
6/27/2023	12:03	10.098684	9.845916653	2.5	0.252767549
6/27/2023	1:07	8.2842518	9.874873783	19.2	-1.590621986
6/27/2023	2:04	10.070315	9.848460951	2.2	0.221853737
6/27/2023	3:00	10.139784	9.879344573	2.56	0.260439648
6/27/2023	4:03	10.649962	9.278610819	12.87	1.371351388
6/27/2023	5:04	9.3519267	9.361000867	0.09	-0.009074131
6/27/2023	6:01	9.3020988	7.890783595	15.17	1.411315202
6/28/2023	6:03	7.4030611	6.873438991	7.15	0.529622101
6/28/2023	7:00	7.4271441	7.412387691	0.19	0.014756443
6/28/2023	8:01	7.591357	9.066962251	19.43	-1.475605204
6/28/2023	9:04	9.9749241	9.892776537	0.82	0.082147565
6/28/2023	10:01	10.528115	10.01974607	4.82	0.508368894
6/28/2023	11:02	10.385018	10.24174749	1.37	0.143270745
6/28/2023	12:03	9.8818042	10.04168137	1.61	-0.159877212
6/28/2023	1:12	10.877689	10.04361538	7.66	0.834073253
6/28/2023	2:04	9.598388	9.950862523	3.67	-0.352474517
6/28/2023	3:03	8.807023	9.613084267	9.15	-0.806061312
6/28/2023	4:00	8.9187841	9.26928879	3.92	-0.350504652
6/28/2023	6:01	8.5233741	7.663093229	10.09	0.860280821
6/29/2023	6:05	5.9939614	6.860234064	14.45	-0.866272637
6/29/2023	7:01	8.6448826	7.138762883	17.42	1.50611967
6/29/2023	8:02	8.9516992	8.572308008	4.23	0.37939116
6/29/2023	9:00	10.235701	9.066078686	11.42	1.169622046
6/29/2023	10:08	9.9744585	9.719363261	2.55	0.255095206
6/29/2023	11:04	10.01909	9.23542221	7.82	0.783668226
6/29/2023	12:06	10.428246	10.04336037	3.69	0.384885298
6/29/2023	1:02	10.393631	9.18033309	11.67	1.213297672
6/29/2023	2:09	10.552186	9.346774154	11.42	1.205412226
6/29/2023	3:04	7.3907985	9.719001618	31.5	-2.328203096
6/29/2023	4:02	8.5699754	8.897262524	3.81	-0.327287147
6/29/2023	5:00	7.6357869	8.332294521	9.12	-0.69650766
6/29/2023	6:01	8.3116439	6.924400436	16.69	1.387243512
6/30/2023	6:04	5.0172798	6.775905929	35.05	-1.758626092
6/30/2023	7:01	7.2800083	6.884265357	5.43	0.395742896

6/30/2023	9:00	9.593628	7.951841609	17.11	1.641786426
6/30/2023	10:01	9.4486484	9.161017275	3.04	0.287631085
6/30/2023	11:02	9.9065329	10.15585277	2.51	-0.249319859
6/30/2023	12:00	10.035436	9.708744511	3.25	0.326691933
6/30/2023	1:02	9.8416653	10.06041324	2.22	-0.218747904
6/30/2023	2:05	9.4174358	8.759300547	6.98	0.658135292
6/30/2023	3:01	8.8204041	8.100584979	8.16	0.719819086
6/30/2023	4:03	8.3850323	7.817486978	6.76	0.567545309
6/30/2023	5:03	8.2430195	7.136107016	13.42	1.106912453
6/30/2023	6:00	6.6214057	6.690254083	1.03	-0.068848432

**Appendix C: Time Pharmaceutical Factory, Nawalpur, Nepal, Hourly
Meteorological Data Report Logsheet**

Date	Time	Irradiance (W/m²)	Temperature (°C)	DC Output Power (W)
5/1/23	6:02	21.65	20.9	770
5/1/23	7:03	83.86	23.49	3410
5/1/23	8:04	109.04	25.93	2480
5/1/23	9:02	207.52	27.58	3770
5/1/23	10:03	192.89	28.43	13070
5/1/23	11:04	250.45	28.76	13520
5/1/23	12:02	348.25	28.76	10880
5/1/23	13:04	448.11	28.8	14820
5/1/23	14:00	402.88	28.65	11590
5/1/23	15:02	384.69	28.3	18800
5/1/23	16:09	260.02	27.72	11050
5/1/23	17:06	106.81	27.01	5380
5/1/23	18:03	22.69	25.94	730
5/2/23	6:02	53.2	22.02	1130
5/2/23	7:04	192.73	24.23	5310
5/2/23	8:00	339.84	25.99	11320
5/2/23	9:03	384.06	26.79	10060
5/2/23	10:00	454.28	27.26	10890
5/2/23	11:01	485.56	27.69	15760
5/2/23	12:03	612.54	27.98	21240
5/2/23	13:05	593.23	27.85	19120
5/2/23	14:01	489.16	27.55	50180
5/2/23	15:03	396.9	27.34	16280
5/2/23	16:00	236.47	27	12480
5/2/23	17:01	109.1	26.16	4620
5/2/23	18:03	29.37	24.81	1170
5/3/23	6:01	63.95	22.13	850
5/3/23	7:02	208.27	24.69	7710
5/3/23	8:04	384.65	27.53	11620
5/3/23	9:01	624.01	29.73	22540
5/3/23	10:02	743.77	30.76	29270
5/3/23	11:00	784.19	31.06	35790
5/3/23	12:04	688.41	31.33	37760
5/3/23	13:00	674.72	31.96	34150
5/3/23	14:02	440.6	32.4	36440
5/3/23	15:04	140.24	32.22	16590
5/3/23	16:00	67.81	31.44	4240
5/3/23	17:01	50.25	30.46	860
5/3/23	18:04	15.96	29.04	400
5/4/23	6:00	13.73	21.77	970

5/4/23	7:02	51.53	24.18	3300
5/4/23	8:04	113.57	26.95	5600
5/4/23	9:00	156.34	28.81	2480
5/4/23	10:01	226.34	30.02	12030
5/4/23	11:03	432.41	31.01	4380
5/4/23	12:04	398.84	31.82	9420
5/4/23	13:01	541.19	32.24	33800
5/4/23	14:03	577.5	32.33	22200
5/4/23	15:05	544.59	31.95	40590
5/4/23	16:01	380.68	31.19	31360
5/4/23	17:03	189.29	30	19250
5/4/23	18:05	36.18	27.87	3670
5/5/23	6:04	107.23	21.37	1610
5/5/23	7:00	299.68	24.57	3020
5/5/23	8:02	536.22	27.86	8070
5/5/23	9:04	763.02	29.96	18940
5/5/23	10:01	909.95	31.6	28790
5/5/23	11:02	937.15	32.98	36780
5/5/23	12:04	889.04	34.04	43270
5/5/23	13:01	923.64	34.7	45520
5/5/23	14:03	759.88	34.88	42340
5/5/23	15:05	653.96	34.55	36830
5/5/23	16:01	454.12	33.76	29420
5/5/23	17:13	231.18	32.45	6140
5/5/23	18:00	45.09	29.87	2110
5/6/23	6:04	116.99	23.01	1210
5/6/23	7:01	308.87	26.19	2910
5/6/23	8:02	537.53	29.87	8110
5/6/23	9:05	742.09	32.37	18270
5/6/23	16:04	456.6	35.4	26440
5/7/23	6:04	108.77	25.08	1220
5/7/23	7:00	280.02	28.55	3540
5/7/23	8:02	477.95	31.4	8410
5/7/23	9:03	706.52	33.29	17190
5/7/23	10:02	903.2	34.71	26170
5/7/23	11:04	986.15	35.87	34420
5/7/23	12:02	964.37	36.75	39830
5/7/23	13:04	933.41	37.29	42090
5/7/23	14:01	784.93	37.49	41490
5/7/23	15:03	587.48	37.16	35980
5/7/23	16:03	397.11	36.36	25050
5/7/23	17:05	209.88	35.04	14060
5/7/23	18:02	47.59	31.96	1590
5/8/23	6:03	121.72	23.69	1260
5/8/23	7:04	292.62	27.34	3420
5/8/23	8:03	494.67	30.7	8510

5/8/23	9:03	731.7	33.76	17900
5/8/23	10:01	911.52	36.01	27090
5/8/23	11:02	984.93	37.79	34700
5/8/23	12:03	980.09	39	39500
5/8/23	13:04	940.3	39.33	40210
5/8/23	14:00	759.01	38.56	24420
5/8/23	15:02	520.5	37.62	18010
5/8/23	16:03	329.75	36.62	12270
5/8/23	17:04	181.33	35.05	19290
5/8/23	18:01	38.23	32.01	4970
5/9/23	6:02	126.23	24.37	1310
5/9/23	7:04	345.47	28.21	3450
5/9/23	8:00	558.83	31.69	8010
5/9/23	9:02	767.65	34.39	17450
5/9/23	10:03	919.96	36.34	26970
5/9/23	13:31	954.69	39.09	39550
5/9/23	14:00	857.32	39	37810
5/9/23	15:02	680.25	38.39	32490
5/9/23	16:04	478.09	37.3	25430
5/9/23	17:02	253.67	35.81	14190
5/9/23	18:04	51.13	32.62	2420
5/10/23	6:03	123.97	24.35	1280
5/10/23	7:04	321.06	29.18	3770
5/10/23	8:01	536.91	33.05	7890
5/10/23	9:03	753.94	35.03	15540
5/10/23	10:04	947.8	36.19	25180
5/10/23	11:01	1022.89	37.07	32280
5/10/23	12:04	994.82	37.65	37840
5/10/23	13:03	973.93	37.85	39730
5/10/23	14:00	836.06	37.65	39010
5/10/23	15:02	671.55	36.99	35540
5/10/23	16:04	467.1	35.92	25100
5/10/23	17:02	252.02	34.37	15010
5/10/23	18:03	50.42	30.43	2960
5/11/23	6:01	118.05	22.67	1260
5/11/23	7:03	311.95	27.69	3620
5/11/23	8:04	532.12	31.7	8340
5/11/23	9:01	734.77	34.04	16750
5/11/23	10:04	936.83	35.47	26200
5/11/23	11:02	1009.28	36.57	33300
5/11/23	12:01	985.86	37.34	39270
5/11/23	13:03	959.77	37.7	42700
5/11/23	14:01	850.32	37.69	41090
5/11/23	15:02	681.23	37.21	34480
5/11/23	16:04	470.52	36.31	25370
5/11/23	17:00	242.33	34.92	13030

5/11/23	18:01	47.71	31.48	2450
5/12/23	6:03	105.04	23.55	1160
5/12/23	7:04	274.92	28.21	3860
5/12/23	8:00	473.88	32.01	7740
5/12/23	9:03	659.72	34.55	15450
5/12/23	10:04	830.54	36.15	23250
5/12/23	11:01	977.3	37.26	29910
5/12/23	12:03	896.02	37.85	34270
5/12/23	13:05	862.45	38.13	36920
5/12/23	14:01	757.16	38.05	35180
5/12/23	15:00	592.29	37.46	29360
5/12/23	16:01	415.51	36.62	19600
5/12/23	17:03	204.76	35.35	10180
5/12/23	18:05	39.75	32.48	1850
5/13/23	6:03	82.92	24.91	1090
5/13/23	7:04	249.95	28.9	4200
5/13/23	8:00	421.24	31.62	7750
5/13/23	9:03	597.14	33.75	14420
5/13/23	10:00	818.31	35.44	20950
5/13/23	11:01	800.37	36.78	27270
5/14/23	6:33	82.14	25.51	2270
5/14/23	7:01	233.75	29.05	3660
5/14/23	11:46	798.56	37.71	28740
5/14/23	12:01	799.62	38.5	29090
5/14/23	13:02	747.89	38.97	31250
5/14/23	14:03	642.61	39.05	28210
5/14/23	15:04	485.88	38.73	24690
5/14/23	16:00	319.53	37.95	5350
5/14/23	17:02	158.79	36.65	500
5/15/23	6:03	88.98	25.43	1490
5/15/23	7:05	251.91	28.62	4460
5/15/23	8:02	437.2	31.19	9440
5/15/23	9:00	610.93	32.86	17390
5/15/23	10:02	749.72	34.33	26370
5/15/23	12:04	839.55	36.29	37530
5/15/23	13:01	792.04	36.58	40100
5/15/23	14:02	718.92	36.42	19100
5/15/23	15:01	600.61	36.06	33110
5/15/23	16:01	384.05	35.06	22730
5/15/23	17:13	191.42	33.64	10330
5/15/23	18:00	44.03	31.2	3270
5/16/23	6:04	98.71	24.15	1550
5/16/23	7:00	272.23	27.19	4410
5/16/23	8:02	472.7	30.58	9680
5/16/23	9:04	646.7	33.1	18610
5/16/23	10:00	869.93	34.82	25950

5/16/23	11:01	879.03	36.13	33420
5/16/23	12:03	773.83	37.09	38160
5/16/23	13:00	751.48	37.58	38620
5/16/23	14:01	591.21	37.63	37930
5/16/23	15:03	523.09	37.07	31770
5/16/23	16:00	340.66	36.19	23430
5/16/23	17:02	185.55	35.05	11560
5/16/23	18:04	40.34	32.51	660
5/17/23	9:03	611.71	33.14	17130
5/17/23	10:00	783.85	34.69	24830
5/17/23	11:02	879.26	35.87	33440
5/17/23	13:37	690.83	37.09	34200
5/17/23	14:04	625.06	37.14	30890
5/17/23	17:00	87.32	34.17	160
5/17/23	18:02	22.98	31.64	180
5/18/23	6:05	84.9	24.4	1730
5/18/23	7:01	233.41	26.69	4360
5/18/23	8:03	390.4	29.48	7860
5/18/23	9:01	572.8	31.43	11550
5/18/23	10:03	717.77	32.99	25830
5/18/23	11:00	790.45	34.3	24930
5/18/23	12:01	827	35.33	37620
5/18/23	13:03	840.88	35.98	40120
5/18/23	14:04	755.29	36.22	38190
5/18/23	15:01	602.19	36.05	32250
5/18/23	16:18	399.22	35.28	20130
5/18/23	17:00	202.81	33.97	12390
5/18/23	18:01	47.76	31.72	3210
5/19/23	6:00	106.31	25.15	1530
5/19/23	7:01	290.8	28.08	4830
5/19/23	9:02	650.26	32.29	18510
5/19/23	10:04	810.59	33.74	27360
5/19/23	11:00	818.71	35.08	34460
5/19/23	13:05	713.35	36.72	15080
5/19/23	14:51	645.02	37.01	37200
5/19/23	15:03	551.06	36.9	31190
5/19/23	16:04	358.7	36.41	10100
5/19/23	17:01	170.43	35.26	12600
5/19/23	18:00	43.17	31.76	1680
5/30/23	7:27	336.3	31.08	4650
5/30/23	8:01	556.76	33.87	8370
5/30/23	9:04	780.46	35.48	18380
5/30/23	10:00	921.6	36.72	27650
5/30/23	11:05	972.38	37.77	35930
5/30/23	12:01	975.31	38.48	40050
5/30/23	13:03	939.37	38.88	41590

5/30/23	14:05	856.82	38.94	40410
5/30/23	15:04	699.06	38.62	36250
5/30/23	16:06	506.3	37.9	28950
5/30/23	17:01	286.62	36.62	14380
5/30/23	18:09	78.93	33.89	4350
5/31/23	6:03	135.95	28.82	1920
5/31/23	7:04	333.23	31.96	5140
5/31/23	8:05	537.62	35.1	9080
5/31/23	9:04	682.6	36.99	17550
5/31/23	10:05	888.96	38.4	26680
5/31/23	11:03	945.19	39.5	34320
5/31/23	12:03	927.78	40.3	38100
5/31/23	13:02	933.08	40.73	40980
5/31/23	14:01	835.29	40.7	38840
5/31/23	16:03	494.78	38.98	28690
5/31/23	17:00	283.1	37.39	16050
5/31/23	18:02	79.95	35.04	4860
6/1/2023	6:04	151.83	26.58	1660
6/1/2023	7:00	362.65	29.8	3470
6/1/2023	8:02	578.56	32.85	8440
6/1/2023	9:03	778.26	35.08	18050
6/1/2023	10:00	919.71	36.72	26910
6/1/2023	11:01	983.56	37.99	34320
6/1/2023	12:04	978.14	38.94	40060
6/1/2023	13:00	954.46	39.55	41420
6/1/2023	2:01	855.31	39.66	41010
6/1/2023	3:09	707.11	39.23	36380
6/1/2023	4:00	516.68	38.25	29970
6/1/2023	5:23	289.41	36.69	13400
6/1/2023	6:04	79.68	33.94	4570
6/2/2023	1:20	949.05	38.84	41300
6/2/2023	2:00	853.29	38.67	39070
6/2/2023	3:02	690.23	38.27	37090
6/2/2023	4:17	503.43	37.53	25300
6/2/2023	5:19	277.55	36.28	13320
6/2/2023	6:00	77.38	33.59	4750
6/3/2023	6:01	154.1	27.2	1680
6/3/2023	7:02	360.02	30.58	3560
6/3/2023	8:04	574.41	33.62	8830
6/3/2023	9:01	791.71	35.67	17430
6/3/2023	10:04	931.86	37.06	26650
6/3/2023	11:05	993.27	38.12	34440
6/3/2023	12:02	986.3	38.85	39070
6/3/2023	1:03	958.76	39.17	41210
6/3/2023	2:04	852.52	39.11	39240
6/3/2023	3:00	691.38	38.71	37660

6/3/2023	4:02	497.06	37.91	29950
6/3/2023	5:40	291.95	36.53	10070
6/3/2023	6:11	81.88	33.76	4260
6/4/2023	6:02	150.56	27.87	1500
6/4/2023	7:03	362.19	31.29	3290
6/4/2023	8:00	581.46	34.19	7610
6/4/2023	9:02	780.87	35.89	16730
6/4/2023	10:08	924.37	37.25	26890
6/4/2023	11:00	986.34	38.38	33310
6/4/2023	12:08	973.65	39.23	38370
6/4/2023	1:14	946.21	39.79	40560
6/4/2023	2:00	860.86	39.94	40280
6/4/2023	3:06	710.12	39.69	36440
6/4/2023	4:04	518.56	38.92	28600
6/4/2023	5:00	293.77	37.58	18330
6/4/2023	6:01	83.29	34.65	5510
6/5/2023	6:04	111.59	27.82	1700
6/5/2023	7:00	287.53	31.4	4340
6/5/2023	8:02	457.19	34.68	8510
6/5/2023	9:04	598.18	36.71	13920
6/5/2023	10:00	697.12	37.93	13270
6/5/2023	11:03	770.28	38.8	17210
6/5/2023	12:04	719.77	39.37	22660
6/5/2023	1:00	721.27	39.72	13080
6/5/2023	2:02	656.77	39.78	33520
6/5/2023	3:00	558.61	39.47	33780
6/5/2023	4:01	371.55	38.77	24500
6/5/2023	5:04	202.23	37.59	15990
6/5/2023	6:01	63.82	35.3	4560
6/6/2023	6:03	122.28	28.65	1320
6/6/2023	7:04	301.21	32.21	3480
6/6/2023	8:01	490.29	35.22	7510
6/6/2023	9:03	671.55	36.98	15850
6/6/2023	10:04	869.31	38.37	24210
6/6/2023	11:01	907.46	39.43	31190
6/6/2023	12:02	805.76	40.12	36320
6/6/2023	1:04	825.05	40.45	39810
6/6/2023	2:00	685.93	40.39	39610
6/6/2023	3:01	615.7	39.98	34130
6/6/2023	4:02	454.22	39.14	25860
6/6/2023	5:00	254.88	37.82	14880
6/6/2023	6:01	68.04	35.44	3790
6/7/2023	6:02	125.42	29.33	1540
6/7/2023	7:04	310.68	33.08	4360
6/7/2023	8:00	499.99	35.75	8500
6/7/2023	9:03	694.05	37.33	16290

6/7/2023	10:00	894.65	38.59	24090
6/7/2023	11:02	957.26	39.66	31650
6/7/2023	12:03	922.75	40.41	36090
6/7/2023	13:00	850	40.87	38600
6/7/2023	2:01	751.08	40.99	37990
6/7/2023	3:03	613.67	40.58	34970
6/7/2023	4:00	443.42	39.78	26600
6/7/2023	5:01	256.48	38.49	16270
6/7/2023	6:03	77.41	35.96	4230
6/8/2023	6:02	139.2	29.82	1280
6/8/2023	7:03	336.66	33.49	3580
6/8/2023	8:04	538.42	36.79	8170
6/8/2023	9:02	733.34	38.61	16000
6/8/2023	10:05	917.09	39.83	24650
6/8/2023	11:01	971.09	40.8	31930
6/8/2023	12:02	953.95	41.44	36910
6/8/2023	1:04	876.01	41.76	39670
6/8/2023	2:01	808.15	41.73	39360
6/8/2023	3:00	670.41	41.3	32130
6/8/2023	4:02	489.02	40.49	25330
6/8/2023	5:04	271.82	39.2	14950
6/8/2023	6:00	75.17	36.57	4990
6/9/2023	6:02	118.15	30.23	1660
6/9/2023	7:04	285.81	34.15	5030
6/9/2023	8:01	493.91	37.15	6440
6/9/2023	9:03	666.29	38.96	15310
6/9/2023	10:00	872.94	40.3	22540
6/9/2023	11:01	916.75	41.33	29160
6/9/2023	12:02	867.84	41.98	34420
6/9/2023	1:03	829.58	42.3	36550
6/9/2023	2:01	730.2	42.26	35390
6/9/2023	3:02	611.33	41.86	30280
6/9/2023	4:00	424.43	41.01	24080
6/9/2023	5:01	249.57	39.65	13520
6/9/2023	6:04	73.02	36.76	3190
6/10/2023	6:02	125.58	29.52	1280
6/10/2023	7:04	307.49	31.87	3340
6/10/2023	8:00	486.29	33.94	7230
6/10/2023	9:03	673.55	36.01	15280
6/10/2023	10:04	829.46	37.69	23400
6/10/2023	12:00	882.77	39.98	34570
6/10/2023	1:01	852.55	40.57	37970
6/10/2023	2:03	742.91	40.7	36780
6/10/2023	3:00	605.12	40.48	33640
6/10/2023	4:01	434.59	39.75	25040
6/10/2023	5:03	237.89	38.64	14330

6/10/2023	6:00	67.73	36.86	4160
6/11/2023	6:04	95.28	30.06	1560
6/11/2023	7:00	246.28	33.04	3920
6/11/2023	8:02	416.42	35.6	7600
6/11/2023	9:04	590.62	37.2	14580
6/11/2023	10:01	809.13	38.62	21510
6/11/2023	11:03	807.71	39.83	27650
6/11/2023	12:05	693.61	40.72	32240
6/11/2023	1:01	663.88	41.25	36380
6/11/2023	2:02	591.42	41.38	33270
6/11/2023	3:00	487.33	41.09	24310
6/11/2023	5:00	175.12	39.15	9860
6/11/2023	6:01	47.23	36.62	3110
6/12/2023	6:01	79.49	30.58	900
6/12/2023	7:02	203.21	32.56	3650
6/12/2023	9:04	540.29	36.72	13170
6/12/2023	10:01	760.47	37.85	21890
6/12/2023	11:00	807.75	38.56	27660
6/12/2023	12:04	737.33	38.77	31530
6/12/2023	1:00	716.3	38.9	15880
6/12/2023	2:02	606.22	38.87	17690
6/12/2023	3:04	492.09	38.52	12570
6/12/2023	4:04	322.2	37.67	4190
6/12/2023	5:00	171.47	36.38	12750
6/12/2023	6:02	50.62	34.69	3190
6/13/2023	6:03	82.58	28.34	2240
6/13/2023	7:04	233.74	30.52	3730
6/13/2023	8:00	400.47	32.91	5940
6/13/2023	9:05	684.21	34.53	15010
6/13/2023	10:28	725.88	35.79	25510
6/13/2023	11:00	751.79	36.81	27970
6/13/2023	12:01	676.8	37.61	15050
6/13/2023	1:03	602.03	38.05	9960
6/13/2023	2:00	482.71	38.31	36130
6/13/2023	3:01	380.98	38.12	29250
6/13/2023	4:03	313.41	37.54	20860
6/13/2023	5:04	157.24	36.62	6010
6/13/2023	6:01	50.78	35.15	650
6/14/2023	6:04	89.31	28.12	1680
6/14/2023	7:00	237.83	30.94	3720
6/14/2023	8:02	394.38	33.27	8410
6/14/2023	9:03	556.16	34.42	19900
6/14/2023	10:04	773.64	36.2	26830
6/14/2023	11:01	836.98	38.15	33350
6/14/2023	12:03	794.12	39.3	38290
6/14/2023	1:04	689.62	39.93	39920

6/14/2023	2:00	620.81	39.98	38810
6/14/2023	3:03	535.14	39.43	33560
6/14/2023	4:00	289.2	38.52	4990
6/14/2023	5:02	146.8	36.94	6300
6/14/2023	6:03	63.7	34.4	1860
6/15/2023	6:03	113.05	29.04	1570
6/15/2023	7:00	272.27	32	3530
6/15/2023	9:01	607.45	37.8	17170
6/15/2023	11:02	899.29	40.43	33900
6/15/2023	12:03	822.68	41.16	13280
6/15/2023	13:00	754.9	41.43	41100
6/15/2023	2:02	756.85	41.44	16040
6/15/2023	3:04	622.55	40.83	33440
6/15/2023	4:00	375.81	39.65	25400
6/15/2023	5:02	240.66	37.87	11480
6/15/2023	6:04	70.23	35.37	4030
6/16/2023	6:03	123.47	29.09	1650
6/16/2023	7:04	313.53	31.73	4160
6/16/2023	8:00	509.37	34.2	8350
6/16/2023	9:03	740.88	36.36	16880
6/16/2023	11:02	931.77	39.74	33260
6/16/2023	12:04	869.52	40.69	37130
6/16/2023	13:00	803.99	41.13	41470
6/16/2023	2:02	746.41	41.19	38890
6/16/2023	3:04	636.9	40.81	35330
6/16/2023	4:00	398.72	40.01	17410
6/16/2023	5:02	222.54	38.7	18360
6/16/2023	6:04	66.15	36.63	4400
6/17/2023	6:03	124.31	29.73	1610
6/17/2023	7:04	291.17	32.79	3900
6/17/2023	8:00	503.18	35.3	8210
6/17/2023	9:03	715.9	37.23	17130
6/17/2023	10:04	880.57	38.8	25920
6/17/2023	11:00	947.62	40.05	31900
6/17/2023	12:03	899.25	40.92	36840
6/17/2023	1:04	825.93	41.45	40400
6/17/2023	2:00	705.97	41.59	38750
6/17/2023	3:03	544.77	41.17	33220
6/17/2023	4:04	361.5	40.26	7780
6/17/2023	5:01	182.02	38.69	6270
6/17/2023	6:03	73.23	35.76	1710
6/18/2023	6:04	109.58	29.3	1620
6/18/2023	7:00	278.69	31.85	3480
6/18/2023	9:18	651.13	36.2	19300
6/18/2023	10:02	866.51	37.17	25460
6/18/2023	11:04	903.74	38.06	33350

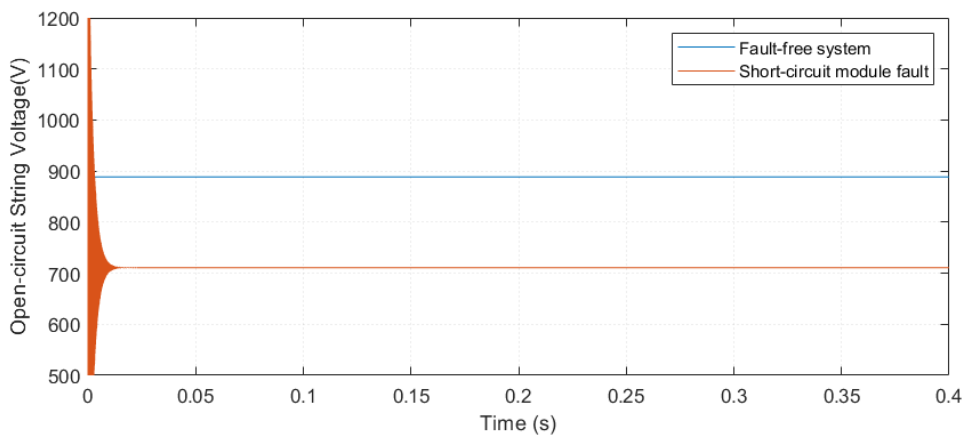
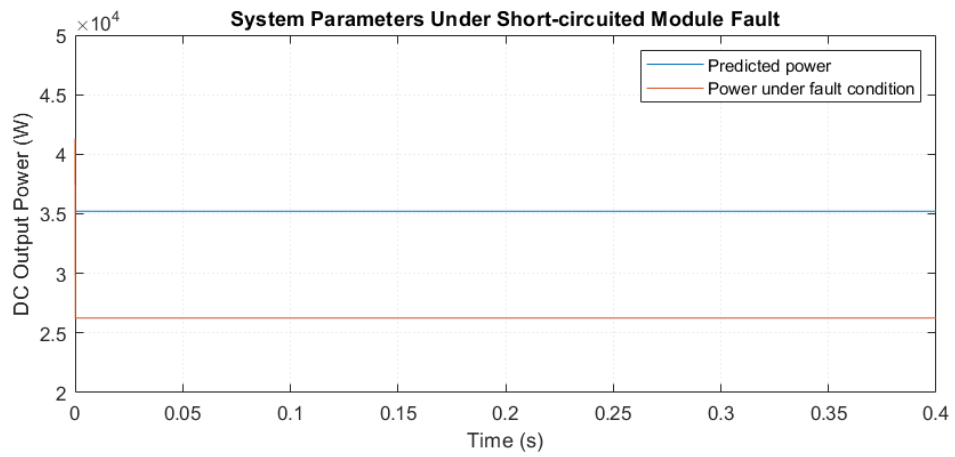
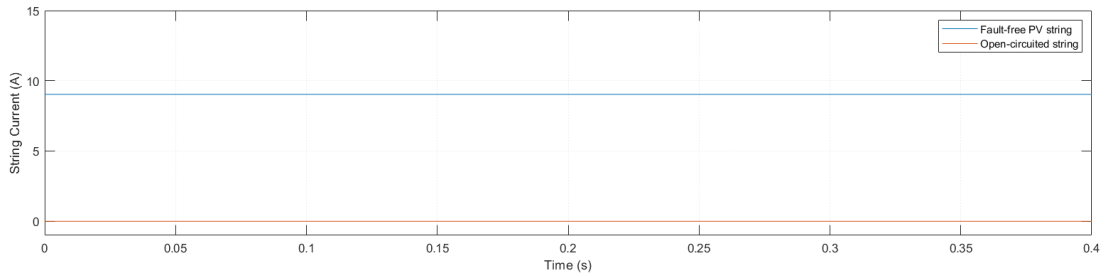
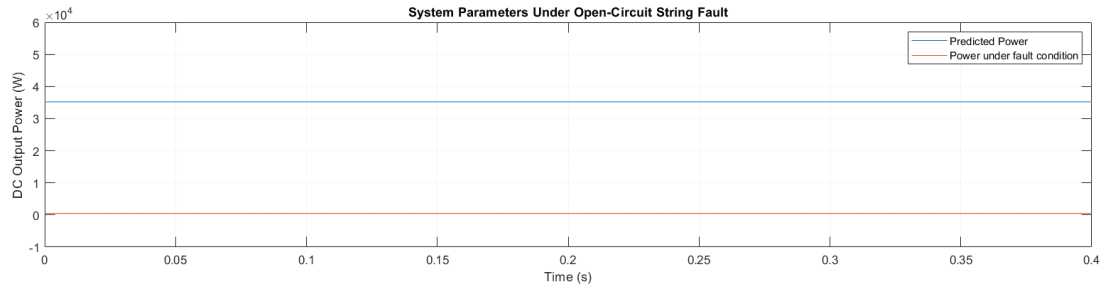
6/18/2023	1:04	714.33	38.53	34110
6/18/2023	2:01	698.88	38.64	4470
6/18/2023	3:04	407.59	38.37	6980
6/18/2023	4:00	131.12	38.05	3100
6/18/2023	6:03	41.46	35.08	1820
6/19/2023	6:02	109.3	29.8	1760
6/19/2023	7:03	280.51	32.15	4440
6/19/2023	9:04	643.17	35.02	17880
6/19/2023	10:00	814.7	36.12	27090
6/19/2023	11:02	870.78	37.22	34260
6/19/2023	12:04	807.8	38.11	38690
6/19/2023	1:00	786.13	38.65	41330
6/19/2023	2:02	719.49	38.87	28740
6/19/2023	3:04	549.3	38.69	13180
6/19/2023	4:00	384.75	38.26	12690
6/19/2023	5:02	195.88	37.37	850
6/19/2023	6:04	66.86	35.49	250
6/20/2023	6:03	69.4	30.15	2730
6/20/2023	7:05	208.88	32.65	4720
6/20/2023	8:00	353.27	34.4	9590
6/20/2023	9:01	453.82	35.66	15890
6/20/2023	10:00	306.59	36.97	4400
6/20/2023	11:00	200.23	38.18	2320
6/20/2023	12:03	247	39.01	12160
6/20/2023	3:03	558.3	39.51	19150
6/20/2023	4:00	421.87	38.65	15420
6/20/2023	5:02	240.93	37.37	19350
6/20/2023	6:00	74.91	35.6	7200
6/21/2023	6:04	43.35	29.73	1440
6/21/2023	7:01	102.87	32.12	3220
6/21/2023	8:02	220.64	34.16	15080
6/21/2023	9:00	390.44	35.58	21800
6/21/2023	10:01	532.09	37.06	11100
6/21/2023	11:04	665.16	38.12	30450
6/21/2023	12:00	751.9	38.74	26050
6/21/2023	1:02	795.2	39.12	41780
6/21/2023	2:03	729.27	39.17	43670
6/21/2023	3:00	578.9	38.94	37210
6/21/2023	4:01	390.01	38.35	28600
6/21/2023	6:02	65.67	35.85	1540
6/22/2023	8:00	331.56	33.39	8190
6/22/2023	10:00	729.76	36.11	28160
6/22/2023	11:00	815.02	37.16	34800
6/22/2023	12:03	607.48	37.88	16810
6/22/2023	1:02	703.73	38.05	42330
6/22/2023	2:03	557.58	37.73	45680

6/22/2023	3:03	467.47	37.2	16140
6/22/2023	4:00	313.55	36.65	13810
6/22/2023	5:02	166.62	35.79	14980
6/22/2023	6:03	50.62	34.65	2620
6/23/2023	6:01	22.45	29.37	5640
6/23/2023	7:02	60.64	30.61	2200
6/23/2023	8:03	96.18	31.85	8280
6/23/2023	9:01	168.18	33.37	3000
6/23/2023	10:00	308.1	35.05	8740
6/23/2023	11:02	560.76	36.57	18910
6/23/2023	12:02	740.49	37.86	26800
6/23/2023	1:04	806.31	38.65	46770
6/23/2023	3:00	608.59	39.1	46350
6/23/2023	4:02	425.63	38.62	16720
6/23/2023	5:04	236.93	37.62	16600
6/23/2023	6:00	79.77	36.26	8950
6/24/2023	7:01	64.67	30.33	510
6/24/2023	8:03	85.43	31.25	880
6/24/2023	9:04	68.88	32.35	2550
6/24/2023	10:03	108.77	33.6	6090
6/24/2023	11:05	190.84	34.78	13710
6/24/2023	12:01	341.46	35.36	26830
6/24/2023	1:03	515.7	35.94	10300
6/24/2023	2:00	450.74	36.08	6600
6/24/2023	3:01	383.97	36.08	42760
6/24/2023	4:01	275.95	35.79	33060
6/24/2023	5:02	144.36	34.93	19650
6/24/2023	6:04	62.42	33.68	1680
6/25/2023	6:02	79.95	28.88	530
6/25/2023	7:03	196.9	30.45	2370
6/25/2023	8:00	314.91	32.05	2640
6/25/2023	9:02	477.67	33.69	9790
6/25/2023	10:05	561.29	35.25	21020
6/25/2023	2:04	599.42	38.5	45900
6/25/2023	3:02	472.2	38.66	13350
6/25/2023	4:04	370.65	38.24	33460
6/25/2023	5:00	213.07	37.15	24580
6/25/2023	6:02	77.89	35.54	4130
6/26/2023	6:01	76.23	29	500
6/26/2023	7:02	207.33	29.78	5960
6/26/2023	8:04	332.73	30.91	10700
6/26/2023	9:00	596.44	31.99	21720
6/26/2023	10:02	764.25	32.89	29220
6/26/2023	11:03	768.26	33.69	35550
6/26/2023	12:01	703.07	34.34	40200
6/26/2023	1:02	744.28	34.94	42630

6/26/2023	2:04	675.79	35.69	27750
6/26/2023	3:01	581.73	36.07	34890
6/26/2023	4:02	427.75	35.97	26540
6/26/2023	5:03	235.63	35.37	22300
6/26/2023	6:04	89.21	34.13	6110
6/27/2023	6:04	73.96	27.66	1170
6/27/2023	7:00	225.89	29.44	4720
6/27/2023	8:02	350.24	31.54	7630
6/27/2023	9:04	473.63	33.33	15680
6/27/2023	10:00	581.48	34.62	17000
6/27/2023	11:02	707.34	35.62	18580
6/27/2023	12:03	631.25	36.26	24310
6/27/2023	1:07	639.63	36.47	3960
6/27/2023	2:04	556.07	36.34	23630
6/27/2023	3:00	543.58	35.82	25330
6/27/2023	4:03	413.02	34.87	42190
6/27/2023	5:04	246.52	33.6	11520
6/27/2023	6:01	82.19	31.87	10960
6/28/2023	6:03	55.39	26.98	1640
6/28/2023	7:00	156.88	28.62	1680
6/28/2023	8:01	280.6	30.27	1980
6/28/2023	9:04	468.94	31.62	21480
6/28/2023	10:01	617.45	32.94	37350
6/28/2023	11:02	724.91	34.12	32370
6/28/2023	12:03	717.3	34.87	19570
6/28/2023	1:12	728.84	34.99	52980
6/28/2023	2:04	642.41	34.67	14740
6/28/2023	3:03	543.13	34.01	6680
6/28/2023	4:00	361.41	33.13	7470
6/28/2023	6:01	76.27	30.87	5030
6/29/2023	6:05	44.87	26.38	400
6/29/2023	7:01	136.41	27.8	5680
6/29/2023	8:02	236.51	29.55	7720
6/29/2023	9:00	352.6	30.98	27880
6/29/2023	10:08	458.54	32.12	21470
6/29/2023	11:04	481.1	32.88	22450
6/29/2023	12:06	613.79	33.26	33800
6/29/2023	1:02	503.4	33.23	32650
6/29/2023	2:09	531.94	32.87	38260
6/29/2023	3:04	448.05	32.13	1620
6/29/2023	4:02	327.3	31.25	5270
6/29/2023	5:00	173.49	30.26	2070
6/29/2023	6:01	65.93	29.12	4070
6/30/2023	6:04	22.95	26.15	150
6/30/2023	7:01	57.45	26.87	1450
6/30/2023	9:00	224.25	28.76	14670

6/30/2023	10:01	342.91	29.3	12690
6/30/2023	11:02	448.8	29.4	20060
6/30/2023	12:00	418.1	29.4	22820
6/30/2023	1:02	441.05	29.33	18800
6/30/2023	2:05	279.11	29.33	12300
6/30/2023	3:01	189.76	29.41	6770
6/30/2023	4:03	164.26	29.3	4380
6/30/2023	5:03	100.43	28.89	3800
6/30/2023	6:00	25.02	28.12	750

Appendix D: System Parameters During Open-Circuit String Fault and Module Fault



Machine Learning Approach for Fault Detection and Diagnosis of PV Modules

ORIGINALITY REPORT

17%

SIMILARITY INDEX

PRIMARY SOURCES

1	elibrary.tucl.edu.np Internet	360 words — 1%
2	www.researchgate.net Internet	360 words — 1%
3	www.mdpi.com Internet	344 words — 1%
4	Abdelkader El Kounni, Hassan Radoine, Hicham Mastouri, Hicham Bahi, Abdelkader Outzourhit. "Solar Power Output Forecasting Using Artificial Neural Network", 2021 9th International Renewable and Sustainable Energy Conference (IRSEC), 2021 Crossref	244 words — 1%
5	core.ac.uk Internet	173 words — 1%
6	www.scilit.net Internet	164 words — 1%
7	www.hindawi.com Internet	162 words — 1%
8	Lian Lian Jiang, Douglas L. Maskell. "Automatic fault detection and diagnosis for photovoltaic systems	161 words — 1%

using combined artificial neural network and analytical based methods", 2015 International Joint Conference on Neural Networks (IJCNN), 2015

Crossref

-
- | | | |
|----|--|------------------|
| 9 | ijeecs.iaescore.com
Internet | 143 words — 1% |
| 10 | elibrary.tucl.edu.np:8080
Internet | 105 words — < 1% |
| 11 | www.worlddata.info
Internet | 102 words — < 1% |
| 12 | Ghada M. El-Banby, Nada M. Moawad, Belal A. Abouzalm, Wessam F. Abouzaid, E. A. Ramadan. "Photovoltaic system fault detection techniques: a review", Neural Computing and Applications, 2023
Crossref | 91 words — < 1% |
| 13 | res.mdpi.com
Internet | 70 words — < 1% |
| 14 | Dolf Gielen, Francisco Boshell, Deger Saygin, Morgan D. Bazilian, Nicholas Wagner, Ricardo Gorini. "The role of renewable energy in the global energy transformation", Energy Strategy Reviews, 2019
Crossref | 63 words — < 1% |
| 15 | thecleverprogrammer.com
Internet | 46 words — < 1% |
| 16 | www.extrica.com
Internet | 45 words — < 1% |
| 17 | K. Ranjith Kumar, M. Surya Kalavathi. "Artificial intelligence based forecast models for predicting | 43 words — < 1% |

-
- 18 eprints.whiterose.ac.uk 40 words — < 1%
Internet
-
- 19 ideas.repec.org 40 words — < 1%
Internet
-
- 20 A. AALLOUCHE, H. OUADI. "Online fault detection and identification for an isolated PV system using ANN", IFAC-PapersOnLine, 2022 39 words — < 1%
Crossref
-
- 21 Banalaxmi Brahma, Rajesh Wadhvani. "Solar Irradiance Forecasting Based on Deep Learning Methodologies and Multi-Site Data", Symmetry, 2020 39 words — < 1%
Crossref
-
- 22 hdl.handle.net 36 words — < 1%
Internet
-
- 23 Moajjem Hossain Chowdhury, Md Nazmul Islam Shuzan, Muhammad E.H. Chowdhury, Zaid B. Mahbub et al. "Estimating Blood Pressure from the Photoplethysmogram Signal and Demographic Features Using Machine Learning Techniques", Sensors, 2020 35 words — < 1%
Crossref
-
- 24 Kingston, Samuel Ray. "Algorithms Using Spread Spectrum Time Domain Reflectometry (SSTDR) for Fault Detection and Location in Electrical Systems", The University of Utah, 2023 34 words — < 1%
ProQuest
-
- 25 Ihsan Ullah Khalil, Azhar Ul-Haq, Yousef Mahmoud, Marium Jalal, Muhammad Aamir, Mati Ullah Ahsan, Khalid Mehmood. "Comparative Analysis of 33 words — < 1%

Photovoltaic Faults and Performance Evaluation of its Detection Techniques", IEEE Access, 2020

Crossref

26 repository.enp.edu.dz 30 words — < 1%

Internet

27 Elyes Garoudja, Aissa Chouder, Kamel Kara, Santiago Silvestre. "An enhanced machine learning based approach for failures detection and diagnosis of PV systems", Energy Conversion and Management, 2017

Crossref

28 Ojaswa Yadav, Ramani Kannan, Sheikh T. Meraj, Ammar Masaoud. "Machine Learning Based Prediction of Output PV Power in India and Malaysia with the Use of Statistical Regression", Mathematical Problems in Engineering, 2022

Crossref

29 dir.indiamart.com 28 words — < 1%

Internet

30 m.moam.info 28 words — < 1%

Internet

31 rdoc.univ-sba.dz 28 words — < 1%

Internet

32 www.scirp.org 27 words — < 1%

Internet

33 Zixia Yuan, Guojiang Xiong, Xiaofan Fu. "Artificial Neural Network for Fault Diagnosis of Solar Photovoltaic Systems: A Survey", Energies, 2022

Crossref

34

Internet

25 words — < 1%

35

Yassine Chouay, Mohammed Ouassaid. "An intelligent method for fault diagnosis in photovoltaic systems", 2017 International Conference on Electrical and Information Technologies (ICEIT), 2017

Crossref

23 words — < 1%

36

livrepository.liverpool.ac.uk

Internet

21 words — < 1%

37

Laxmikant D. Jathar, S. Ganesan, Umesh Awasarmol, Keval Nikam et al. "Comprehensive review of environmental factors influencing the performance of photovoltaic panels: Concern over emissions at various phases throughout the lifecycle", Environmental Pollution, 2023

Crossref

20 words — < 1%

38

Risenmay, Matthew Allan. "Application of Supervised Machine Learning to Search for Nuclear Fallout Analytes that Identify Explosive Type", North Carolina State University, 2023

ProQuest

20 words — < 1%

39

Varaha Satra Bharath Kurukuru, Ahteshamul Haque, Mohammed Ali Khan, Subham Sahoo, Azra Malik, Frede Blaabjerg. "A Review on Artificial Intelligence Applications for Grid-Connected Solar Photovoltaic Systems", Energies, 2021

Crossref

20 words — < 1%

40

Vipinkumar Shriram Meshram, Alberto Reatti. "Performance Analysis of Zeta Converter for Photovoltaic Powered Micromobility Charging Station", 2023 AEIT International Annual Conference (AEIT), 2023

Crossref

20 words — < 1%

41	m.scirp.org Internet	20 words — < 1%
42	Payman Goodarzi, Steffen Klein, Andreas Schütze, Tizian Schneider. "Comparing Different Feature Extraction Methods in Condition Monitoring Applications", 2023 IEEE International Instrumentation and Measurement Technology Conference (I2MTC), 2023 Crossref	19 words — < 1%
43	fr.scribd.com Internet	19 words — < 1%
44	latamt.ieeer9.org Internet	19 words — < 1%
45	keep.lib.asu.edu Internet	18 words — < 1%
46	lib.icimod.org Internet	18 words — < 1%
47	lup.lub.lu.se Internet	18 words — < 1%
48	openrepository.aut.ac.nz Internet	18 words — < 1%
49	qspace.qu.edu.qa Internet	18 words — < 1%
50	Connor Scott, Momina Ahsan, Alhussein Albarbar. "Machine learning for forecasting a photovoltaic (PV) generation system", Energy, 2023 Crossref	17 words — < 1%
51	pubmed.ncbi.nlm.nih.gov Internet	

17 words — < 1%

52 utpedia.utp.edu.my
Internet

17 words — < 1%

53 beei.org
Internet

16 words — < 1%

54 etd.aau.edu.et
Internet

16 words — < 1%

55 J.-S.R. Jang, Chuen-Tsai Sun. "Neuro-fuzzy modeling and control", Proceedings of the IEEE, 1995
Crossref

15 words — < 1%

56 mdpi-res.com
Internet

15 words — < 1%

57 "Artificial Intelligence and Renewables Towards an Energy Transition", Springer Science and Business Media LLC, 2021
Crossref

14 words — < 1%

58 "Soft Computing in Condition Monitoring and Diagnostics of Electrical and Mechanical Systems", Springer Science and Business Media LLC, 2020
Crossref

14 words — < 1%

59 Muhammad Saad Iqbal, Yasir Amir Khan Niazi, Umer Amir Khan, Bang-Wook Lee. "Real-time fault detection system for large scale grid integrated solar photovoltaic power plants", International Journal of Electrical Power & Energy Systems, 2021
Crossref

14 words — < 1%

60 Siva Ramakrishna Madeti, S.N. Singh. "A comprehensive study on different types of faults and detection techniques for solar photovoltaic system", Solar Energy, 2017

14 words — < 1%

Crossref

61 pdfcoffee.com

Internet

14 words — < 1%

62 www.arxiv-vanity.com

Internet

14 words — < 1%

63 "Advances in Robotics, Automation and Data Analytics", Springer Science and Business Media LLC, 2021

Crossref

13 words — < 1%

64 Ikechukwu Etienne Umeonyiagu, Chidozie Chukwuemeka Nwobi-Okoye. "Modelling and multi objective optimization of bamboo reinforced concrete beams using ANN and genetic algorithms", European Journal of Wood and Wood Products, 2019

Crossref

13 words — < 1%

65 www.csagroup.org

Internet

13 words — < 1%

66 www.ncbi.nlm.nih.gov

Internet

13 words — < 1%

67 Ao Dong, Yingying Zhao, Xiwei Liu, Li Shang, Qi Liu, Dahai Kang. "Fault Diagnosis and Classification in Photovoltaic Systems Using SCADA Data", 2017 International Conference on Sensing, Diagnostics, Prognostics, and Control (SDPC), 2017

Crossref

12 words — < 1%

68 Lina M. Shaker, Ahmed Alamiery, Wan Nor Roslam Wan Isahak, Waleed Khalid Al-Azzawi. "Corrosion in solar cells: challenges and solutions for enhanced performance and durability", Journal of Optics, 2023 12 words — < 1%
Crossref

69 Saba Gul, Azhar Ul Haq, Marium Jalal, Almas Anjum, Ihsan Ullah Khalil. "A Unified Approach for Analysis of Faults in Different Configurations of PV Arrays and Its Impact on Power Grid", Energies, 2019 12 words — < 1%
Crossref

70 Seinuk, Matthew. "Foundation and Flood Protection Design in Flood Zones.", The Cooper Union for the Advancement of Science and Art, 2020 12 words — < 1%
ProQuest

71 mech.pcampus.edu.np 12 words — < 1%
Internet

72 9pdf.net 11 words — < 1%
Internet

73 DASH, PRADHAN, PANDA. "Application of Artificial Intelligence Techniques for Classification and Location of Faults on Thyristor-Controlled Series-Compensated Line", Electric Power Components and Systems, 2003 11 words — < 1%
Crossref

74 Junjie Wang, Dedong Gao, Shaokang Zhu, Shan Wang, Haixiong Liu. "Fault diagnosis method of photovoltaic array based on support vector machine", Energy Sources, Part A: Recovery, Utilization, and Environmental Effects, 2019 11 words — < 1%
Crossref

-
- 75 Robert Babuška, Henk Verbruggen. "Data-driven Construction of Transparent Fuzzy Systems", IFAC Proceedings Volumes, 2001
Crossref 11 words — < 1%
-
- 76 Xiaolei Yu, Yujun Zhou, Zhenlu Liu, Zhimin Zhao. "An optimal measurement method for spatial distribution of radio frequency identification multi-tag based on image analysis and PSO", Transactions of the Institute of Measurement and Control, 2019
Crossref 11 words — < 1%
-
- 77 krishi.icar.gov.in
Internet 11 words — < 1%
-
- 78 Roshan Pandey, Rajendra Shrestha, Nawraj Bhattarai, Rabin Dhakal. "Problems identification and performance analysis in small hydropower plants in Nepal", International Journal of Low-Carbon Technologies, 2023
Crossref 10 words — < 1%
-
- 79 dspace.khazar.org
Internet 10 words — < 1%
-
- 80 flipkarma.com
Internet 10 words — < 1%
-
- 81 repository.ruforum.org
Internet 10 words — < 1%
-
- 82 studentrepo.iium.edu.my
Internet 10 words — < 1%
-
- 83 www.adb.org
Internet 10 words — < 1%
-
- 84 assets.researchsquare.com

Internet

9 words — < 1%

85 awyungsource.ecrater.com

Internet

9 words — < 1%

86 dspace.lib.ntua.gr

Internet

9 words — < 1%

87 eprints.nottingham.ac.uk

Internet

9 words — < 1%

88 pure.kfupm.edu.sa

Internet

9 words — < 1%

89 repository.library.carleton.ca

Internet

9 words — < 1%

90 timesofindia.indiatimes.com

Internet

9 words — < 1%

91 topics.nytimes.com

Internet

9 words — < 1%

92 web.stanford.edu

Internet

9 words — < 1%

93 www.eemj.icpm.tuiasi.ro

Internet

9 words — < 1%

94 Adel Mellit, Soteris Kalogirou. "Artificial intelligence and internet of things to improve efficacy of diagnosis and remote sensing of solar photovoltaic systems: Challenges, recommendations and future directions", Renewable and Sustainable Energy Reviews, 2021

Crossref

8 words — < 1%

95 Amit Dhoke, Rahul Sharma, Tapan Kumar Saha. "An approach for fault detection and location in solar PV systems", Solar Energy, 2019

Crossref

8 words — < 1%

96 Bashar Hammad, Mohammad Al-Abed, Ahmed Al-Ghandoor, Ali Al-Sardeah, Adnan Al-Bashir.

"Modeling and analysis of dust and temperature effects on photovoltaic systems' performance and optimal cleaning frequency: Jordan case study", Renewable and Sustainable Energy Reviews, 2018

Crossref

8 words — < 1%

97 Boris Pokrić, Nigel M. Allinson, John R. Helliwell. "Integration of macromolecular diffraction data using radial basis function networks", Journal of Synchrotron Radiation, 2000

Crossref

8 words — < 1%

98 Fauzan Hanif Jufri, Seongmun Oh, Jaesung Jung. "Development of Photovoltaic abnormal condition detection system using combined regression and Support Vector Machine", Energy, 2019

Crossref

8 words — < 1%

99 Gokmen, Nuri, Engin Karatepe, Berk Celik, and Santiago Silvestre. "Simple diagnostic approach for determining of faulted PV modules in string based PV arrays", Solar Energy, 2012.

Crossref

8 words — < 1%

100 Haizheng Wang, Jian Zhao, Qian Sun, Honglu Zhu. "Probability modeling for PV array output interval and its application in fault diagnosis", Energy, 2019

Crossref

8 words — < 1%

101 R. Fazai, K. Abodayeh, M. Mansouri, M. Trabelsi, H. Nounou, M. Nounou, G.E. Georghiou. "Machine learning-based statistical testing hypothesis for fault detection in photovoltaic systems", Solar Energy, 2019

Crossref

8 words — < 1%

102 W. Chine, A. Mellit, A. Massi Pavan, S.A. Kalogirou. "Fault detection method for grid-connected photovoltaic plants", Renewable Energy, 2014

Crossref

8 words — < 1%

103 Yasemin Onal, Umit Cigdem Turhal. "Discriminative common vector in sufficient data Case: A fault detection and classification application on photovoltaic arrays", Engineering Science and Technology, an International Journal, 2021

Crossref

8 words — < 1%

104 Yin, Yong, Chaoyong Zhang, and Yu Li. "A two-stage data fusion model for wireless sensor networks", International Journal of Sensor Networks, 2014.

Crossref

8 words — < 1%

105 Ying Su, Jingna Pan, Haifei Wu, Shuang Sun, Zubing Zou, Jiaqi Li, Bingrong Pan, Honglu Zhu. "Dynamic probability modeling of photovoltaic strings and its application in fault diagnosis", Energy Reports, 2022

Crossref

8 words — < 1%

106 bura.brunel.ac.uk

Internet

8 words — < 1%

107 cupdf.com

Internet

8 words — < 1%

108 digitalcommons.lsu.edu

Internet

8 words — < 1%

109	dr.library.brocku.ca Internet	8 words — < 1%
110	dspace2020.uniten.edu.my:8080 Internet	8 words — < 1%
111	ekhsuir.kspu.edu Internet	8 words — < 1%
112	etd.astu.edu.et Internet	8 words — < 1%
113	github.com Internet	8 words — < 1%
114	uvadoc.uva.es Internet	8 words — < 1%
115	worldwidescience.org Internet	8 words — < 1%
116	www.ee.iitb.ac.in Internet	8 words — < 1%
117	www.hackerrank.com Internet	8 words — < 1%
118	www.idin.org Internet	8 words — < 1%
119	Abdou Latif Bonkaney, Madougou Saidou, Rabani Adamou. "Impact of Climatic Parameters on the Performance of Solar Photovoltaic (PV) Module in Niamey", Smart Grid and Renewable Energy, 2017 Crossref	7 words — < 1%

120 Ghada Shaban Eldeghady, Hanan Ahmed Kamal, Mohamed A. Moustafa Hassan. "Fault diagnosis for PV system using a deep learning optimized via PSO heuristic combination technique", Electrical Engineering, 2023

Crossref

7 words — < 1%

121 Joardar, Biresk Kumar. "Machine Learning-Enabled Vertically Integrated Heterogeneous Manycore Systems for Big-Data Analytics", Washington State University, 2020

ProQuest

7 words — < 1%

122 Mahmudul Islam, Masud Rana Rashel, Md Tofael Ahmed, A. K. M. Kamrul Islam, Mouhaydine Tlemçani. "Artificial Intelligence in Photovoltaic Fault Identification and Diagnosis: A Systematic Review", Energies, 2023

Crossref

7 words — < 1%

123 Ryszard M. Czarny. "The Nordic Dimension of Energy Security", Springer Science and Business Media LLC, 2020

Crossref

7 words — < 1%

124 Zhicong Chen, Yixiang Chen, Lijun Wu, Shuying Cheng, Peijie Lin. "Deep residual network based fault detection and diagnosis of photovoltaic arrays using current-voltage curves and ambient conditions", Energy Conversion and Management, 2019

Crossref

7 words — < 1%

125 scholarworks.boisestate.edu

Internet

7 words — < 1%

126 www.gecekitapligi.com

Internet

7 words — < 1%

127 Ahteshamul Haque, Kurukuru Varaha Satya Bharath, Mohammed Ali Khan, Irshad Khan, Zainul Abdin Jaffery. "Fault diagnosis of Photovoltaic Modules", Energy Science & Engineering, 2019

6 words — < 1%

Crossref

128 Amith Khandakar, Muhammad E. H. Chowdhury, Monzure- Khoda Kazi, Kamel Benhmed et al. "Machine Learning Based Photovoltaics (PV) Power Prediction Using Different Environmental Parameters of Qatar", Energies, 2019

6 words — < 1%

Crossref

129 Andreas Livera, Marios Theristis, George Makrides, George E. Georghiou. "Recent advances in failure diagnosis techniques based on performance data analysis for grid-connected photovoltaic systems", Renewable Energy, 2019

6 words — < 1%

Crossref

130 Bayu Sutanto, Hector Iacovides, Adel Nasser, Andrea Cioncolini et al. "Design and analysis of passively cooled floating photovoltaic systems", Applied Thermal Engineering, 2023

6 words — < 1%

Crossref

131 Prince D. N. Ncube, Edson L. Meyer, Zelalem S. Shibeshi. "Towards the Development of a Photovoltaic Array Fault Detection and Diagnosis (PVAFFD) System", 2021 International Conference on Electrical, Computer and Energy Technologies (ICECET), 2021

6 words — < 1%

Crossref

132 S. Sumathi, L. Ashok Kumar, P. Surekha. "Solar PV and Wind Energy Conversion Systems", Springer Science and Business Media LLC, 2015

6 words — < 1%

Crossref

133

Ye Zhao, Brad Lehman, Jean-Francois de Palma, Jerry Mosesian, Robert Lyons. "Fault analysis in solar PV arrays under: Low irradiance conditions and reverse connections", 2011 37th IEEE Photovoltaic Specialists Conference, 2011

Crossref

6 words — < 1%

EXCLUDE QUOTES ON

EXCLUDE SOURCES < 6 WORDS

EXCLUDE BIBLIOGRAPHY ON

EXCLUDE MATCHES < 6 WORDS



त्रिभुवन विश्वविद्यालय
Tribhuvan University
इन्जिनियरिङ अध्ययन संस्थान
Institute of Engineering

डीनको कार्यालय OFFICE OF THE DEAN

GPO box- 1915, Pulchowk, Lalitpur
Tel: 977-5-521531, Fax: 977-5-525830
dean@ioe.edu.np, www.ioe.edu.np
गोश्वारा पो. व. न- १९१५, पुल्चोक, ललितपुर
फोन- ५५२१५३१, फ्याक्स- ५५२५८३०

Date: November 26, 2023

To Whom It May Concern:

This is to certify that the paper titled “*Machine Learning Approach for Fault Detection and Diagnosis of Solar Modules*” (Submission# 536) submitted by **Kabina Maharjan** as the first author has been accepted after the peer-review process for presentation in the 14th IOE Graduate Conference being held during Nov 29 to Dec 1, 2023. Kindly note that the publication of the conference proceedings is still underway and hence inclusion of the accepted manuscript in the conference proceedings is contingent upon the author’s presence for presentation during the conference and timely response to further edits during the publication process.

Bhim Kumar Dahal, PhD
Convener,
14th IOE Graduate Conference

